

**- SPONGISTATIN 1 -**

NOVEL MODES OF ACTION AS A POTENT ANTICANCER AGENT



Dissertation zur Erlangung des Doktorgrades  
der Fakultät für Chemie und Pharmazie  
der Ludwig-Maximilians-Universität München



- SPONGISTATIN 1 -

NOVEL MODES OF ACTION AS  
A POTENT ANTICANCER AGENT

**Uta Monika Schneiders**

aus  
Saarbrücken  
2008



## Erklärung

Diese Dissertation wurde im Sinne von §13 Abs. 3 der Promotionsordnung vom 29. Januar 1998 von Frau Prof. Dr. A. M. Vollmar betreut.

## Ehrenwörtliche Versicherung

Diese Dissertation wurde selbständig, ohne unerlaubte Hilfe erarbeitet.

München, am 24.07.2008

---

Uta Monika Schneiders

Dissertation eingereicht am: 24.07.2008

1. Gutachter: Prof. Dr. Angelika M. Vollmar

2. Gutachter: Prof. Dr. Christian Wahl-Schott

Mündliche Prüfung am: 26.09.2008



dedicated to my family



"Every great advance in science has issued from a new audacity of imagination."

- John Dewey -



## **CONTENTS**

## TABLE OF CONTENTS

<b>I</b>	<b>INTRODUCTION</b> .....	<b>1</b>
1	NATURAL PRODUCTS IN CANCER THERAPY .....	1
1.1	MARINE-DERIVED ANTICANCER AGENTS .....	2
1.2	MICROTUBULES AS TARGET IN CANCER THERAPY .....	3
2	THE SPONGISTATINS.....	5
3	AIM OF THE STUDY .....	8
4	PROGRAMMED CELL DEATH.....	8
5	APOPTOSIS SIGNALING PATHWAYS.....	11
5.1	CASPASES .....	11
5.1.1	GENERAL FEATURES AND CLASSIFICATION OF CASPASES .....	11
5.1.2	SUBSTRATE CLEAVAGE.....	14
5.1.3	REGULATION OF CASPASES.....	14
5.2	EXTRINSIC APOPTOTIC PATHWAY .....	16
5.3	INTRINSIC APOPTOTIC PATHWAY.....	18
5.3.1	REGULATION BY BCL-2 FAMILY MEMBERS.....	20
5.3.2	BH3-ONLY PROTEINS .....	23
6	APOPTOSIS AS A BARRIER TO METASTASIS.....	26
6.1	THE METASTATIC CASCADE .....	26
6.2	APOPTOSIS IN THE METASTATIC PROCESS .....	27
<b>II</b>	<b>MATERIALS AND METHODS</b> .....	<b>33</b>
1	MATERIALS.....	33
1.1	SPONGISTATIN 1 .....	33
1.2	REAGENTS .....	33
1.3	TECHNICAL EQUIPMENT .....	34
2	CELL CULTURE.....	34
2.1	CELL LINES.....	34
2.2	CULTIVATION.....	35
2.3	SEEDING FOR EXPERIMENTS .....	36
2.4	FREEZING AND THAWING.....	36
3	FLOW CYTOMETRY .....	37
3.1	INTRODUCTION .....	37
3.2	NICOLETTI ASSAY .....	39
3.3	BAX ACTIVATION.....	40
4	MTT VIABILITY ASSAY .....	40
5	COLONY FORMATION ASSAY.....	41
6	<i>IN VITRO</i> METASTASIS ASSAYS .....	42
6.1	CELL PROLIFERATION.....	42

---

6.2	CELL MIGRATION ASSAY / WOUND HEALING ASSAY .....	42
6.3	CELL INVASION ASSAY.....	43
6.4	ADHESION ASSAY .....	44
6.5	INDUCTION OF ANOIKIS.....	45
7	MICROSCOPY .....	45
7.1	LIGHT MICROSCOPY .....	45
7.2	FLUORESCENCE MICROSCOPY .....	46
7.3	CONFOCAL LASER SCANNING MICROSCOPY.....	46
8	WESTERN BLOT.....	48
8.1	SAMPLE PREPARATION .....	48
8.1.1	WHOLE CELL LYSATES.....	48
8.1.2	CYTOSOLIC AND MITOCHONDRIA CONTAINING FRACTIONS .....	49
8.1.3	NUCLEI ISOLATION .....	50
8.1.4	TUBULIN FRACTIONATION.....	50
8.2	PROTEIN QUANTIFICATION .....	51
8.3	SDS-PAGE.....	51
8.4	WESTERN BLOTTING AND DETECTION .....	53
8.5	MEMBRANE STRIPPING .....	56
8.6	STAINING OF GELS AND MEMBRANES .....	56
9	IMMUNOPRECIPITATION .....	57
10	GENE SILENCING BY RNA INTERFERENCE .....	59
11	STATISTICS.....	60
<b>III</b>	<b>RESULTS.....</b>	<b>63</b>
1	CYTOTOXICITY OF SPONGISTATIN 1.....	63
1.1	APOPTOSIS INDUCTION BY SPONGISTATIN 1 .....	63
1.1.1	CHARACTERISTIC APOPTOTIC FEATURES CAUSED BY SPONGISTATIN 1 63	
1.1.2	SPONGISTATIN 1 INHIBITS METABOLIC ACTIVITY.....	64
1.1.3	DNA FRAGMENTATION IN DIFFERENT CANCER CELL LINES.....	65
1.1.4	SPONGISTATIN 1 INDUCES CELL CYCLE ARREST AT G2/M PHASE.....	66
1.2	SPONGISTATIN 1 STRONGLY INHIBITS CLONOGENIC SURVIVAL OF TUMOR CELLS.....	68
2	ANTIMETASTATIC PROPERTIES OF SPONGISTATIN 1 <i>IN VITRO</i> .....	72
2.1	SPONGISTATIN 1 REVEALS ANTIPROLIFERATIVE PROPERTIES .....	73
2.2	SPONGISTATIN 1 INHIBITS TUMOR CELL MIGRATION.....	74
2.3	EFFECTS OF SPONGISTATIN 1 ON TUMOR CELL INVASION .....	75
2.4	SPONGISTATIN 1 INHIBITS THE ADHESION OF CANCER CELLS.....	75
2.5	FAK IS DEPHOSPHORYLATED BY SPONGISTATIN 1 .....	76
2.6	SPONGISTATIN 1 INDUCES APOPTOSIS IN ANOIKIS - RESISTANT CELLS.....	77

2.7	INVOLVEMENT OF BCL-2 AND BCL-X <sub>L</sub> IN METASTASIS .....	79
3	SIGNAL TRANSDUCTION PATHWAYS IN SPONGISTATIN 1-INDUCED APOPTOSIS.....	80
3.1	RELEASE OF PROAPOPTOTIC PROTEINS FROM MITOCHONDRIA .....	81
3.2	MINOR ROLE OF CASPASES IN SPONGISTATIN 1-INDUCED APOPTOSIS..	83
3.3	SPONGISTATIN 1-INDUCED APOPTOSIS INVOLVES AIF AND ENDO G, BUT NOT OMI/HTRA2 .....	86
3.4	BID IS NOT ENGAGED IN SPONGISTATIN 1-MEDIATED CELL DEATH.....	90
3.5	MAJOR ROLE OF BIM IN SPONGISTATIN 1-INDUCED APOPTOSIS .....	92
3.5.1	SPONGISTATIN 1 FREES BIM FROM ITS SEQUESTRATION BY MICROTUBULES .....	92
3.5.2	SPONGISTATIN 1 DISRUPTS THE MCL-1/BIM COMPLEX .....	93
3.5.3	BIM KNOCKDOWN PREVENTS CELL DEATH BY SPONGISTATIN 1.....	95
3.5.4	BIM FUNCTIONS AS A PROAPOPTOTIC FACTOR UPSTREAM OF MITOCHONDRIA.....	96
<b>IV</b>	<b>DISCUSSION.....</b>	<b>101</b>
1	SPONGISTATIN 1, A POTENT ANTICANCER AGENT.....	101
2	ANTIMETASTATIC EFFECTS OF SPONGISTATIN 1.....	102
2.1	SPONGISTATIN 1 INFLUENCES CRITICAL STEPS IN THE METASTATIC PROCESS.....	102
2.2	APOPTOSIS AND METASTASIS .....	104
2.3	CONCLUSION AND FURTHER DIRECTIONS .....	105
3	APOPTOTIC SIGNALING PATHWAYS .....	106
3.1	INVOLVEMENT OF THE INTRINSIC APOPTOTIC PATHWAY .....	106
3.2	CASPASE-INDEPENDENT MECHANISMS.....	107
3.3	INVOLVEMENT OF BIM .....	109
3.4	CONCLUSION.....	111
<b>V</b>	<b>SUMMARY .....</b>	<b>116</b>
<b>VI</b>	<b>REFERENCES.....</b>	<b>119</b>
<b>VII</b>	<b>APPENDIX.....</b>	<b>131</b>
1	ABBREVIATIONS.....	131
2	ALPHABETICAL LIST OF COMPANIES .....	135
3	PUBLICATIONS.....	138
3.1	POSTER PRESENTATIONS.....	138
3.2	ORIGINAL PUBLICATIONS.....	138
3.3	BOOK CONTRIBUTIONS .....	138
4	CURRICULUM VITAE.....	139
5	ACKNOWLEDGEMENTS .....	140

**INDEX OF FIGURES**

Figure I.1: Polymerization of microtubules (modified from [13]).....	4
Figure I.2: Marine sponges. ....	6
Figure I.3: Chemical structure of the spongistatins.....	7
Figure I.4: Overview of apoptotic and necrotic cell death.....	9
Figure I.5: Classification of caspases based on their prodomain structure.....	12
Figure I.6: Schematic representation of the proteolytic caspase activation. ....	13
Figure I.7: Schematic diagram of the structure of mammalian IAP family members. ....	15
Figure I.8: The extrinsic apoptotic pathway. ....	17
Figure I.9: The intrinsic apoptotic pathway.....	20
Figure I.10 Subfamilies of Bcl-2 related proteins. ....	22
Figure I.11: Modes of post-translational regulation of BH3-only proteins. ....	24
Figure I.12: Differing binding profiles and apoptotic potency of BH3-only proteins. ....	24
Figure I.13: Direct and indirect activation models for Bax and Bak. ....	25
Figure I.14: The metastatic cascade (adapted from [101]).....	26
Figure I.15: Focal adhesion kinase structural features. ....	28
Figure I.16: Integrin signaling pathway.....	28
Figure I.17: Resistance of anoikis is a crucial feature of metastatic cells. ....	29
Figure II.1: Hydrodynamic focusing in the flow chamber. ....	37
Figure II.2: Optical bench diagram of a flow cytometer (adapted from [114]). ....	38
Figure II.3: Histogram of untreated and treated PI-stained cells.....	39
Figure II.4: Reduction of MTT to the blue formazan. ....	41
Figure II.5: Quantitative evaluation of S.CO LifeSciences.....	43
Figure II.6: Schematic diagram of the chemoinvasion assay. ....	44
Figure II.7: Chemical structure of Hoechst 33342.....	46
Figure II.8: LSM 510 Meta beam path (adapted from [119]). ....	47
Figure II.9: HRP-luminol reaction.....	55
Figure II.10: Short interfering RNA. ....	59
Figure III.1: Morphological alterations in spongistatin 1-treated MCF-7 cells. ....	64
Figure III.2: Spongistatin 1 induces dose- and time-dependent cell death in MCF-7.....	64
Figure III.3: Spongistatin 1 induces dose- and time-dependent DNA fragmentation. ....	66
Figure III.4: Spongistatin 1 induces cell cycle arrest in L3.6pl cells. ....	67
Figure III.5: Spongistatin 1 shows long term effects on the clonal tumor cell growth. ....	72
Figure III.6: Spongistatin 1 significantly inhibits tumor cell proliferation after 72 h.....	73
Figure III.7: Spongistatin 1 reduces tumor cell migration. ....	74
Figure III.8: Effect of spongistatin 1 on tumor cell invasion. ....	75
Figure III.9: Spongistatin 1 inhibits adhesion of L3.6pl cells.....	76
Figure III.10: Spongistatin 1 dephosphorylates FAK at Tyr397. ....	77

---

Figure III.11: Spongistatin 1 induces apoptosis in anoikis-resistant tumor cells.....	78
Figure III.12: Inactivation of antiapoptotic Bcl-2 family proteins. ....	78
Figure III.13: Bcl-2 and Bcl-x <sub>L</sub> knockdown sensitizes L3.6pl cells to anoikis.....	79
Figure III.14: Involvement of Bcl-2 and Bcl-x <sub>L</sub> in cell migration. ....	80
Figure III.15: Spongistatin 1 induces the intrinsic apoptotic pathway by activation of Bax and inactivation of Bcl-2 and Bcl-x <sub>L</sub> . ....	82
Figure III.16: Spongistatin 1 induces the release of proapoptotic proteins from mitochondria. ....	83
Figure III.17: Marginal participation of the caspases in spongistatin 1-induced cell death. .....	84
Figure III.18: Spongistatin 1 induces cell death mainly independent of caspases in several cancer cell lines. ....	85
Figure III.19: The pan-caspase-inhibitors zVAD.fmk and Q-VD-OPh exhibit equal effects in MCF-7 cells.....	86
Figure III.20: Spongistatin 1 induces the translocation of AIF and EndoG to the nucleus..	88
Figure III.21: AIF and EndoG, but not Omi /HtrA2, assume a functional role in spongistatin 1-induced apoptosis. ....	90
Figure III.22: Bid is not cleaved to its active form tBid upon spongistatin 1 treatment. ....	91
Figure III.23: Bid is not involved in spongistatin 1-induced cell death. ....	91
Figure III.24: Spongistatin 1 depolymerizes tubulin, thereby releasing Bim from its sequestration at microtubules. ....	93
Figure III.25: Bim is constitutively associated with Bcl-2, Bcl-x <sub>L</sub> and Bax. ....	93
Figure III.26: Spongistatin 1 disrupts the Mcl-1 / Bim complex. ....	94
Figure III.27: Bim and Mcl-1 are not degraded upon spongistatin 1-treatment. ....	95
Figure III.28: Bim siRNA inhibits spongistatin 1-induced cell death.....	95
Figure III.29: Bim functions as a proapoptotic regulator upstream of mitochondria.....	96
Figure III.30: Bim is involved in the caspase-independent apoptotic pathway.....	97
Figure III.31: Bim and EndoG are the major regulators of spongistatin 1-induced cell death.....	98
Figure IV.1: Proposed mechanism of spongistatin 1-induced apoptosis. ....	112

---

**INDEX OF TABLES**

Table I.1: Representative anticancer drugs from natural origin in development or clinical use .....	1
Table I.2: Marine-derived anticancer drugs [9, 10].....	3
Table I.3: Antimitotic drugs, their binding sites on tubulin and their stages in clinical development [13].....	5
Table I.4: Results of comparative antitumor evaluations of spongistatins 1-3 in the NCI <i>in vitro</i> primary screen [16].....	6
Table I.5: Results of comparative antitumor evaluations of spongistatins 1, 4 and 5 in the NCI <i>in vitro</i> primary screen [17].....	6
Table I.6: Characteristics of different types of cell death. ....	10
Table II.1: Summary of used cancer cell lines.....	35
Table II.2: Freezing medium. ....	36
Table II.3 PAA-concentration in the separating gel. ....	52
Table II.4: Primary antibodies.....	54
Table II.5: Secondary antibodies.....	55
Table III.1: Orthotopic pancreatic tumor model. ....	73



# INTRODUCTION

## I INTRODUCTION

### 1 NATURAL PRODUCTS IN CANCER THERAPY

Cancer is one of the biggest causes of death in developed countries despite the global efforts and the major advances achieved in the last decades. Currently, there are three principal ways of treating cancer: surgery, radiotherapy and chemotherapy. Surgery and/or radiotherapy are frequently used as first line therapy in treating primary cancers. However, more effective anticancer therapies are required for most patients to achieve a complete eradication of the disease. Chemotherapeutical drugs alone or in combination with other additional treatments as anti-angiogenic and immune therapies are needed to combat disseminated cancer that cannot be cured solely by surgical excision.

Natural products have played a major role in the treatment of diseases since ancient times. For instance, the plant *Catharanthus roseus* was used as a hypoglycaemic agent in many parts of Asia, but it was not until 1958 that the main constituents vincristine and vinblastine were found to reveal cytotoxic properties [1]. These agents were first introduced in the late 1960s and have contributed significantly to the successful treatment of many cancers. Nature is an attractive source of new therapeutic candidate compounds because of the tremendous chemical diversity in millions of species of plants, animals, marine organisms and microorganisms [2, 3]. For the past three decades natural products have been the mainstay of cancer chemotherapy. The importance of natural products in the tumor therapy can be realized by the fact that over 60% of the drugs approved for treatment of cancer are either of natural origin or their derivatives [4].

**Table I.1: Representative anticancer drugs from natural origin in development or clinical use**

Drug	Source	Status in clinical trial
<b>Plant-derived anticancer drugs</b>		
Etoposide	<i>Podophyllum peltatum</i>	Phase III/IV
Vinblastine, Vincristine	<i>Catharanthus roseus (Vinca rosea)</i>	Phase III/IV
Paclitaxel	<i>Taxus brevifolia</i>	Phase III/IV
Docetaxel	<i>Taxus baccata</i>	Phase III/IV
Topotecan, Irinotecan	<i>Camptotheca accuminata</i>	Phase I/II
Combretastatin A-4	<i>Combretum caffrum</i>	Phase I/II
<b>Microbe-derived anticancer drugs</b>		
Bleomycin	<i>Streptomyces verticillus</i>	Phase III/IV
Daunomycin, Doxorubicin	<i>Streptomyces sp.</i>	Phase III/IV
Epothilones A-D	<i>Sorangium cellulosum</i>	Phase III/IV

The National Cancer Institute (NCI) started in 1960 with a large-scale screening program for natural antitumor agents primary effective against leukemia. The most significant drug to emerge from this program was taxol, obtained from the bark of the pacific yew *Taxus brevifolia*. In 1985, the NCI introduced a new program in which extracts from plants,

animals and microorganisms are screened against a panel of 60 human tumor cell lines derived from different solid human cancer types (colon, brain, breast, kidney, ovary, prostate). Examples of very promising antineoplastic agents and their status in clinical trials are listed in Table I.1.

## 1.1 MARINE-DERIVED ANTICANCER AGENTS

A wide range of chemotherapeutic agents used in cancer therapy induce death in the malignant cells through apoptosis (described in I.5) or other forms of programmed cell death (described in I.4). Inability of tumor cells to undergo apoptosis is one of the fundamental hallmarks of cancer and also the major contributor to drug resistance developed by many tumor cells [5]. Hence, the identification of potent drugs promoting unusual apoptotic mechanisms is a valuable strategy to overcome chemoresistance [6].

In this respect, the chemical and biological diversity of the marine environment is a productive source for the discovery of new anticancer drugs. Most sessile marine invertebrates contain a primitive immune system and produce toxic chemicals as a form of defense. Many of these products regulate specific biological functions and exert pharmacologic activity due to their specific interactions with cellular structures, receptors and enzymes [7]. Because these substances become immediately diluted by large volumes of seawater, they need to be highly potent on a molecular basis. The majority of the marine natural products has been isolated from sponges, molluscs, bryozoans, tunicates and marine microorganisms including fungi, bacteria and cyanobacteria. The relationship between marine sponges and medicines goes back to Alexandrian physicians as first described by the Roman historian Plinius in the first century [8]. However, the development of marine compounds as therapeutic agents is still in its infancy due to the technical difficulties in collecting marine organisms. Pharmaceutical interest in marine sponges evolved in the early 1950s through the discovery of the nucleosides spongothymidine and spongouridine in the marine sponge *Cryptothecia crypta* [8]. These nucleotides were the basis for the synthesis of Ara-C, the first marine-derived anticancer agent, which is currently used in the treatment of leukemia and lymphoma. The systematic investigation of the marine environment is reflected in the discovery of approximately 16,000 novel marine-derived products till date [4]. So far, no drug from marine sources, whether isolated or by total synthesis, has made it to the commercial sector in any disease. However, some of the most promising antitumor compounds currently in various phases of human clinical trials for treatment of different cancer types (Table I.2) were isolated from marine invertebrates or their associated microbes, and it may be expected that this number will increase in future.

**Table I.2: Marine-derived anticancer drugs [9, 10].**

Compound	Source	Chemical class	Molecular target	Status in clinical trial
Ascididemin	<i>Didemnum sp.</i>	aromatic alkaloid	caspase-2, mitochondria	preclinical
Bryostatin 1	<i>Bugula neritina</i>	macrocyclic lactone	PKC	Phase II
Discodermolide	<i>Discodermia dissolute</i>	lactone	tubulin	Phase II
Dolastatin 10	<i>Dolabella auricularia</i>	linear peptide	tubulin	Phase I/II
Dolastatin 15	<i>Dolabella auricularia</i>	linear peptide	tubulin	preclinical
Ecteinascidin 743	<i>Ecteinascidia turbinata</i>	tetrahydroisoquinolone alkaloid	tubulin	Phase II
Eleutherobin	<i>Eleutherobia sp. / Erythropodium caribaeorum</i>	diterpene glycoside	tubulin	preclinical
Halichondrin B	<i>Halichondria okadai</i>	macrocyclic polyether	tubulin	preclinical
Kahalalide F	<i>Elysia refuscens / Bryopsis sp.</i>	cyclic depsipeptide	lysosomes	Phase II
Sarcodictyin	<i>Sarcodictyon roseum</i>	diterpene	tubulin	preclinical

## 1.2 MICROTUBULES AS TARGET IN CANCER THERAPY

Microtubules, the key components of the cytoskeleton, are filamentous, hollow cylindrical structures that are essential in all eukaryotic cells. Their dynamic instability is a crucial and indispensable property in the regulation of the development and maintenance of cell shape, in the transport of vesicles and organelles throughout the cell, in cell signaling as well as cell division and mitosis. Microtubules are composed of globular  $\alpha$ -tubulin and  $\beta$ -tubulin that are tightly bound together by noncovalent bonds. Tubulin subunits have a binding site for GTP and assemble head-to-tail to each other mediated by GTP/GDP exchange, following the same direction and leading to a distinct structural polarity (Figure I.1). Microtubules are highly dynamic polymers and their polymerization dynamics are thoroughly regulated, e.g. through binding of various regulatory proteins including dynein and kinesin motor proteins to soluble tubulin and to microtubule surfaces [11, 12].

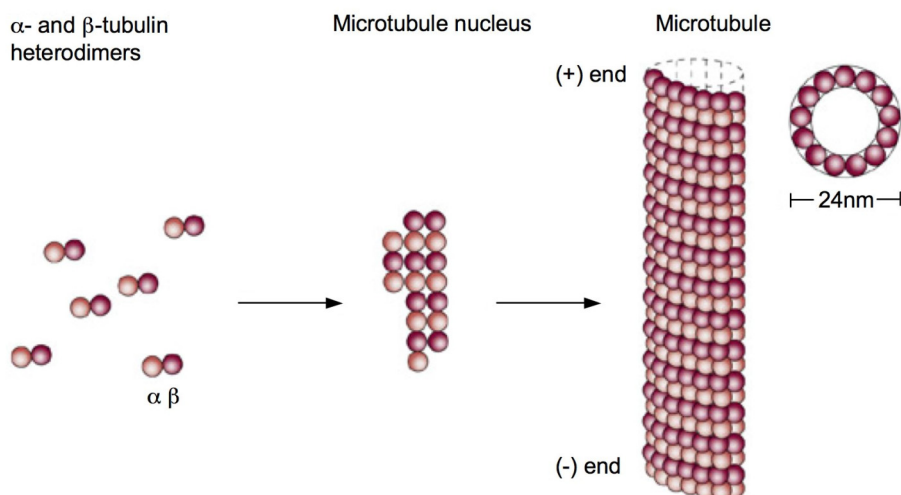


**Figure I.1: Polymerization of microtubules (modified from [13]).**

Heterodimers of  $\alpha$ - and  $\beta$ -tubulin assemble to form a short microtubule nucleus. Nucleation is followed by elongation of the microtubule at both ends building a cylinder that is composed of tubulin heterodimers arranged head-to-tail in 13 protofilaments.

The crucial role of microtubules in vital functions including mitosis, motility and cell-cell contacts makes microtubules an important target for cancer chemotherapy [13]. In this context, a chemically diverse group of anticancer drugs targeting microtubules and their dynamics, has been used with great success in the treatment of cancer (Table I.3). Microtubules seem to be targeted in favor by natural products, since most of the microtubule interacting agents are derived from natural origin. All of the antimetabolic drugs studied so far induce apoptosis in a variety of cell types. These compounds act by binding to specific sites on the tubulin dimer and can be classified into three major categories based on their respective tubulin binding domains including the “vinca alkaloid” domain, the “colchicine” domain and the “paclitaxel” domain (Table I.3).

Based on their influence on microtubule dynamics, antimetabolic drugs are divided into two groups: Some of these compounds including *Vinca* alkaloids and colchicine inhibit microtubule polymerization, whereas others (taxanes) stabilize microtubules. But although these compounds exert opposite effects on microtubules, both types share the common property of suppressing microtubule dynamics and thereby microtubule function, leading to the disruption of the mitotic spindle function and blocking cell cycle progression. This failure to proceed through the cell cycle is usually followed by the activation of apoptosis.

**Table I.3: Antimitotic drugs, their binding sites on tubulin and their stages in clinical development [13].**

Drug	Binding domain	Therapeutical use	Status in clinical trial
Vinblastine	<i>Vinca</i> domain	Hodgkin's disease, testicular germ-cell cancer	In clinical use, 22 combination trials in progress
Vincristine	<i>Vinca</i> domain	Leukemia, lymphomas	In clinical use, 108 combination trials in progress
Vinorelbine	<i>Vinca</i> domain	Solid tumors, lymphomas, lung cancer	In clinical use, 29 Phase I-III clinical trials (single and in combination)
Dolastatins	<i>Vinca</i> domain	Potential vascular targeting agents	Phase I/II
Colchicine	Colchicine domain	Non-neoplastic diseases	Failed trials because of toxicity
Combretastatins	Colchicine domain	Potential vascular targeting agents	Phase I/II
Paclitaxel (Taxol)	Taxane site	Ovarian, breast and lung tumors, Kaposi's sarcoma; trials with numerous other tumors	In clinical use; 207 Phase I-III trials in USA
Docetaxel (Taxotere)	Taxane site	Prostate, brain and lung tumors	8 Phase I-III trials in USA
Epothilones	Taxane site	Paclitaxel-resistant tumors	Phase I-III

## 2 THE SPONGISTATINS

The spongistatins, a family of macrocyclic lactone polyethers, are promising anticancer compounds isolated from marine sponges. Up to now, seven members of this family have been discovered by Prof. G. R. Pettit [14] in the Eastern Indian Ocean *Hyrtios erecta* (spongistatins 1-3) [15, 16] and in the African marine sponge *Spirastrella spinispirulifera* (spongistatins 4-7) [17, 18] (Figure I.2). In 1988 his group collected 400 kg (wet wt) of the dark brown to black *Spongia* sp. (family Spongiidea, class Demospongiae) from the Eastern Indian Ocean, Republic of Maldives, and made an extraction with methanol followed by dichlormethane-methanol. The obtained fraction was separated by LH-20 Sephadex gel permeation and high-performance liquid chromatography to receive colorless spongistatin 1 as an amorphous powder (mp 161-162°C).



**Figure I.2: Marine sponges.**

Left panel: Eastern Indian Ocean *Hyrtios erecta* (Spongia) [19]

Right panel: African *Spirastrella spinispirulifera* (Prolifera) [20]

All of the spongistatins have exceptionally potent and selective inhibitory activity against a subset of the U.S. National Cancer Institute's (NCI) panel of 60 human cancer cell lines [21] (Table I.4, Table I.5), suggesting that they may employ novel mechanisms of action different from any other anticancer agent. Spongistatin 1, first introduced as a broad-spectrum antifungal compound [22], represents the most extraordinarily potent substance ( $GI_{50}$  typically  $2.5-3.5 \times 10^{-11}$  M) presently known against a variety of highly chemoresistant tumor types tested in the NCI screen. Thus, spongistatin 1 may have bright prospects in getting a potent anticancer agent in the future.

**Table I.4: Results of comparative antitumor evaluations of spongistatins 1-3 in the NCI *in vitro* primary screen [16].**

Spongistatin	Mean panel $GI_{50}/10^{-10}$ mol l <sup>-1</sup>	Compare correlation coefficient
1	1.48	1.00
2	8.51	0.83
3	8.32	0.90

All compounds were tested in quadruplicate at each of three different concentration ranges ( $10^{-7}$ ,  $10^{-8}$ ,  $10^{-9}$  mol l<sup>-1</sup> upper limits, log<sub>10</sub> dilutions x 5) against the entire panel of 60 human tumor cell lines comprising the NCI screen.

**Table I.5: Results of comparative antitumor evaluations of spongistatins 1, 4 and 5 in the NCI *in vitro* primary screen [17].**

Spongistatin	Mean panel $GI_{50} \times 10^{-10}$ mol dm <sup>-3</sup>	Compare correlation coefficient
1	1.17	1.00
4	1.02	0.93
5	1.23	0.92

All compounds were tested in quadruplicate at each of five different concentration ranges ( $10^{-8}$ ,  $10^{-9}$ ,  $10^{-10}$ ,  $10^{-11}$ ,  $10^{-12}$  mol dm<sup>-3</sup>) against the entire panel of 60 human tumor cell lines comprising the NCI screen.

The macrocyclic lactone polyether spongistatin 1 contains 23 chiral centers and two spiroketal pyran groups. Even though spongistatins are structurally complex (Figure I.3), the total synthesis of spongistatin 1 has been recently accomplished [23].

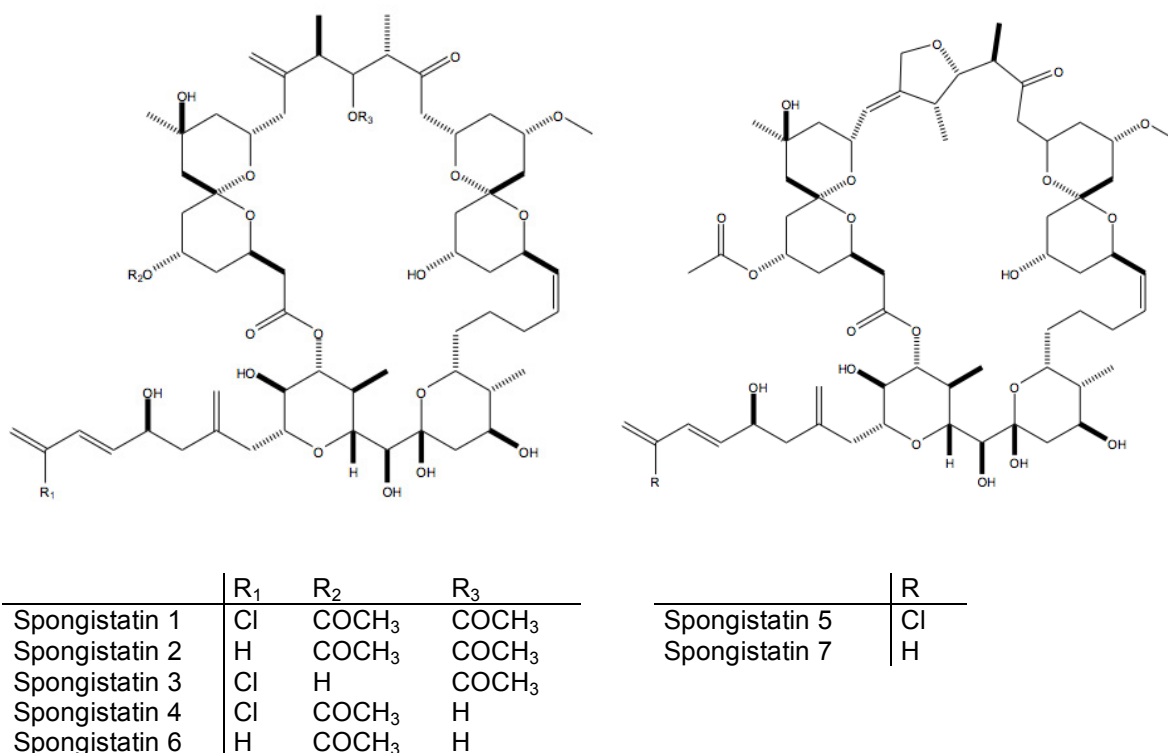


**Figure I.3: Chemical structure of the spongistatins.**

Bai et al. revealed spongistatin 1 as a potent mitosis inhibiting and tubulin depolymerizing natural product [24]. Spongistatin 1 was shown to inhibit microtubule assembly, the binding of vinblastine and GTP to tubulin as well as the displacement of GDP bound in the exchangeable binding site of tubulin [25, 26]. The proposed binding pocket for spongistatin 1 is in close proximity to the GDP exchange site on the  $\beta$ -subunit of the tubulin heterodimer. Studies of structure-activity relationships indicated that the two spiroketal groups serve as critical binding components of spongistatin 1. The binding of spongistatin 1 to this pocket may hinder interdimer interactions of tubulin and contribute to the tubulin depolymerizing activity of spongistatin 1.

Despite the knowledge of spongistatin 1 as a tubulin-depolymerizing agent and its exceeding anticancer activity observed in the NCI screen, the underlying mechanisms leading to spongistatin 1-induced cytotoxicity remain to be explored.

### 3 AIM OF THE STUDY

The main problems in chemotherapy are the often developed resistance of tumor cells to anticancer drugs as well as the metastatic spread of tumor cells in distant organs. For this reason, chemotherapeutic agents in clinical trials often show limited success, emphasizing the need for the development of new and effective chemotherapeutic agents that can target the metastatic process as well as multiple signaling pathways to resensitize cancer cells to chemotherapy. Although spongistatin 1 proved to be an extremely potent agent against a subset of human tumor cell lines including highly chemoresistant tumor types in the screening program of the National Cancer Institute (NCI), up to now less work has been done to elucidate the effects of spongistatin 1 on the combat of cancer. Recently, spongistatin 1 was shown to have an apoptosis-inducing effect in A549 cells by activating caspase-3 and by the cleavage of vimentin [27]. Moreover, our working group characterized spongistatin 1 as a novel promising therapeutic agent for the treatment of leukemic tumor cells especially in the clinical highly relevant situation of chemoresistance due to overexpression of XIAP [28].

These impressive results in leukemic cells encourage to elucidate the activity and underlying cytotoxic mechanisms of spongistatin 1 in metastatic cancer cells and chemoresistant solid tumors. For this purpose, two different models were pursued:

First, the impact of spongistatin 1 on the basic processes during the metastatic spread were monitored *in vitro* using the highly invasive pancreatic cancer cell line L3.6pl, thereby focusing on the involvement of antiapoptotic events during the metastatic cascade.

Secondly, the apoptotic signaling pathway induced by spongistatin 1 was clarified in the human breast cancer cell line MCF-7 in respect to overcome chemoresistance, heading at identifying exceptional or unusual signaling.

### 4 PROGRAMMED CELL DEATH

The balance between cell division and cell death is essential for the development and maintenance of tissue homeostasis of multicellular organisms. Deregulation of either process has a variety of pathological consequences leading to disturbed embryogenesis, neurodegenerative diseases, autoimmunity and the development of cancer. Thus, the equilibrium between life and death is tightly controlled [29-31]. Dispensable or potentially dangerous cells are forced to die by a process called programmed cell death (PCD) and are removed by phagocytosis to prevent a host immune response. PCD can be defined as a coordinated sequence of events based on cellular metabolism that occurs at specific points of development and leads to cell destruction [32]. The most common and best

characterized form of PCD is apoptosis, a term first introduced in 1972 by Kerr et al. [33, 34] to describe a form of cell death in mammals distinctive to necrosis. The word apoptosis derives from the Greek denoting a “falling off”, as leaves from a tree [35]. Apoptosis is characterized by the activation of a specific family of cysteine proteases, called caspases, followed by typical caspase-mediated biochemical and morphological changes including cell shrinkage with cytoskeletal rearrangements, mitochondrial outer membrane permeabilization, nuclear condensation and cleavage of the chromatin by endonucleases, remodeling and blebbing of the plasma membrane. The morphological alterations are a consequence of highly conserved, genetically controlled molecular and biochemical events and culminate in the fragmentation of the cell into so called “apoptotic bodies”. These compact membrane-enclosed structures contain cytosol and cell organelles, that are engulfed by macrophages without inciting the inflammation [36, 37]. A hallmark of apoptosis is the exposure of phosphatidylserine on the cell surface, which mediates their recognition and phagocytosis by macrophages [38].

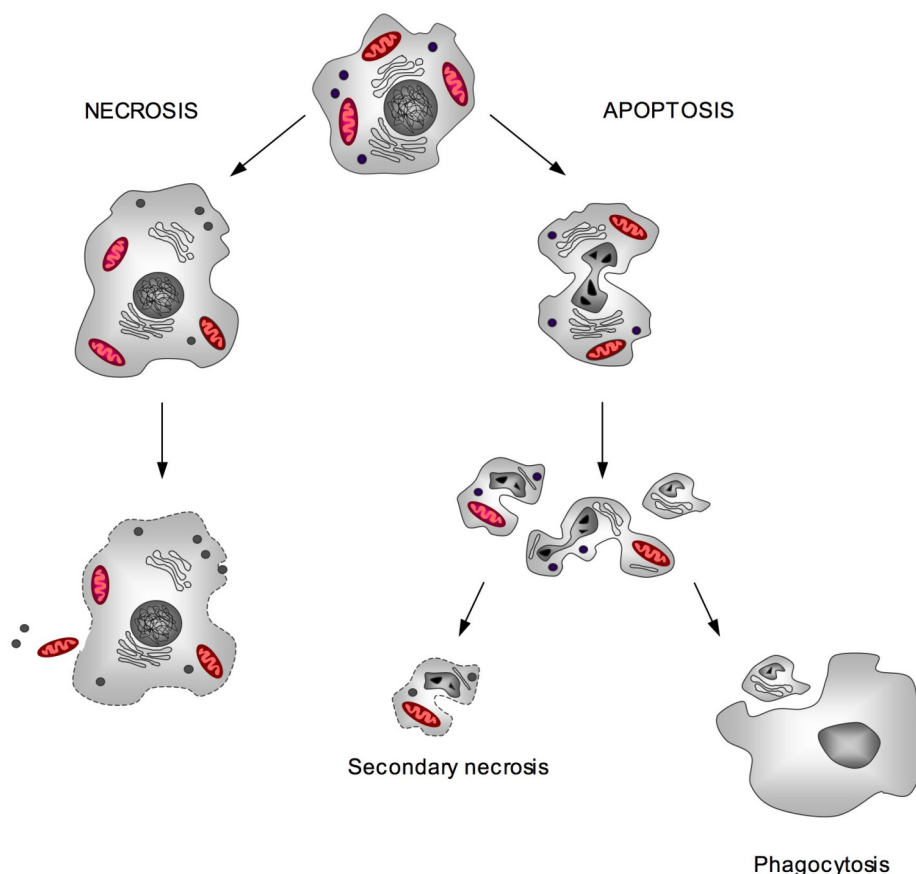


**Figure I.4: Overview of apoptotic and necrotic cell death.**

Apoptosis is characterized by morphological changes of the cell like cell shrinkage, chromatin condensation and fragmentation of the cell in membrane enclosed apoptotic bodies. These are engulfed by macrophages (phagocytosis), thus preventing inflammation. In contrast, in necrosis the cell swells and the membrane ruptures, releasing the cellular content into the surrounding tissue and thereby inducing inflammation.

Whereas apoptosis is an inherent, controlled cellular death program, the conceptual counterpart, necrosis, is an uncontrolled, passive mode of cell death that occurs after exposure to high concentrations of detergents, ionophores, oxidants or as consequence of pathophysiological conditions, such as hyperthermia, hypoxia, ischemia or infection [35, 39]. As shown in Figure I.4, there are many observable morphological and biochemical differences between necrosis and apoptosis. Necrotic cell death is characterized by cellular swelling and rupture of the plasma membrane. Due to the ultimate breakdown of the plasma membrane, potentially inflammatory cellular contents are released into the extracellular fluid provoking a substantial inflammatory response [40]. Typical features of apoptotic cell death like DNA fragmentation, membrane blebbing (zeiosis) and formation of apoptotic bodies are absent in necrosis.

In recent years, it has become evident that the classic dichotomy of apoptosis versus necrosis is a simplification of highly complex processes. Although caspase-mediated apoptosis is the most common cell death program, the process of caspase activation is not the only determinant of life and death in PCD [41]. Indeed, various forms of alternative cell death pathways, even in the complete absence of caspases, have been described, sharing the common feature that they are executed by active cellular processes. This distinguishes them from accidental necrosis [37, 41, 42]. Despite the numerous models proposed to characterize the various modes of PCD, exclusive definitions do not exist due to the overlap and shared signaling pathways between the different death programs. Table I.6 [43] gives an overview of the classification of different modes of PCD according to morphological changes and biochemical features of the dying cell.

**Table I.6: Characteristics of different types of cell death.**

Type of cell death	Morphological changes			Biochemical features
	Nucleus	Cell membrane	Cytoplasm	
Apoptosis	chromatin condensation, nuclear fragmentation, DNA laddering	blebbing	fragmentation, formation of apoptotic bodies, preservation of organelles	caspase-dependent
Necrosis	clumping and random degradation of nuclear DNA	swelling, rupture	increased vacuolation, organelle degradation, mitochondrial swelling	no energy requirement
Autophagy	partial chromatin condensation, no DNA laddering	blebbing	increased number of autophagic vesicles, organelle degradation	caspase-independent, increased lysosomal activity
Mitotic catastrophe	multiple micronuclei, nuclear fragmentation	no consensus on the distinctive morphological appearance by now		caspase-independent (at early stage)

## 5 APOPTOSIS SIGNALING PATHWAYS

Apoptosis is an evolutionary conserved and tightly regulated cell death program that can be triggered by several stimuli, including intracellular stress and receptor-mediated signaling. In the classical apoptotic signaling pathway, the activation of the caspase-family of cysteine-proteases builds the core of the mechanisms leading to cell death.

### 5.1 CASPASES

Caspases (cysteine aspartate specific proteases) are an evolutionarily ancient class of intracellular proteases and common to multicellular organisms that irreversibly commit a cell to die. Although the first caspase, interleukin-1 $\beta$ -converting enzyme (ICE, caspase-1), was identified in humans, the critical involvement of caspases in the apoptotic process was discovered in the nematode worm *Caenorhabditis elegans*, first documented in 1993 by Yuan et al. [44]. In this model organism, apoptosis was determined by three genes including an inhibitor (*ced-9*), an activator (*ced-4*) and an executor (*ced-3*). The identification of the *ced-3* (cell death abnormality-3) gene, encoding a cysteine protease that is closely related to the mammalian ICE, led to the discovery of the whole family of proteases. Since then, at least 14 distinct mammalian caspases have been identified, of which there are 11 of human origin and 3 of murine origin [45]. Some of them are implicated in apoptosis (caspases-2, -3, -6, -7, -8, -9, -10 and -12), while others are involved in activation of proinflammatory cytokines (caspase-1, -4, -5, -13) or in keratinocyte differentiation (caspase-14). Apart from caspases, other proteases are engaged in the characteristic apoptotic morphology including other cystein proteases such as calpains, cathepsins (lysomal proteases) or serine proteases [46]. They contribute to the acitvation of caspases or mediate caspase-independent cell death and are often mutually activated by caspases in an amplification loop.

#### 5.1.1 GENERAL FEATURES AND CLASSIFICATION OF CASPASES

Caspases are synthesized as a single-chain of inactive zymogens consisting of an N-terminal prodomain of variable length followed by a large subunit with a molecular weight of about 20 kDa (p20), a small subunit of about 10 kDa (p10) and a linker region connecting these catalytic subunits [47]. Based on the structures of the prodomains and their functions, caspases are typically divided into three major groups. Caspases with large prodomains (> 90 residues) are classified by their phylogenetic relationship in inflammatory caspases (caspase-1, -4, -5, -13) and initiator caspases (caspase-2, -8, -9, -10 and -12), while caspases with short prodomains (20-30 residues) belong to the effector caspases (caspase-3, -6, -7) [48, 49] (Figure I.5).

**Initiator caspases**

Procaspase-8, -10



Procaspase-1, -2, -4, -5, -9, -12, -13

**Effector caspases**

Procaspase-3, -6, -7, -14

**Figure I.5: Classification of caspases based on their prodomain structure.**

Initiator caspases contain long prodomains, procaspase-8 and -10 carry two repeats of the DED, whereas other initiator caspases possess a CARD domain. Caspases-3, -6 and -7 are apoptotic effector caspases with short prodomains. Prodomains are followed by the large subunit (~20 kDa), a linker region and the small subunit (~10 kDa).

The large prodomains of procaspases comprise structural motifs in the death domain superfamily including the death domain (DD), the death effector domain (DED) and the caspase recruitment domain (CARD). These structures are essential for the homotypic interaction with other proteins and reveal an important role in apoptotic signaling. DEDs and CARDS are responsible for the recruitment of initiator caspases into death- and inflammation-inducing signaling complexes, resulting in proteolytic autoactivation of caspases that subsequently initiates inflammation and apoptosis [47]. Two tandem DEDs are found in both procaspase-8 and -10, while the procaspases-1, -2, -4, -5, -9, -12 and -13 are characterized by the CARD domain (Figure I.5) [50].

Although caspase zymogens contain a small amount of catalytic activity, they are kept in check by a variety of regulatory molecules. Thus, caspases as inactive enzyme precursors require a conformational change and usually have to be cleaved to become an active enzyme. Mature caspases are heterotetramers formed by an association of two heterodimers derived from two precursor molecules, with each comprising the large (p20) and the small (p10) subunit (Figure I.6) [48, 51]. The tetramer contains two active sites, positioned at opposite ends of the molecule and comprising amino acids of the large and the small subunits.

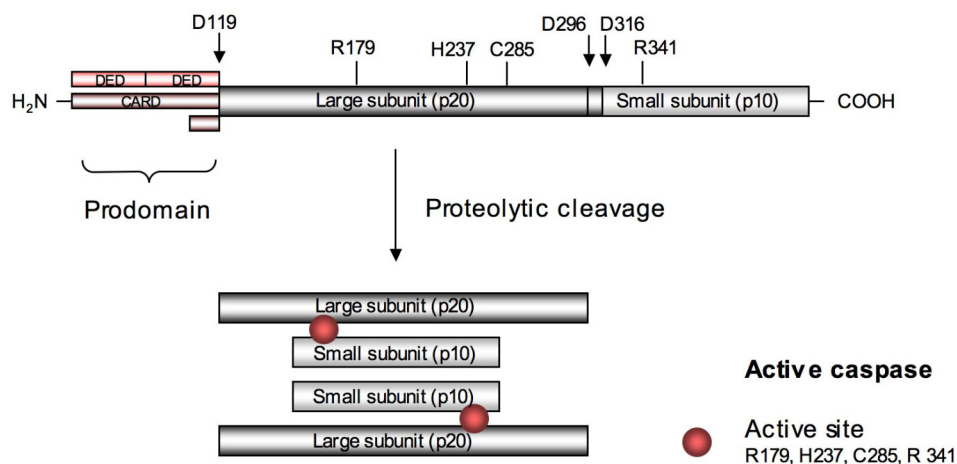


**Figure I.6: Schematic representation of the proteolytic caspase activation.**

Activation proceeds by cleavage of the N-terminal domain at Asp 119, Asp 296 and Asp 316 (all caspase-1 numbering convention) leading to a large (p20) and a small (p10) subunit. The activity and specificity determining residues (R179, H237, C285 and R341) are brought into the necessary structural arrangement for catalysis. C285 is the catalytic nucleophile. The active caspase is a tetramer of two heterodimers, each comprising a large and a small subunit and an active site.

The activation of effector caspases is performed by initiator caspases through removal of the N-terminal prodomain and the linker peptide within the protease domain by internal cleavage at specific Asp residues causing the separation of the large and the small subunits. As a consequence, the active site loops undergo drastic conformational changes resulting in the catalytical activation of the enzyme [51]. The effector caspases are able to directly degrade multiple substrates including the structural and regulatory proteins in the nucleus, cytoplasm and cytoskeleton, leading ultimately to cell death. Initiator caspases, however, undergo autocatalytic intrachain cleavage, a process usually requiring and facilitated by multicomponent complexes, which have modest effect on catalytic activity compared with the effector caspases. Upon recruitment to large protein complexes, initiator caspases are brought into close proximity by virtue of their long DED and CARD domains. The dimerization of inactive monomers is sufficient to trigger the activation and processing of procaspases [52]. Up to now, the involvement of different multicomponent protein complexes is described. For example, the apoptosome is responsible for the activation of caspase-9, whereas the assembly of the death-inducing signaling complex (DISC) is indispensable for the activation of caspase-8. Furthermore, the inflammasome facilitates the activation of proinflammatory caspases and the PIDDosome underlies the activation of caspase-2.

### 5.1.2 SUBSTRATE CLEAVAGE

Caspases are specific cysteine proteases that recognize at least four (caspase-2 five) contiguous amino acids in their substrates, P4-P3-P2-P1. Typically, the cleavage point occurs after the C-terminal residue (P1), which is usually an aspartate. The preferred P3 position is a glutamine residue for all mammalian caspases, whereas the preference in the P4 position varies among different groups of caspases and contributes to their substrate specificity. Thus the general recognition sequence can be described as X-Gln-X-Asp [48, 53]. The use of the Cys side chain as a nucleophile during peptide bond hydrolysis is common to several protease families. However, the primary specificity for Asp is very rare among proteases, of the currently known proteases only the serine protease granzyme B shares this primary specificity [54].

A tremendous variety of proteins in apoptosis signal transduction is cleaved by caspases. Overall, more than 280 caspase substrates are identified so far. The proteolytic cleavage can either induce the functional inhibition or activation of these mediators, turning off cell-protective mechanisms and activating pathways that lead to cell destruction [55]. Proteolysis of certain components by effector caspases is associated with distinct morphological changes of cell death. For example, cleavage of PARP (poly ADP-ribose polymerase) inhibits DNA repair, whereas cleavage of ICAD (inhibitor of caspase-activated DNase) by caspase-3 liberates the active CAD (caspase-activated DNase) nuclease that mediates DNA fragmentation. Caspases destroy several proteins involved in the maintenance of the cytoskeletal structure, such as focal adhesion kinases or paxillin, resulting in cell shrinkage and cell detachment. Initiator caspases are able to activate effector caspases but may target also many other proteins in the cell. In this respect, the most prominent caspase-8 substrate is the BH3-only protein Bid. After proteolytic cleavage, Bid translocates to mitochondria, thus promoting release of cytochrome c. Furthermore, cell-protective proteins as c-FLIP (cellular FADD-like ICE-inhibitory protein), Bcl-2, Bcl-x<sub>L</sub> or Akt can be inactivated by caspases. The conversion of antiapoptotic into proapoptotic regulators constitutes a positive feedback loop in the apoptosis signaling pathway [50, 55].

### 5.1.3 REGULATION OF CASPASES

Because caspases execute a central role in the apoptotic process, inappropriate activation of caspases leads to a fatal outcome. Therefore, their expression and activation states need to be tightly regulated. Caspases are regulated by transcriptional and posttranslational mechanisms. Endogenous caspase inhibitors block either the activation of caspases or the

proteolytic effect of activated caspases. The major regulation checkpoints are found at the level of the activation of initiator caspases.

The conserved family of inhibitors of apoptosis proteins (IAPs) potently inhibits the enzymatic activity of mature caspases and additionally removes caspases through proteasomal degradation. The IAP protein family, originally discovered in the genome of baculovirus on the basis of its apoptosis-suppression potential in infected host cells, comprises at least eight mammalian members (Figure I.7) [53]. Three conserved structural domains are characteristic of IAP proteins: BIR (baculoviral IAP repeat), RING (RING zinc-finger) and CARD (caspase-activating and recruitment domain). The BIR domains, the hallmark of the IAP family, are ~80-amino acid zinc-binding domains responsible for the binding of caspases. XIAP (X-chromosome-linked inhibitor of apoptosis) is the most thoroughly characterized mammalian IAP member and also the most potent inhibitor of cell death *in vitro*, bearing three BIR domains with different functions. BIR3 is involved in inhibition of caspase-9, whereas the linker region between BIR1 and BIR2 selectively targets caspase-3 and -7 [56, 57]. Except for survivin, all IAPs are comprised of a C-terminal RING (really interesting new gene) domain, a E3 ligase that presumably directly targets the IAP to the ubiquitin proteasome degradation system. The third structural motif, the CARD domain, is found in c-IAP1 and c-IAP2 and functions as protein-protein interaction domain which mediates the oligomerization with other CARD-containing proteins [58, 59] (Figure I.7, modified from [53]).

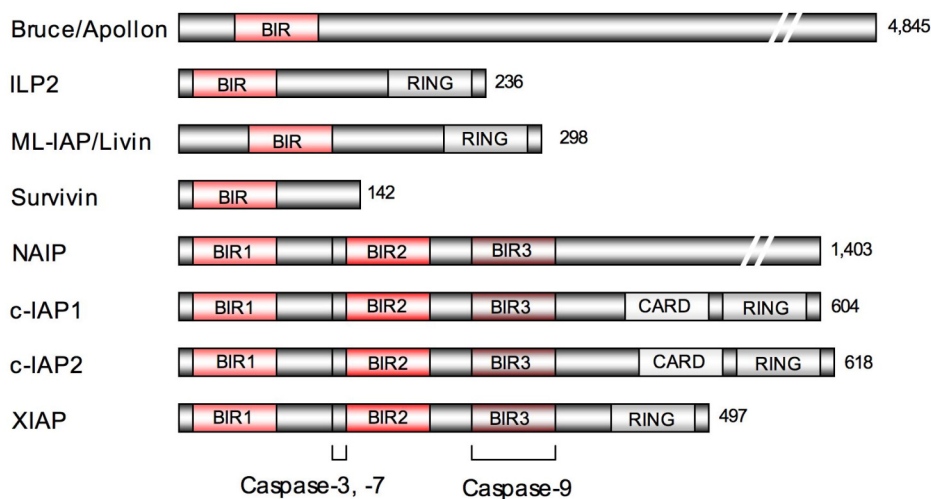


**Figure I.7: Schematic diagram of the structure of mammalian IAP family members.**

The eight members of the IAP family contain at least one BIR domain. Additionally, most IAPs have other distinct functional domains, such as the CARD domain and the RING domain, functioning as a E3 ligase that presumably directly targets to proteasomal degradation. *BIR*, baculoviral IAP-repeat; *c-IAP*, cellular IAP; *IAP*, inhibitor of apoptosis protein; *ILP*, IAP-like protein; *ML-IAP*, melanoma IAP; *NAIP*, neuronal apoptosis-inhibitory protein; *XIAP*, X-chromosome-linked IAP).

The activities of IAPs are antagonized by a group of proteins containing a conserved four-residue IAP-binding motif (IBM) (Ala-Val-Pro-Ile), such as the mitochondrial proteins Smac and Omi/HtrA2 [60, 61].

IAPs are not the only endogenous inhibitors of caspases. In contrast to the IAPs, which effect specifically caspase-3, -7 and -9, the baculoviral protein p35 is a pan-caspase inhibitor targeting most caspases through the formation of an inhibitory complex. Another pan-caspase inhibitor is poxvirus CrmA (cytokine response factor A) protein, a member of the serine protease inhibitor (serpin) family, which inhibits apoptosis via covalent modifications of the caspase active center. Thus, CrmA inhibits not only cysteine but also serine proteases, e.g. granzyme B [48, 62].

## 5.2 EXTRINSIC APOPTOTIC PATHWAY

In mammals, a wide array of external signals triggers two major apoptotic responses, namely the extrinsic pathway (death receptor pathway) or the intrinsic pathway (mitochondrial pathway) within the cell, depending on the origin of death stimuli. The death receptor pathway is activated by apoptotic stimuli comprising extrinsic signals such as the binding of death inducing ligands to cell surface receptors. Death receptors are members of the tumor necrosis factor (TNF) receptor gene superfamily and share similar cysteine-rich extracellular domains. In addition, death receptors are defined by a cytoplasmic domain of about 80 amino acids called the "death domain" (DD), which plays a crucial role in transmitting the death signal from the cell's surface to intracellular signaling pathways [5]. Among them, the death receptors including TNFR1 (TNF receptor-1), CD95 (or APO-1/Fas) and the TRAIL (TNF-related apoptosis-inducing ligand) receptors DR4 (death receptor-4) and DR5 are best characterized for the induction of apoptosis. Decoy receptors, such as the soluble Fas, DcR3, constitute a negative regulatory mechanism of the extrinsic pathway. Due to lack of a functional death domain, these decoy receptors are unable to elicit the activation of the downstream apoptotic signaling pathway. However, they can compete for the binding of death ligands in order to block apoptosis triggered by death receptors [29, 63]. The extrinsic pathway is activated by the ligation of death receptors to their cognate ligands resulting in receptor trimerization, clustering of the death domains and recruitment of adaptor molecules, such as Fas-associated death domain (FADD), through homophilic interaction mediated by the death domain. FADD in turn recruits procaspase-8 (or procaspase-10) by its death effector domain (DED) to the activated CD95 receptor to form the CD95 death-inducing signaling complex (DISC). Within the DISC, procaspase-8 is autocatalytically cleaved by induced proximity and dimerization. Caspase-8 is released from the DISC as an active heterotetramer which is able to activate downstream effector caspases such as caspase-3. According to their requirement for mitochondrial pathway in CD95-induced apoptosis,

two distinct prototypic cell types have been identified. In type I cells, caspase-8 is activated at the DISC in quantities sufficient to directly activate downstream effector caspases. However, in type II cells efficient activation of effector caspases depends on a mitochondrial amplification loop that relies on caspase-8 mediated cleavage of Bid and subsequent release of mitochondrial proapoptotic factors leading to cell death (Figure I.8). The identification of Bid as a caspase-8 substrate established a link between the extrinsic and the intrinsic pathway [29]. The DISC complex formation downstream of other death receptors (DR4/5, TNFR1) is similar to the CD95 pathway.

Signaling by death receptors can be negatively regulated by proteins that associate with their cytoplasmic domains, for example c-FLIP. The two splice variants of c-FLIP have sequence homology to caspase-8 and caspase-10, but lack enzymatic activity. Consequently, the recruitment of c-FLIP to the DISC instead of procaspase-8 or -10 can block caspase activation [63].

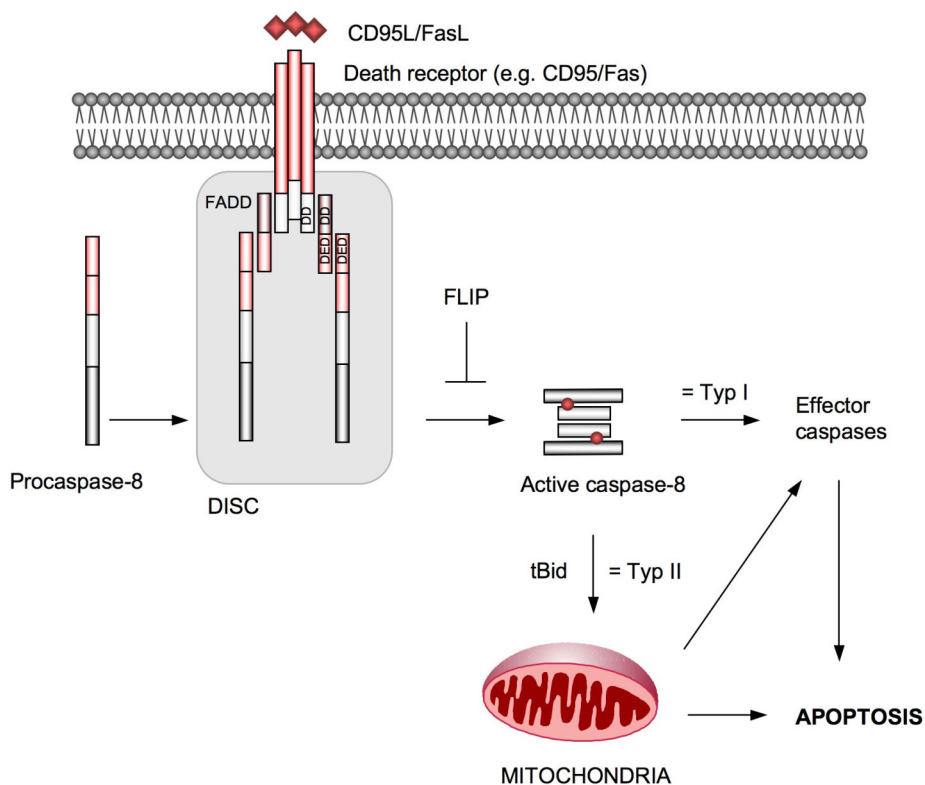


**Figure I.8: The extrinsic apoptotic pathway.**

Binding of death ligands to their receptors leads to receptor trimerization and formation of the death inducing signaling complex (DISC). In the DISC, the initiator caspase-8 is recruited by the adaptor protein FADD via interaction with the death effector domain (DED) and is activated by autocatalytic cleavage. An amplification of the apoptotic signal is possible upon caspase-8 mediated cleavage of Bid which in turn translocates to mitochondria leading to apoptosis. As a negative regulator, FLIP is able to bind to DISC preventing the activation of caspase-8.

### 5.3 INTRINSIC APOPTOTIC PATHWAY

Intrinsic apoptotic pathways are initiated within the cell. The most important turning point in the course of the intrinsic apoptotic process occurs in the mitochondria [64]. Apart from being the main energy producers of the cell, mitochondria are crucial organelles regulating and mediating apoptotic cell death [29, 63]. Numerous cytotoxic stimuli originating from inside the cell including DNA-damage, oxidative stress, actions of some oncoproteins and tumor suppressor genes or signals induced by chemotherapeutic agents can converge on the mitochondria to induce outer membrane permeabilization (MOMP). This permeabilization, mainly mediated and controlled by Bcl-2 family members (described in I.5.3.1), causes the dissipation of the mitochondrial membrane potential ( $\Delta\Psi_m$ ), which is required for mitochondrial function as ion transport or energy conservation. Upon disruption of the outer mitochondrial membrane, a set of proteins that normally resides in the space between the inner and outer mitochondrial membranes is released into the cytosol causing either the activation of caspases or acting as caspase-independent cell death effectors. These apoptogenic proteins include cytochrome c, Smac/DIABLO (second mitochondria-derived activator of caspases/direct IAP binding protein with low pI), Omi/HtrA2 (high temperature requirement protein A2), AIF (apoptosis-inducing factor) and EndoG (endonuclease G) [65].

Cytochrome c, an essential component of electron transport in the ATP-generating respiratory chain, is considered to be among the major steps in the intrinsic death pathway. Once cytochrome c escapes into the cytosol, it is captured by the C-terminal region of Apaf-1 (apoptotic protease activating factor 1), a cytosolic protein with an N-terminal caspase-recruitment domain (CARD). Binding of cytochrome c facilitates the association of ATP/dATP with Apaf-1 exposing the CARD. Further oligomerization results in a wheel-shaped heptameric structure containing seven cytochrome c/Apaf-1 complexes. This large multi-protein complex is termed apoptosome and functions as a platform to recruit and activate procaspase-9 via CARD-CARD interactions, thereby triggering the caspase cascade leading to cell death [66-68].

Other proteins released from mitochondria, such as Smac/DIABLO and Omi/HtrA2, facilitate caspase activation through neutralizing endogenous inhibitors of caspases, the inhibitor of apoptosis proteins (IAPs). Smac and its murine homolog DIABLO are the best known antagonists of IAPs, removing IAP-mediated inhibition of active initiator and effector caspases. Smac acts as a homodimer, exposing the conserved four-residue IAP-binding motif (IBM) (Ala-Val-Pro-Ile) at its N-terminus, which is required to recognize a hydrophobic groove in the BIR2 and BIR3 domain of IAPs. Caspase-9 contains a similar recognition motif (Ala-Thr-Pro-Phe), enabling Smac/DIABLO to compete with caspase-9 for binding to the BIR3 domain of IAPs. The binding site of the IBM sequence of

Smac/DIABLO maps also to the BIR2 motif. Although the IAP fragment responsible for inhibiting caspase-3 and -7 is the linker between BIR1 and BIR2, steric clashes allow competition with caspase-3 and -7 [69].

The mammalian serine protease Omi/HtrA2, a member of the HtrA protein family, possesses an IBM, similar to Smac/DIABLO. Omi/HtrA2 executes an essential role in mitochondrial homeostasis, but the molecular targets and interaction partners in the mitochondrion are as yet undefined. Omi/HtrA2 unleashes caspase activity in a biphasic process that frees the active forms of caspase-3, -7 and -9 by proteolytically removing their natural inhibitors. The IBM, presented in a trimeric configuration, sequesters IAP proteins in a first step. The protease activity of Omi/HtrA2 may then drive the reaction through the degradation of bound IAP proteins [70]. Besides its caspase-dependent cytotoxicity, Omi/HtrA2 also contributes to apoptosis in a caspase-independent way. This function is independent of its IAP-binding activity, but rather depends on the serine protease activity of Omi/HtrA2 [66].

Mitochondria can also release factors involved in caspase-independent cell death including the apoptosis-inducing factor (AIF) [71] and endonuclease G (EndoG) [72, 73]. AIF is a mitochondrial flavoprotein first identified and characterized in the laboratory of Guido Kroemer. Under apoptosis-inducing conditions, AIF is transported to the nucleus where it initiates ATP-independent nuclear chromatin condensation as well as large-scale (50kb) DNA fragmentation. The molecular mechanism as to how AIF exerts its cytotoxic activity is unknown. AIF has no intrinsic nuclease activity and its oxidoreductase activity is not required for its apoptogenic function. AIF has been reported [71, 74] being not able to cleave DNA by itself, but recruiting or activating endonucleases to facilitate DNA fragmentation and chromatin condensation [75]. In mammalian cells, cyclophilin A, a peptidyl-propyl *cis-trans* isomerase, cooperates with AIF to induce the breakdown of DNA [76].

Upon apoptotic stimuli, endonuclease G, like AIF, is released from the mitochondrial intermembrane space and translocates to the nucleus where it causes oligonucleosomal DNA fragmentation. EndoG-induced DNA degradation was observed to be caspase-independent [71, 72], suggesting an important role of EndoG in bringing about caspase-independent cell death.

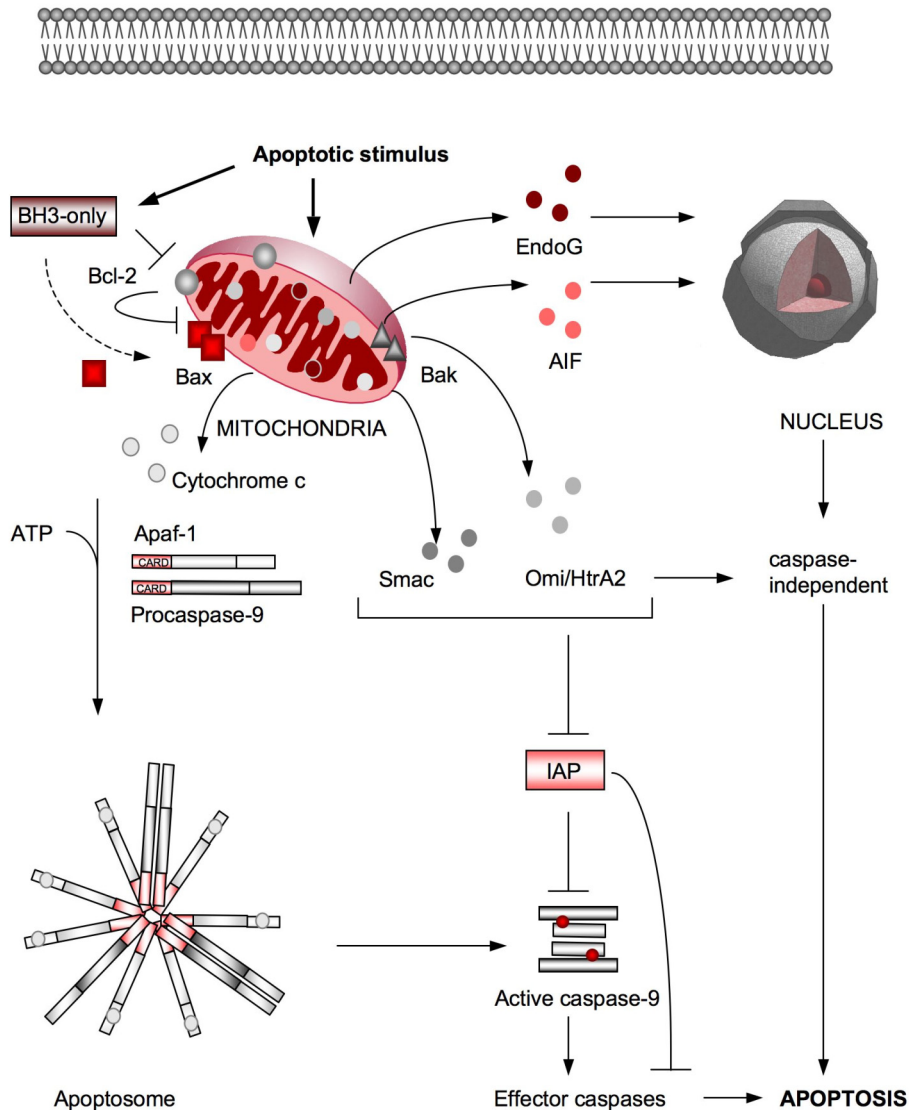


**Figure I.9: The intrinsic apoptotic pathway.**

Mitochondria are the central organelles in the intrinsic apoptotic pathway. Many apoptotic stimuli like chemotherapeutic agents induce mitochondrial membrane permeabilization (MMP) and the release of proapoptotic proteins from mitochondria to the cytosol. Cytochrome c binds and activates Apaf-1, which in turn recruits procaspase-9 to the apoptosome leading to autoactivation of caspase-9 and further activation of downstream effector caspases. Smac and Omi/HtrA2 abolish the negative regulation of the caspases by IAP. AIF, EndoG and Omi/HtrA2 are supposed to induce caspase-independent cell death. The intrinsic apoptotic pathway is regulated by the Bcl-2 family proteins. Antiapoptotic Bcl-2 proteins inhibit the release of mitochondrial proteins whereas the proapoptotic members contribute to MMP.

### 5.3.1 REGULATION BY BCL-2 FAMILY MEMBERS

The process of mitochondrial release of proapoptotic factors such as cytochrome c to the cytosol is elegantly regulated through members of the Bcl-2 protein family. The Bcl-2 (B cell lymphoma) family is an evolutionary conserved group of proteins, acting as potent regulators of the intrinsic apoptotic pathway by influencing the permeability of the outer

mitochondrial membrane [77, 78]. The fate of the cell depends to a great degree on the precise balance of function between pro- and antiapoptotic Bcl-2 proteins. Thus, the Bcl-2 family functions as a “life/death switch” determining whether or not the stress apoptotic pathway should be activated. The founding member is Bcl-2, first identified as a protooncogene involved in human follicular B cell lymphoma and homologue to the *C. elegans ced-9* gene [79, 80]. In mammals, the Bcl-2 family has at least 20 relatives all of which share one to four conserved Bcl-2 homology domains (BH) [77]. The BH domains roughly correspond to  $\alpha$ -helices defining both structure and function. Their three-dimensional structure is well studied and comprises amphiphilic  $\alpha$ -helices surrounding two central hydrophobic  $\alpha$ -helices. A hydrophobic groove formed by BH1, BH2 and BH3 can bind the BH3  $\alpha$ -helix of an interacting BH3-only protein (described in I.5.3.2).

The Bcl-2 protein family possesses both antiapoptotic and proapoptotic members which are divided into three subclasses defined by structural and functional similarities within the four conserved Bcl-2 homology domains (BH 1-4) (Figure I.10).

The first subfamily contains prosurvival members, protecting cells exposed to diverse cytotoxic conditions. These members are characterized by four short BH domains and a hydrophobic carboxy-terminal domain which anchors the proteins to intracellular membranes of organelles such as the outer mitochondrial membrane, the endoplasmic reticulum (ER) and the nuclear envelope. Bcl-2 is an integral membrane protein, whereas Bcl-w and Bcl-x<sub>L</sub> only becomes tightly associated with the membrane after a cytosolic signal. Proposed mechanisms to explain the antiapoptotic function of prosurvival Bcl-2 family members include their ability to heterodimerize with proapoptotic Bcl-2 family members thereby sequestering these proteins [81]. The activity of Bcl-2 is linked to the phosphorylation/dephosphorylation status, the phosphorylation of Ser70 of Bcl-2 abrogates its antiapoptotic properties [11]. Several studies have demonstrated that Bcl-2 phosphorylation can be specifically induced by drugs affecting microtubule dynamics and is not seen by DNA damaging agents, suggesting a role for Bcl-2 as the “guardian of microtubule integrity” [82]. The number of phosphorylated sites depends on the intensity of kinase activation. Mitotic arrest induces the phosphorylation of Bcl-2 on its serine and threonine residues Ser70, Ser87 and Tyr69. A variety of different kinases have been implicated in the phosphorylation of Bcl-2, including JNK, c-RAF, ERK1/2, CDK1, PKA and PKC $\alpha$  [83]. Bcl-2 is phosphorylated and thereby inactivated at the G<sub>2</sub>/M phase of normally cycling cells as well as in cells arrested at the G<sub>2</sub>/M phase following treatment with microtubule-damaging compounds. The persistent Bcl-2 inactivation through phosphorylation during G<sub>2</sub>/M arrest is an important determinant of the induction of apoptosis by microtubule-active drugs. In addition, proteolytic cleavage of Bcl-2 at Asp34 by caspase-3 converts it from an antiapoptotic to a proapoptotic protein [84].

The second group includes Bcl-2 proteins with proapoptotic activity, e.g. Bax and Bak which are structurally similar to the antiapoptotic members but lacking the BH4 domain. In healthy cells, Bax is found as a monomer either in the cytosol or loosely attached to the outer mitochondrial membrane. Contrary to Bax, Bak has an anchor attaching it to the outer mitochondrial membrane in a complex with the voltage-dependent anion channel (VDAC). In response to cytotoxic stimuli, Bax translocates to mitochondria and both Bax and Bak undergo a conformational change in the N-terminus that exposes the formerly buried 6A7 epitope. This conformational change is necessary to create homo-oligomers, insert into the mitochondrial membrane and form protein-permeable pores. Intermembrane mitochondrial proteins like cytochrome c are released through these channels. Another model describes the interaction of Bax and Bak with one or more components of the permeability transition pore complex (PTPC), formed by the adenine nucleotide translocator (ANT, inner mitochondrial membrane), the voltage-dependent anion channel (VDAC, outer mitochondrial membrane) and other proteins [78, 85].

The third subfamily, the proapoptotic BH3-only proteins, only sharing sequence homology with the short BH3 domain, constitutes a key group of proapoptotic proteins. This subfamily includes at least eight members: Bid, Bik, Bad, Bim, Bmf, Hrk, Noxa and Puma. Apart from the BH3 domain, these proteins are largely unrelated in sequence to either Bcl-2 or each other.

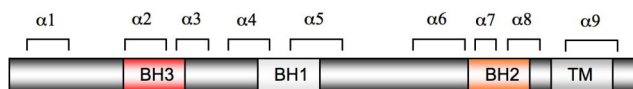
#### Pro-survival

Bcl-2 family: Bcl-2, Bcl-x<sub>L</sub>, A1, Bcl-w, Mcl-1



#### Pro-apoptosis

Bax family: Bax, Bak, Bok



#### BH-3 only family:

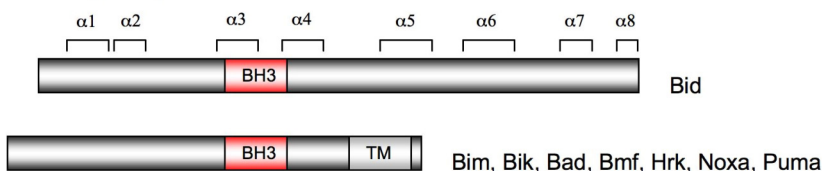


**Figure I.10 Subfamilies of Bcl-2 related proteins.**

Bcl-2 family members share at least one highly conserved BH domain. Most members have a carboxy-terminal hydrophobic domain that aids association with the intracellular membranes. *BH*, Bcl-2 homology; *TM*, transmembrane domain.

Pro- and antiapoptotic proteins can heterodimerize and seemingly titrate one other's function. It is hypothesized that the antiapoptotic proteins inhibit the proapoptotic proteins through binding of the BH3 domains, thus sequestering their proapoptotic abilities [86, 87]. The ratio between pro- and antiapoptotic proteins may determine the susceptibility of a cell to apoptosis.

### 5.3.2 BH3-ONLY PROTEINS

The activation of BH3-only proteins is regulated at the post-translational level by a variety of strategies (Figure I.11) [77, 88]. The regulation of Bid occurs through proteolytic cleavage by caspase-8 to its active truncated form tBid followed by myristoylation upon the activation of death receptors [89]. These events may trigger rearrangement and exposure of the BH3 domain, allowing Bid to bind and inactivate prosurvival molecules. Furthermore, Bid can be cleaved independent of death receptors by caspase-3, calpains, cathepsins or granzyme B [88]. After truncation, tBid is proposed to induce the oligomerization of Bax and Bak resulting in the release of proapoptotic proteins from mitochondria to the cytosol. Bid plays an important role in the mitochondrial apoptotic pathway as it has been identified as the molecular linker bridging various peripheral death pathways to the central mitochondrial release of proapoptotic proteins [90].

Bim and Bmf are sequestered by binding to dynein light chains (DLC) associated with microtubules and the actin cytoskeleton, respectively. Bim (Bcl-2 interacting mediator of cell death) exists in three major isoforms that are generated by alternative splicing: Bim<sub>EL</sub> (extra long), Bim<sub>L</sub> (long) and Bim<sub>S</sub> (short). In contrast to Bim<sub>EL</sub> and Bim<sub>L</sub>, Bim<sub>S</sub> does not appear to interact with the microtubule complex, yet is still capable of exerting proapoptotic activities. In healthy cells, most of the major Bim isoform molecules (Bim<sub>EL</sub>, Bim<sub>L</sub>) are bound to the microtubule-associated dynein motor complex by connection to LC8 dynein light chain. Therefore, Bim is unable to promote cell death. Apoptotic stimuli are thought to disrupt this interaction, causing LC8 and Bim to dissociate from the motor complex and translocate together to the mitochondria where Bim is thought to interact with Bcl-2 or its homologues and antagonize their antiapoptotic activity [91]. Moreover, the activity of Bim was shown to be regulated by the antiapoptotic Bcl-2 family member Mcl-1, which possesses a high affinity binding capacity for Bim. Upon apoptotic stimuli, the Mcl-1/Bim complex is disrupted allowing Bim to mediate the apoptotic cascade [92-94]. A similar process occurs with Bmf. Bmf is normally sequestered by the dynein light chain 2, but under certain damage signals such as loss of cell attachment (anoikis) Bmf is unleashed to trigger an apoptotic response.

Bad is switched on and off primarily by rapid changes in phosphorylation, which modulates its protein-protein interactions and its binding to 14-3-3 scaffold proteins. Nonphosphorylated Bad is active due to the exposure of the BH3 domain, while

phosphorylated Bad is sequestered by 14-3-3 molecules. Noxa, Puma and Hrk are regulated at the transcriptional level by p53.

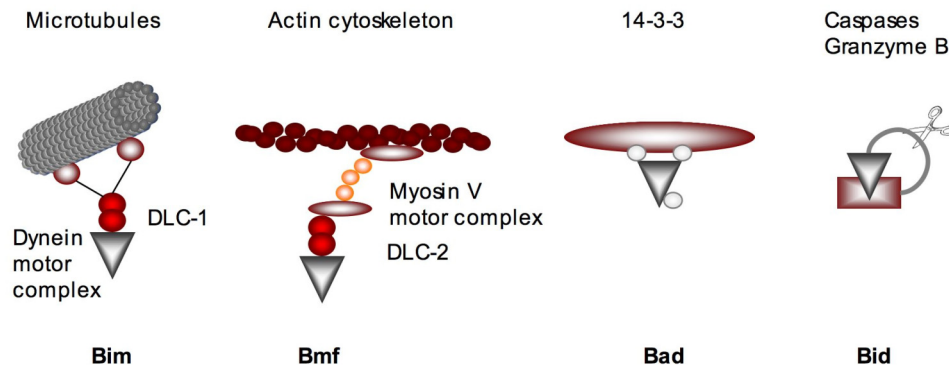


**Figure I.11: Modes of post-translational regulation of BH3-only proteins.**

In healthy cells, BH3-only proteins are held in check by a variety of strategies. Bim and Bmf are sequestered to the microtubules or actin cytoskeleton, respectively, via interaction with a dynein light chain. Phosphorylated Bad is bound by 14-3-3 scaffold proteins. Bid is synthesized as a precursor, which requires proteolytic cleavage to be fully active.

Quantitative assessment of the binding of BH3-only proteins to all Bcl-2 family members have revealed an enormous variety in the affinities of different pairs. Bim, tBid and Puma bind to all five prosurvival Bcl-2 family proteins, whereas other BH3-only proteins exhibit marked selectivity (Figure I.12), e.g. Bad and Bmf bind only Bcl-2, Bcl-x<sub>L</sub> and Bcl-w, Noxa engages only Mcl-1 and A1 [95]. Importantly, the promiscuous binding molecules are much more potent killers than those selectively engaging Bcl-2-like proteins. Therefore, efficient apoptosis requires neutralization of multiple prosurvival proteins.

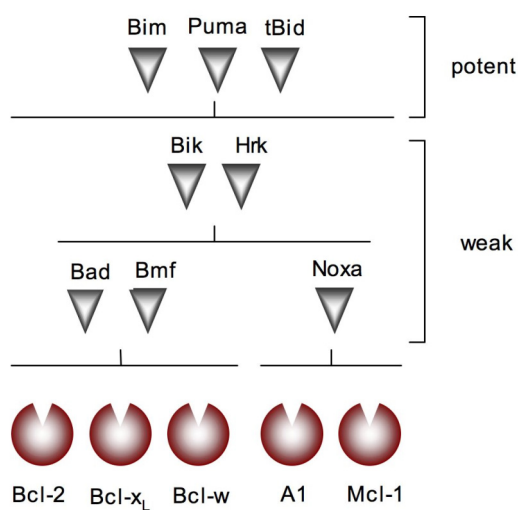


**Figure I.12: Differing binding profiles and apoptotic potency of BH3-only proteins.**

The ability of Bim, Puma and tBid to engage all prosurvival proteins contrasts with the selective binding of others, characterizing them as potent killers.

Because of their multiplicity and complex regulation, BH3-only proteins execute a key role in the control of the intrinsic apoptosis pathway. As the multidomain proapoptotic Bcl-2 members Bax and Bak are constitutively expressed and inactive in nonapoptotic cells, they must be activated by BH3-only proteins to permeabilize the outer mitochondrial membrane [96]. In the signaling cascade, the BH3-only proteins act upstream of Bax and Bak, because they cannot induce apoptosis in cells lacking these two proteins.

Adams et al. [95, 97] describe two distinct models, suggesting how BH3-only proteins induce activation of the proapoptotic Bax and Bak. In the direct activation model (Figure I.13A), certain BH3-only proteins, called *activators* (Bim, tBid and Puma) are able to bind Bax and Bak directly, whereas the remaining BH3-only proteins, termed *sensitizers*, bind only to the prosurvival Bcl-2 family members. Thereby any bound forms of Bim and tBid are displaced from antiapoptotic proteins, allowing them to directly activate Bax and Bak [98]. On the other hand, the indirect activation model (Figure I.13B) describes all the BH3-only proteins engaging only their prosurvival relatives and thus preventing them from neutralizing Bax and Bak activation [99, 100]. As Bim and tBid inhibit all the prosurvival Bcl-2 proteins, they are considered as the most important inducers of apoptosis in this model.

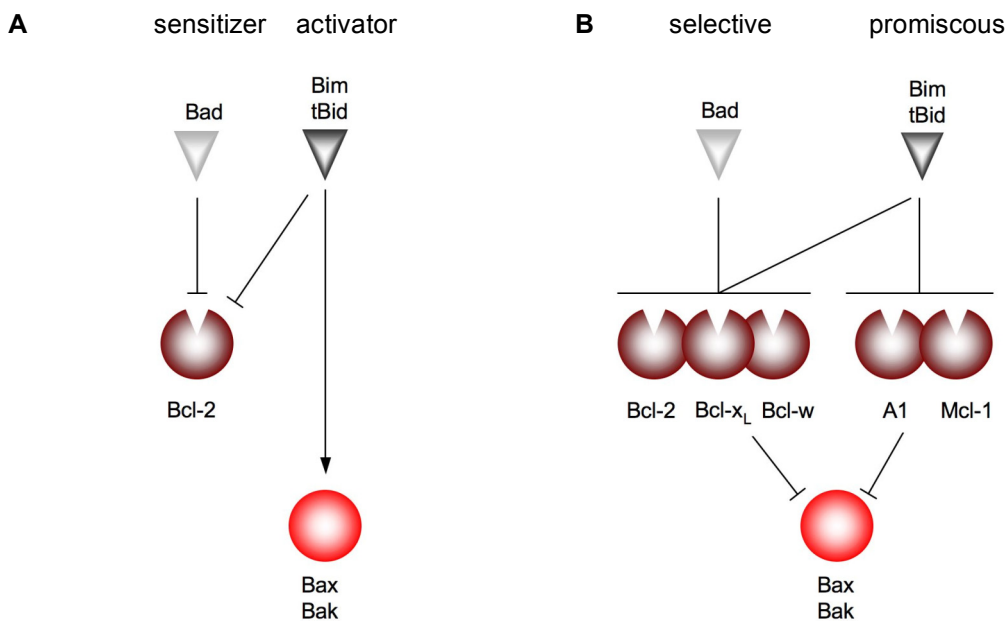


**Figure I.13: Direct and indirect activation models for Bax and Bak.**

(A) In the direct model, the putative activators Bim and tBid bind directly to Bax and Bak causing their activation, whereas the sensitizers only bind to the prosurvival Bcl-2 homologs (Bcl-2).

(B) In the indirect activation model, the BH3-only proteins are proposed to activate Bax and Bak by displacing them from the multiple prosurvival Bcl-2 proteins that sequester their active forms. In this model, Bim and tBid are more potent than Bad and other BH3-only proteins owing to the greater range of prosurvival proteins that they can engage and neutralize.

## 6 APOPTOSIS AS A BARRIER TO METASTASIS

### 6.1 THE METASTATIC CASCADE

Metastasis is the spread of tumor cells from the primary neoplasm to distant organs and their relentless growth, making it one of the most fearsome aspects of cancer. Primary tumors are responsible for only about 10% of cancer deaths, the remaining 90% of patients die from cancerous growths that are discovered at sites far away from the primary tumors. These metastases are formed by cancer cells that have left the primary tumor mass and traveled by either blood or lymphatic vessels to seek out new sites throughout the body where they may form colonies. Such wandering cells are the dangerous manifestations of the cancer process. The understanding of invasion and metastasis is still quite incomplete, explaining why these late steps of tumor progression represent the major unsolved problems of cancer pathology.

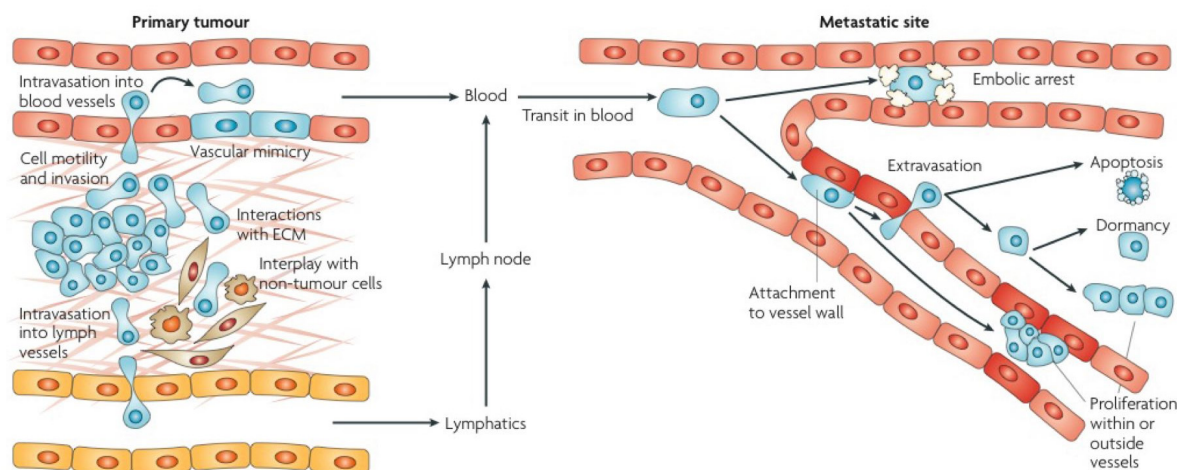


**Figure I.14: The metastatic cascade (adapted from [101]).**

The classical metastatic cascade encompasses intravasation by tumor cells, their circulation in lymph and blood vascular systems, arrest in distant organs, extravasation and growth into metastatic foci.

As illustrated in Figure I.14, metastasis is a complex multi-stage process involving a series of discrete events that occur in sequence. After the initial transformation and onset of primary tumor growth, cells in the primary tumor invade the surrounding stroma and migrate towards blood vessels or lymphatics. Following the entry of cells into the blood vessels (intravasation), the tumor cells are carried by the circulatory system to other parts of the body where they arrest. The arrested cells may proliferate in the vessel or extravasate to grow in a secondary organ (colonization) [102]. The small probability of successfully completing all steps of this cascade explains the low likelihood that any single cancer cell leaving the primary tumor will succeed in becoming the founder of a

distant, macroscopic metastasis. Hence, metastasis is a very inefficient process, only 0.01% of metastatic clonal cancer cells are able to generate metastatic foci.

The ability of cancer cells to undergo migration allows a change of position within the tissues and to enter lymphatic and blood vessels for dissemination into the circulation. To migrate, the cell undergoes a transition from a non-polarized to a polarized state, thereby modifying its shape to interact with the surrounding matrix. These interactions are integrated in the concepts of focal adhesion dynamics, actomyosin polymerization and contraction. In this respect, cell adhesion to the extracellular matrix (ECM) plays a central role in this process [103]. Growing cell protrusions touch the ECM via adhesion molecules, most notably transmembrane receptors of the integrin family, forming focal contacts. The focal contacts are dynamic in assembly and the turnover of adhesion and de-adhesion events allows the cell to move. However, the ECM also provides a barrier towards the advancing cell body. The most critical event in cancer metastasis is the invasion of basement membranes. The degradation of the basement membranes makes the difference between benign and malignant tumors. During the dynamic process of tumor cell invasion, the cell activates specific proteases, such as matrix metalloproteinases (MMP), serine proteinases and cathepsins to degrade matrix components. ECM-degrading enzymes are frequently upregulated in tumor cells thereby facilitating migration and invasion *in vitro* as well as dissemination and metastasis *in vivo*.

## 6.2 APOPTOSIS IN THE METASTATIC PROCESS

Apoptosis is an important mechanism that negatively regulates cancer development. Aberrant cell survival resulting from inhibition of apoptosis is expected to contribute to tumor progression, oncogenesis and resistance to apoptosis, and is one of the required selective advantages that a tumor cell has to form a tumor.

The first step of metastatic dissemination is characterized by the detachment of epithelial cells from the extracellular matrix (ECM) and disruption of the actin skeleton. Detachment of cells from the extracellular matrix often results in apoptotic cell death, termed anoikis, which is derived from the Greek word for "homelessness". The anchorage of cells to components of the extracellular matrix is mainly engaged by integrins, transmembrane cell surface receptors composed of a beta and an alpha chain forming heterodimers [104]. ECM-dependent inhibition of apoptosis is likely to be mediated by the integrin-activated signaling pathway. Upon detachment from the ECM, the proapoptotic Bcl-2 proteins Bim and Bmf are released from its sequestration by the cytoskeleton and trigger the intrinsic apoptotic pathway [105]. Furthermore, proteins involved in integrin-mediated signaling, like focal-adhesion kinase (FAK), are important players in metastasis. FAK is a non-

receptor tyrosine kinase that resides at the intracellular tails of integrins and interacts with various cytoskeletal proteins. It is composed of an N-terminal FERM (protein4.1, ezrin, radixin and moesin homology) domain, a central kinase domain, proline-rich regions (PRR) and a C-terminal focal-adhesion targeting (FAT) domain (Figure I.15).

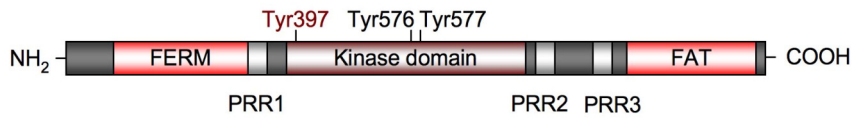


**Figure I.15: Focal adhesion kinase structural features.**

The kinase domain of FAK is flanked by the N-terminus that harbors the FERM domain, and by the C-terminus consisting, in addition to the proline rich domains, of the FAT domain. The autophosphorylation site (Tyr397) as well as the phosphorylation of two important tyrosins, Tyr576 and Tyr577, is required for its activity.

The FERM domain mediates protein-protein interactions and acts as a regulator of FAK activity whereas the proline-rich regions function as binding sites for SRC. FAT promotes colocalization of FAK with integrins and focal contacts. Furthermore, FAK is able to associate with integrins indirectly through binding to integrin-associated proteins such as paxillin and talin (Figure I.16).

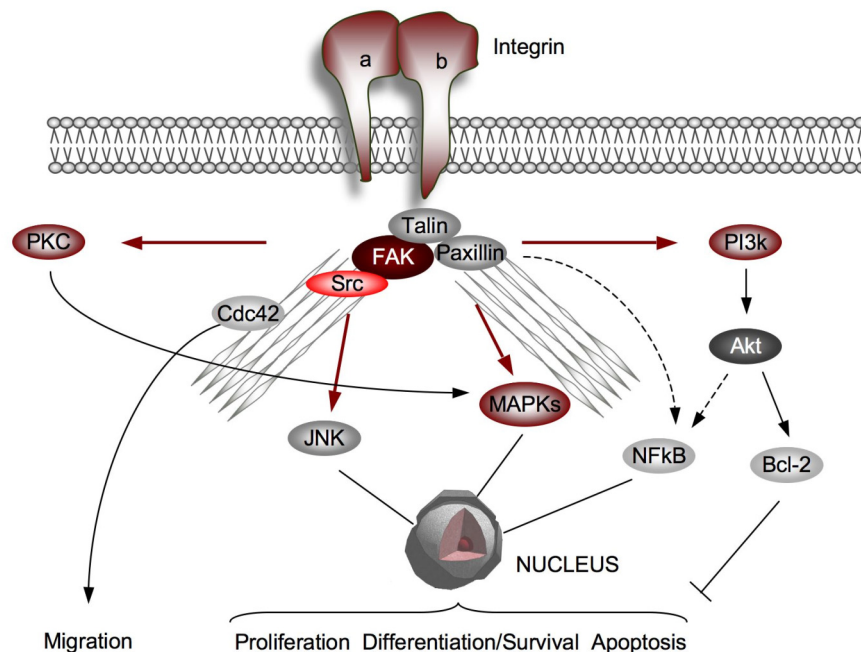


**Figure I.16: Integrin signaling pathway.**

Integrins are heterodimeric transmembrane receptors anchoring the cell to components of the extracellular matrix. The focal adhesion kinase (FAK) functions as a key player in the integrin-mediated signal transduction. Upon integrin ligation FAK is phosphorylated at tyrosin 397 and interacts with numerous signaling molecules. FAK mediates the activation of several mitotic signaling pathways, such as the PI3k, MAPK, JNK and PKC pathway, thereby FAK influences cell adhesion and migration as well as cell-survival pathways.

The activity of FAK is regulated at the post-translational level by phosphorylation. Autophosphorylation of FAK on a particular tyrosine residue, Tyr397, occurs in response to many stimuli, e.g. integrin engagement, thereby recruiting SRC. The association of SRC with FAK leads to a conformational change and activation of the kinase activity of SRC, which in turn phosphorylates FAK at Tyr576 and Tyr577 within the catalytic domain to achieve fully enzymatic activity of FAK. Activated FAK triggers several mitotic signaling pathways, such as phosphoinositide-3-OH kinase (PI3k) pathway with the downstream target protein kinase B (PKB/Akt), the protein kinase C (PKC) pathway and the Jun-NH2-terminal kinase (JNK)/mitogen activated protein kinase (MAPK)-pathway (Figure I.16), thereby influencing cell adhesion, migration and cell survival. Phosphorylation of FAK at Tyr397 has been found in invasive tumors but not in normal epithelial cells [106]. Moreover, FAK is frequently overexpressed in metastatic cancers and its activation seems to be associated with cell survival [106, 107].

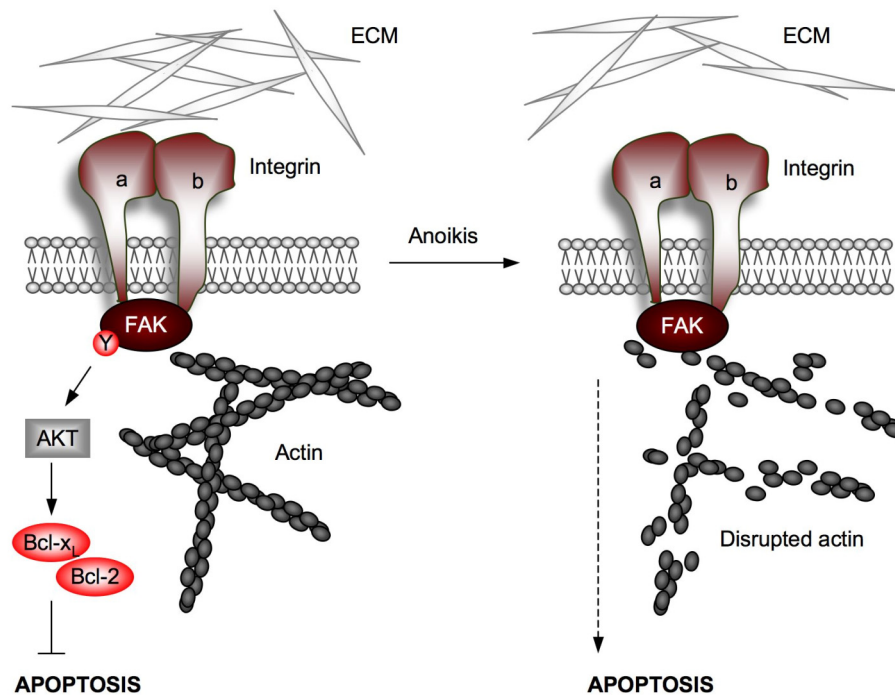


**Figure I.17: Resistance of anoikis is a crucial feature of metastatic cells.**

In the primary tumor, integrin-mediated attachment to the extracellular matrix (ECM) triggers the phosphorylation of FAK leading to the local organization of the cytoskeleton and to cell survival by inducing antiapoptotic pathways. After cell detachment from the ECM, disruption of the actin cytoskeleton results in the loss of survival signals and cell death by mitochondria-mediated apoptosis.

Since metastatic cells have to survive in a detached state during metastasis, it may be necessary for tumor cells to overcome anoikis to disseminate (Figure I.17, modified from [105]). Therefore, metastatic cells are characterized by their resistance to anoikis and their ability to survive in the absence of extracellular matrix components. Several known apoptotic and antiapoptotic proteins are shown to influence both anoikis and metastasis.

Although the precise mechanisms have yet to be studied, resistance of apoptosis may be mediated by dysregulation of Bcl-2 family proteins (described in I.5.3.1) and may play a prominent role both in tumorigenesis and metastasis. In this respect, the expression levels of the antiapoptotic Bcl-2 family proteins Bcl-2 and Bcl-x<sub>L</sub> have been reported to correlate with the metastatic potential. Overexpression of Bcl-2 as well as Bcl-x<sub>L</sub> increases the formation of distant metastases without affecting primary tumor growth [108, 109]. Furthermore, Bcl-x<sub>L</sub> was identified as a suppressor of cytoskeleton-dependent cell death [109].

Moreover, the loss of function of proapoptotic genes such as *BAX* and the downregulation of death-associated protein kinase (DAPK) [110] correlates with the tumor progression and favors metastasis. These studies demonstrate that crucial apoptotic modulators are deregulated in metastatic cancer cells and support the hypothesis that suppression of apoptosis plays an important role during the metastatic process.



## **MATERIALS AND METHODS**

## II MATERIALS AND METHODS

### 1 MATERIALS

#### 1.1 SPONGISTATIN 1

Spongistatin 1, isolated as described in [24], was kindly provided by Prof. G. R. Pettit (Cancer Research Institute, Arizona State University, Tempe, USA). The 10 mM stock solution prepared in DMSO was stored at  $-20^{\circ}\text{C}$ .

#### 1.2 REAGENTS

Reagent	Company
5-Fluoruracil	Sigma, Taufkirchen, Germany
BI-6C9	Sigma, Taufkirchen, Germany
Bradford	Bio-Rad, Munich, Germany
Collagen A	SERVA, Heidelberg, Germany
Collagen G	BIOCHROME AG, Berlin, Germany
Complete <sup>TM</sup>	Roche, Mannheim, Germany
Culture flasks, plates, dishes	TPP, Trasadingen, Switzerland
Cytoskelfix <sup>TM</sup>	Cytoskeleton, Offenbach, Germany
DMEM	PAN Biotech, Aidenbach, Germany
DMSO	Roth GmbH, Karlsruhe, Germany
ECL Plus <sup>TM</sup>	Amersham Biosciences, Freiburg, Germany
FCS gold	PAA Laboratories, Cölbe, Germany
Human FGF-basic	PeptoTech, Rocky Hill, NY, USA
Gemcitabine	Eli Lilly, Bad Homburg, Germany
Hoechst 33342	Sigma, Taufkirchen, Germany
L-glutamine	PAN Biotech, Aidenbach, Germany
Matrigel <sup>TM</sup>	BD Biosciences, Heidelberg, Germany
McCoy's 5a	PAN Biotech, Aidenbach, Germany
MitoTracker Red	Molecular Probes, Karlsruhe, Germany
MTT	Sigma, Taufkirchen, Germany
Penicillin	PAN Biotech, Aidenbach, Germany
Polyacrylamide	Roth GmbH, Karlsruhe, Germany
Poly-HEMA	Sigma, Taufkirchen, Germany
Precision ALL Blue®	Bio-Rad, Munich, Germany
Propidium iodide	Sigma, Taufkirchen, Germany
Q-VD-OPh	Calbiochem, Schwalbach, Germany

RPMI 1640	PAN Biotech, Aidenbach, Germany
Staurosporine	Calbiochem, Schwalbach, Germany
Streptomycin	PAN Biotech, Aidenbach, Germany
Taxol	Sigma, Taufkirchen, Germany
Vinblastine	Sigma, Taufkirchen, Germany
zVAD.fmk	Calbiochem, Schwalbach, Germany

### 1.3 TECHNICAL EQUIPMENT

Axiovert 25 (Zeiss)	Inverted microscope
Axiovert 200 (Zeiss)	Inverted microscope
Curix 60 (Agfa)	Tabletop film processor
FACSCalibur (Becton Dickinson)	Flow cytometer
LSM 510 Meta (Zeiss)	Confocal laser scanning microscope
Nucleofector™ II (Amaxa)	Electroporation device
Odyssey (Li-Cor)	Imaging system for Western Blot analysis
SLT spectra (SLT Labinstruments)	ELISA plate reader
SpectraFluor Plus™ (Tecan)	Plate-reading multifunction photometer
Sunrise™ (Tecan)	Microplate absorbance reader
Vi-Cell™ (Beckman Coulter)	Cell viability analyser

## 2 CELL CULTURE

### 2.1 CELL LINES

The epithelial breast cancer cell line MCF-7 and caspase-3 reconstituted MCF-7 cells (kindly provided by K. Schulze-Osthoff, University of Düsseldorf, Germany) [111] were cultured (37°C and 5% CO<sub>2</sub>) in RPMI 1640 containing 2 mM L-glutamine (PAN Biotech, Aidenbach, Germany) supplemented with 10% heat-inactivated FCS (PAA Laboratories, Cölbe, Germany). The human melanoma cell line SK-Mel-5 was obtained from ATCC American Type Culture Collection (Manassas, USA) and the human pancreatic cancer cells Panc-1 from Prof. Lindl (I.A.Z., Munich, Germany). Both cell lines were cultured in DMEM supplemented with 1 mM sodium pyruvate and 10% FCS. The human prostate cancer cell line LNCaP, (kindly provided by I. Jeremias, Helmholtz Center Munich, Germany) was cultured in RPMI 1640 supplemented with 10% FCS. The human ovarian cancer cell line SK-OV-3, purchased from ATCC, was cultured in McCoy's 5a containing 10% FCS. The human pancreatic cancer cell line L3.6pl [112] (kindly provided by C. Bruns, Klinikum Großhadern, Munich, Germany) was cultured in DMEM supplemented with 1

mM sodium pyruvate, non-essential amino acids and 10% FCS. A summary of all used cancer cell lines is listed in Table II.1.

**Table II.1: Summary of used cancer cell lines.**

<b>Carcinoma cell lines</b>	<b>Derived tumor</b>
L3.6pl	Human pancreatic tumor
LNCaP	Human prostate cancer
MCF-7 +/- caspase-3	Human epithelial breast cancer
Panc-1	Human pancreatic tumor
SK-Mel-5	Human melanoma
SK-OV-3	Human ovarian cancer

## 2.2 CULTIVATION

All cell lines were cultured in tissue culture flasks at 37°C in a humidified atmosphere and 5% CO<sub>2</sub>. Cell concentration and viability was determined by staining cells with trypan blue using a VI-CELL™ cell viability analyzer (Beckman Coulter, Krefeld, Germany).

All used cancer cell lines grow in monolayers adherent to plastic surfaces. Cells were split when reaching 85-90% confluence. To maintain genetic stability, cells were not used for experiments any longer after reaching passage number 20. Briefly, cells were washed in prewarmed PBS (see below) and detached by incubation with 3 ml Trypsin/EDTA (T/E) (see below)/75 cm<sup>2</sup> flask at 37°C. After detaching, the T/E was inactivated by adding 7 ml serum-containing medium. The cell suspension was centrifuged (180 x g, 10 min, RT) and resuspended in fresh medium before transferring to culture flasks. For cultivation of the L3.6pl cell line, the flasks were coated with Collagen G (0.001% in PBS) 30 min before transferring the cells to the flasks.

### PBS (pH 7.4)

NaCl	7.20 g
Na <sub>2</sub> HPO <sub>4</sub>	1.48 g
KH <sub>2</sub> PO <sub>4</sub>	0.43 g
H <sub>2</sub> O	ad 1,000 ml

### Trypsin/EDTA (T/E)

Trypsin	0.50 g
EDTA	0.20 g
PBS	ad 1,000 ml

### 2.3 SEEDING FOR EXPERIMENTS

Carcinoma cell lines were detached with T/E and centrifuged as described in II.2.2. The cell suspensions were analyzed in the VI-CELL™, the concentrations were adjusted to  $0.3 \times 10^6$  cells/ml and the cells were seeded in 6-, 12-, 24- or 96-well plates approximately 16 h before experiments. Similar to cultivation, the 6-, 12-, 24- or 96-well plates were coated with Collagen G (0.001% in PBS) 30 min before seeding L3.6pl cells.

### 2.4 FREEZING AND THAWING

Cryogenic preservation is necessary to obtain a sufficient stock of each cell line. The long term storage in liquid nitrogen protects cells from microbial contamination, genetic and morphological changes and allows using cells of the similar passage number for experiments to increase reproducibility.

Cells in low passages were frozen in special medium (Table II.2) containing higher percentage of serum than culture medium and DMSO as a cryoprotector to avoid cell rupture. After centrifugation ( $180 \times g$ , 10 min,  $4^\circ\text{C}$ ) cells were resuspended in ice-cold freezing medium at a concentration of  $2-3 \times 10^6$  cells/ml. 1.5 ml of the cell suspension was transferred into each cryovial and frozen overnight at  $-20^\circ\text{C}$ . Afterwards, cryovials were kept at  $-80^\circ\text{C}$  for permanent usage or transferred to liquid nitrogen ( $-196^\circ\text{C}$ ) after two days for long-term storage.

**Table II.2: Freezing medium.**

	<b>L3.6pl</b>	<b>LNCaP</b>	<b>MCF-7</b>	<b>Panc-1</b>	<b>SK-Mel-5</b>	<b>SK-OV-3</b>
RPMI 1640	-	70%	70%	-	-	-
DMEM	70%	-	-	70%	80%	-
McCoy's 5a	-	-	-	-	-	85%
FCS gold	20%	20%	20%	20%	10%	10%
DMSO	10%	10%	10%	10%	10%	5%

The frozen cells were thawed in a water bath ( $37^\circ\text{C}$ ) and subsequently diluted 1:10 with prewarmed medium. Cells were centrifuged ( $180 \times g$ , 10 min, RT) to remove dead cells and DMSO. After resuspension in fresh medium, cells were cultured for at least five days before conducting any experiment.

### 3 FLOW CYTOMETRY

#### 3.1 INTRODUCTION

Flow cytometry has become a technology indispensable in the analysis of cell death allowing the measurement of various physical characteristics of single cells or particles suspended in a fluid at the same time. This method is ideally suited for the rapid, reliable and accurate quantitative analysis of selected physical properties of cells, even if these cells form a small population within the mixture of cell types. This analysis is performed at rates of thousands of cells per second. Measurable parameters include particle's relative size, relative granularity of internal complexity and relative fluorescence intensity. The applications of flow cytometry range from the analysis of cell cycle, cell viability, apoptosis, membrane potential, calcium influx, protein expression and localization to the investigation of surface antigens and enzymatic activity.

Flow cytometry uses light scattering, light excitation and the emission of fluorochrome molecules to generate specific multi-parameter data sets from particles and cells in the size range of  $0.5 \mu\text{m}$  to  $40 \mu\text{m}$ . The particles or cells are presented to the laser by the principle of hydrodynamic focusing. In the flow chamber (Figure II.1, modified from [113]) the suspension of single cells emerges from the sample needle into a surrounding sheath fluid moving with greater velocity. The sheath fluid accelerates the particles, restricts them to the center of the sample core and forces them to travel one by one in the central portion of the fluid.

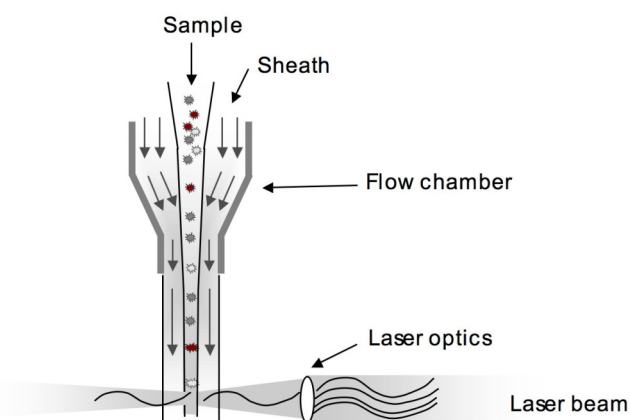


**Figure II.1: Hydrodynamic focusing in the flow chamber.**

When the cells pass the laser beam, the illuminating light is scattered and simultaneously, if particles have been stained with a fluorescent dye capable to absorb the laser light, fluorescence emission occurs. Optical filters collect and send scattered light and emitted fluorescence to different detectors (Figure II.2). Morphological parameters like the relative size and granularity of a cell influence the light scattering. Low angle scattered light

depends on cell size and is measured in line with the laser beam, called forward scatter (FSC). The sideward scatter (SSC) which is perpendicular to the laser, bears information on the cell light refractive and reflective properties and reveals optical inhomogeneity of the cell structure including the results from condensation of the cytoplasm or nucleus and granularity.

Fluorescence was measured using the appropriate filters for the respective fluorochromes (e.g. FL2 for detection of propidium iodide). All measurements were performed on a FACSCalibur (Becton Dickinson, Heidelberg, Germany) equipped with a 488 nm argon laser. Sheath fluid is composed as seen below (FACS buffer).

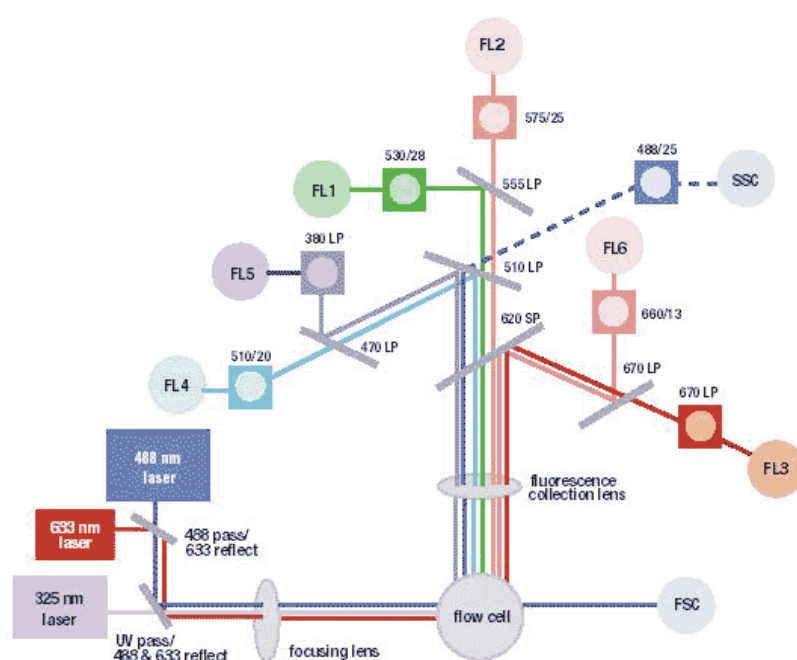


Figure II.2: Optical bench diagram of a flow cytometer (adapted from [114]).

#### FACS buffer

NaCl	8.12 g
KH <sub>2</sub> PO <sub>4</sub>	0.26 g
Na <sub>2</sub> HPO <sub>4</sub>	2.35 g
KCl	0.28 g
Na <sub>2</sub> EDTA	0.36 g
LiCl	0.43 g
NaN <sub>3</sub>	0.20 g
H <sub>2</sub> O	ad 1,000 ml, pH 7.37

### 3.2 NICOLETTI ASSAY

A characteristic event during the apoptotic process is the activation of endogenous endonucleases causing the fragmentation of nuclear DNA into oligonucleosomal-size fragments. Hence, an easy and commonly used assay to quantify apoptotic cell death is the determination of nuclei with a subdiploid DNA content after staining with propidium iodide (PI). Because of its rapidness and simplicity, this method first described by Nicoletti et al. [115] is one of the most widely used for the quantification of apoptosis.

Briefly, cells are permeabilized in a hypotonic buffer (HFS, hypotonic fluorochrome solution) containing the DNA intercalating dye propidium iodide and the resulting red fluorescence is measured by flow cytometry. Figure II.3 shows characteristic histograms of untreated control cells and cells stimulated with spongistatin 1 (500 pM, 48 h) after staining with propidium iodide. Most cells of untreated cell populations are in  $G_0/G_1$  phase containing  $2n$  DNA content. Cells in  $G_2/M$  phase emit a higher amount of fluorescence due to their  $4n$  DNA content, while cells in the S phase appear between the  $G_0/G_1$  and  $G_2/M$  peaks. DNA fragments of apoptotic cells take up less dye and thus appear in a hypodiploid peak “left” to the  $G_0/G_1$  peak in the FL2 histogram.

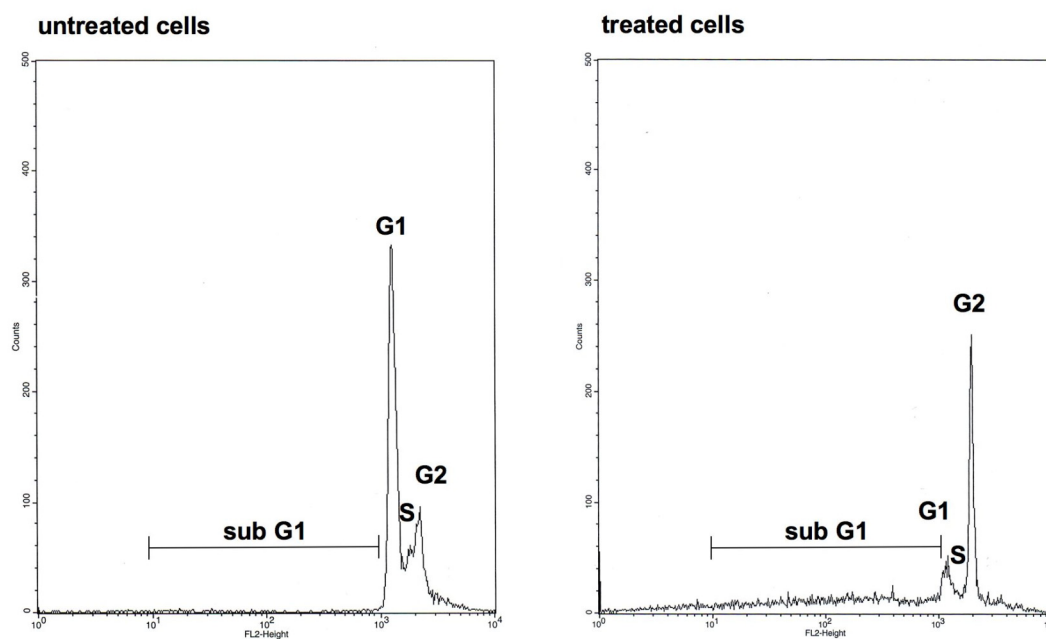


**Figure II.3: Histogram of untreated and treated PI-stained cells.**

Left panel: Untreated MCF-7 cells stained with PI.

Right panel: PI-stained MCF-7 cells stimulated with 500 pM spongistatin 1 for 48 h.

Cells were seeded as described in II.2.3 and either left untreated or stimulated with the desired substances. In some experiments, caspase inhibitors were added 1 hour before stimulation. After various incubation times, cells were harvested by detachment with T/E and centrifugation ( $600 \times g$ , 10 min,  $4^\circ\text{C}$ ) and washed once with cold PBS. Cells were

incubated in 250  $\mu$ l HFS buffer containing PI (see below) overnight at 4°C and analyzed by flow cytometry on a FACSCalibur. The logarithmic mode of FL2 was recorded and the instrument settings were adjusted by assigning a fluorescence intensity of  $10^3$  to the  $G_0/G_1$  peak. The percentage of sub  $G_1$  region was quantified as apoptotic cells. Because of the elevated spontaneous apoptosis rate (about 10%) of cells transfected with siRNA, results of experiments with transfected cells are represented as percental specific apoptosis. Thereby the spontaneous apoptosis rate of the control cells is considered as 0% and the apoptosis rate of the stimulated cells is set in correlation.

#### HFS buffer

---

Prodidium iodide	50 $\mu$ g
Sodium citrate	0.1 % (w/v)
Triton X-100	0.1 % (v/v)
PBS	ad 1 ml

Propidium iodide was added under light protection just before use.

### 3.3 BAX ACTIVATION

Activation of Bax was measured by FACS analysis upon staining of activated Bax with an antibody specifically recognizing the conformationally changed Bax protein. MCF-7 cells were left untreated or treated with spongistatin 1. After 8 h cells were harvested with T/E, washed with PBS and fixed in PBS/0.5% paraformaldehyde on ice for 30 min. Then, cells were washed three times in PBS/1% FCS. Staining with 0.5  $\mu$ g anti-Bax 6A7 was performed in staining buffer (PBS, 1% FCS, 50  $\mu$ g/ml digitonin). After three washing steps, cells were resuspended in staining buffer containing 0.1  $\mu$ g Alexafluor 488-labeled goat-anti-mouse (Molecular Probes, Karlsruhe, Germany) and incubated on ice for 30 min in the dark. Following the incubation step, cells were washed three times and measured by flow cytometry to detect the conformational change of Bax as evidenced by a shift in FL1 channel.

## 4 MTT VIABILITY ASSAY

The mitochondrial respiratory activity is a parameter for cell viability that is used to determine the cytotoxic potential of a substance by the MTT assay. This colorimetric assay utilizes the tetrazolium salt MTT (3-(4,5-dimethylthiazol-2-yl)-2,5-diphenyl tetrazolium bromide) and is based on the reduction of MTT by enzymes of the mitochondrial electron transport assembly which leads to the formation of a blue formazan derivative (Figure II.4). This reduction is proportional to the activity of the assembly and thus to the viability

of the cells. The absorption of the blue formazan derivative can be measured at 550 nm in a spectrophotometer.

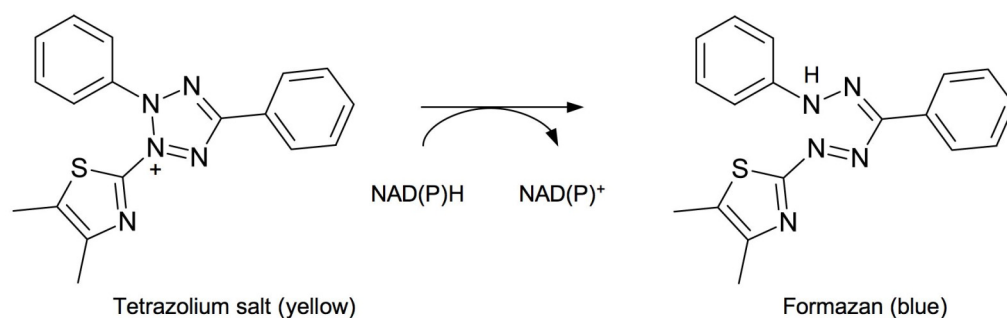


**Figure II.4: Reduction of MTT to the blue formazan.**

The day before stimulation, cells were seeded at a concentration of  $0.15 \times 10^5$  cells/ml in a 96-well plate (100  $\mu$ l per well). After stimulation 10  $\mu$ l MTT solution (stock solution: 5 mg/ml in PBS, sterile filtrated and kept in aliquots at  $-20^\circ\text{C}$ ) was added to each well and incubated at  $37^\circ\text{C}$  for 60 minutes. Afterwards, cells were lysed by adding 190  $\mu$ l DMSO to each well and incubated at room temperature under gentle agitation, protected from light for an additional hour. Finally, the absorption of the solubilized formazan crystals was measured at 550 nm in an ELISA plate reader (SLT spectra, SLT Labinstruments, Crailsheim, Germany).

## 5 COLONY FORMATION ASSAY

The colony formation assay or clonogenic assay is an *in vitro* long term cell survival assay to determine the effectiveness of cytotoxic agents based on the ability of a single cell to grow into a colony. The assay essentially assesses each individual cell in the population to undergo “unlimited” division.

Cells were seeded as described in II.2.2 and left untreated or treated with spongistatin 1 or the respective positive controls for 3 h. Subsequently, cells were harvested with T/E and washed with PBS to remove any remaining substances. 500 cells per well were seeded as triplicate in a 6-well plate using the ViCell™ to determine the cell count. After 7 days of culture, cells were stained with 0.5% crystal violet in 20% methanol and the colonies were scored. Untreated cells were set at 100% viability. Images of the stained colonies were taken with a digital camera (Canon, Krefeld, Germany).

## 6 IN VITRO METASTASIS ASSAYS

### 6.1 CELL PROLIFERATION

In order to assess the effects of spongistatin 1 on cell proliferation, the crystal violet staining assay was performed.

$1.5 \times 10^3$  L3.6pl cells were seeded into flat-bottom 96-well plates coated with Collagen G (0.001% in PBS). 24 h after incubation, cells in a reference plate were stained with crystal violet solution, serving as baseline (CO-0). The cells in the remaining plates were either left untreated or stimulated with increasing concentrations of spongistatin 1 or the respective positive controls. Upon an incubation period of 72 h, the medium was removed and cells were stained with 100  $\mu$ l crystal violet solution for 10 min at room temperature. After five wash steps with distilled water, bound dye was solubilized by the addition of 100  $\mu$ l dissolving buffer to each well. The absorbance was measured at 540 nm in a plate-reading photometer (SPECTRAFluor Plus, Tecan, Crailsheim, Germany).

#### Crystal violet solution

Crystal violet	0.5%
Methanol	20%
H <sub>2</sub> O	

#### Dissolving buffer

Sodium citrate 0.1 M	50%
Ethanol	50%

### 6.2 CELL MIGRATION ASSAY / WOUND HEALING ASSAY

The “wound healing” assay was used to investigate the motility of cancer cells. In this assay, a confluent cell monolayer is wounded and the ability of the cells to migrate and close the artificial scratch is determined.

$3 \times 10^5$  L3.6pl cells were seeded in Collagen G (0.001% in PBS) coated 24-well plates and grown as monolayers until they reach confluence. Afterwards, cells were scratched in a line across the well using a tip of a micropipette. To remove the floating cellular debris, the wounded monolayers were washed twice with PBS and re-fed with growth medium supplemented with 10% FCS. As a negative control, cells were cultured in starving medium without FCS to prevent migration. Cells were left either untreated or stimulated with spongistatin 1 or the respective positive controls. 16 h after stimulation, the area of cell-free wound was detected using an imaging system (TILL Photonics GmbH,

Gräfelfing, Germany) and a CCD-camera connected to an Axiovert 200 microscope (Zeiss, Oberkochen, Germany). The images were analyzed and the percentage of cell-covered area in relation to the total image area was quantified by a specifically designed software (S.CO LifeScience, Garching, Germany) as displayed in Figure II.5. Migration was expressed as the ratio of pixels covered by cells (yellow) and the number of pixels in the wound area (gray).

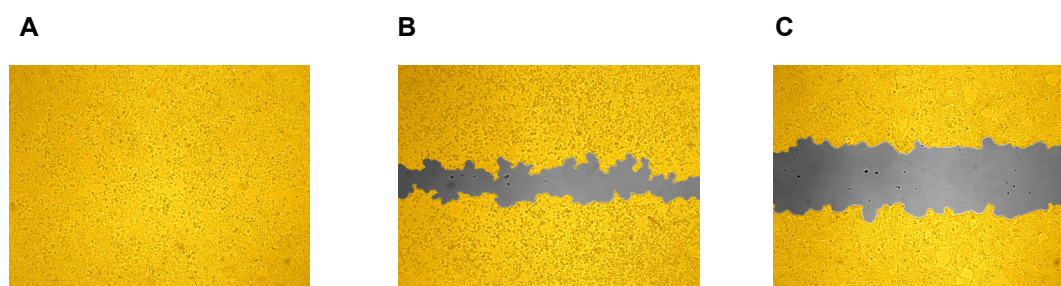


**Figure II.5: Quantitative evaluation of S.CO LifeSciences.**

(A) L3.6pl cells stimulated with growth medium supplemented with 10% FCS. (B) Cells treated with spongistatin 1 (100 pM, 16 h). (C) Cells starved with growth medium without FCS for 16 h. The uncovered area is displayed in gray, whereas the cell-covered area is highlighted in yellow.

### 6.3 CELL INVASION ASSAY

One of the most critical events in cancer metastasis is the invasion of basement membranes. Basal membrane is a thin continuous sheet of extracellular matrix enveloping organs and represents a barrier that tumor cells have to cross in order to disseminate. During the dynamic process of tumor cell invasion, the cell activates specific proteases to degrade matrix components.

In order to evaluate *in vitro* the metastatic potential of cancer cells, a transwell assay, the so-called modified “Boyden chamber” developed 1987 by Albini et al. [116-118] was performed. This assay utilizes a reconstituted basal membrane extracted from the murine Engelbreth-Holm-Swarm sarcoma, commonly known as Matrigel™ with the main components collagen IV, laminin, entactin and perlecan. Matrigel™ can simply be applied in its cold, liquid form over polycarbonate filters (standard size 8 μm) allowing the formation of a polymerized matrix. Several growth factors such as vascular endothelial growth factor, basic fibroblast growth factor and hepatocyte growth factor stimulate cell motility and invasion of target cells, and are frequently used as chemoattractants in the chemoinvasion test. The cell invasion assay can be performed in numerous variations concerning especially the cell type, Matrigel™ concentration, diameter of the polycarbonate filters, chemoattractant and time of incubation.

The invasion assay was carried out in a Boyden chamber with polycarbonate filter inserts for 24-well plates containing 8  $\mu\text{m}$  pores (BioCoat Inserts, Becton Dickinson Labware, Heidelberg, Germany), as illustrated in Figure II.6. Filters were coated on ice with 70  $\mu\text{l}$  Matrigel™ (1:20 in starving medium without FCS).  $1 \times 10^5$  L3.6pl cells were plated in 250  $\mu\text{l}$  of starving medium (culture medium supplemented with 1% FCS) into the upper chamber. The lower chamber was filled with 500  $\mu\text{l}$  of 10% FCS-DMEM supplemented with 100 nM hFGF as chemoattractant. Subsequently, cells in the upper chamber were left untreated or stimulated with spongistatin 1 or taxol as positive control. After incubation for 24 h, noninvaded cells in the inserts were removed with cotton swabs. The invaded cells on the underside were fixed with 4% formaldehyde and stained with crystal violet. The stained cells were washed five times with  $\text{H}_2\text{O}$ , the bound dye was solubilized by addition of 300  $\mu\text{l}$  dissolving buffer to each well (II.6.1). The absorbance was measured at 540 nm in a plate-reading photometer (SPECTRAFluor Plus, Tecan, Crailsheim, Germany).

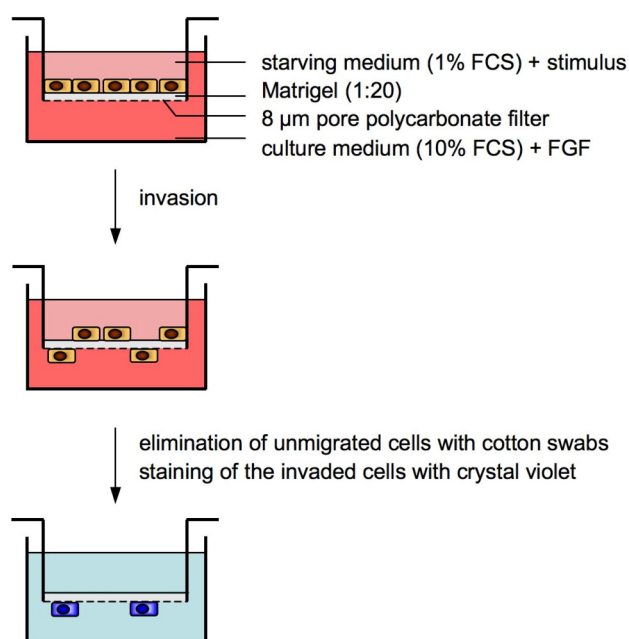


**Figure II.6: Schematic diagram of the chemoinvasion assay.**

## 6.4 ADHESION ASSAY

The significance of aberrant cellular adhesion for cancer metastasis is widely recognized. *In vitro* adhesion assays were performed to evaluate the effects of spongistatin 1 on the adhesive properties of L3.6pl cells. L3.6pl cells were prestimulated under confluent conditions with spongistatin 1 or the respective controls for 3 h. Subsequently, cells were harvested with T/E, seeded in 24-well plates precoated with collagen G (0.001% in PBS) and allowed to adhere for 16 h. Nonadhered cells were removed by gently washing with

PBS and the adhered cells were stained with crystal violet. The stained cells were washed five times with H<sub>2</sub>O, the bound dye was solubilized by addition of 300  $\mu$ l dissolving buffer to each well (II.6.1). The absorbance was measured at 540 nm in a plate-reading photometer (SPECTRAFluor Plus, Tecan, Crailsheim, Germany).

## 6.5 INDUCTION OF ANOIKIS

Anoikis is defined by apoptotic cell death in response to inappropriate cell-matrix interactions and plays a significant role in tumor metastasis. Therefore, DNA-fragmentation of L3.6pl cells was investigated under detached conditions.

To prevent cell adhesion, 24-well plates were coated with a solution of polyhydroxyethylmethacrylate (poly-HEMA, Sigma-Aldrich, Taufkirchen, Germany). Poly-HEMA was dissolved at 10 mg/ml in ethanol at 65°C. To coat 24-well plates, 200  $\mu$ l of poly-HEMA solution was added to each well. The plates were kept at 37°C for at least 3 days until the solvent had completely evaporated. For anoikis induction, L3.6pl cells were harvested with Trypsin/EDTA and transferred to plates coated with poly-HEMA.  $0.15 \times 10^6$  resuspended cells, cultured in growth medium supplemented with 10% FCS, were left untreated or stimulated with spongistatin 1 (SP; 500 pM) for the indicated time points. Subsequently, cells were gently recovered and DNA fragmentation was analyzed by FACS analysis using the Nicoletti method (described in II.5.2).

## 7 MICROSCOPY

### 7.1 LIGHT MICROSCOPY

The characteristic morphological changes of apoptosis as well as other forms of programmed cell death, such as cell shrinkage, swelling or formation of apoptotic bodies, can be easily detected by light microscopy.

$3 \times 10^5$  cells/ml (500  $\mu$ l, 24-well plate) were left untreated or stimulated with the required substances for different time periods. Cells were viewed with an Axiovert 25 microscope (Zeiss, Oberkochen, Germany) at 40 x magnification. Images were obtained with a connected CCD-camera.

## 7.2 FLUORESCENCE MICROSCOPY

Vital staining of DNA with Hoechst 33342 (bisBenzimide) allows the visualization of DNA condensation, a characteristic feature of apoptotic cells, with a fluorescence microscope. Hoechst 33342 is a cell permeable fluorescent dye that intercalates in the DNA due to its planar structure (Figure II.7). Since the DNA is distributed evenly in the nucleus, healthy cells emit only a weak blue fluorescence. Contrary to this, the nucleus of apoptotic cells is smaller and therefore shows a strong signal emitted from the condensed DNA.

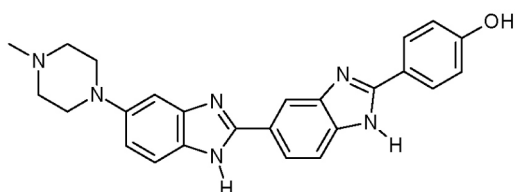


**Figure II.7: Chemical structure of Hoechst 33342.**

$3 \times 10^5$  cells/ml (500  $\mu$ l, 24-well plate) were left untreated or stimulated with spongistatin 1 for 48 h. Hoechst solution (final concentration 5  $\mu$ g/ml) was added to the cells and incubated at 37°C for 5 min. Subsequently, pictures were taken using a CCD-camera connected to an Axiovert 200 microscope (Zeiss, Jena, Germany).

## 7.3 CONFOCAL LASER SCANNING MICROSCOPY

Confocal microscopes are increasingly used in life sciences due to the many advantages they offer. Among them, the extremely high-quality images are obtained with a maximum resolution, three-dimensional information of thick specimens can be received and colocalizations of signals from different fluorochromes can be reliably studied. Confocal can be defined as “having the same focus”, the final image has the same focus as the point of focus in the object. A confocal microscope is able to filter out the out-of-focus light from above and below the point of focus in the object by a pinhole, allowing high-quality images with ultimate resolution.

For the visualization of Omi/HtrA2, AIF, EndoG and tubulin during apoptosis, a LSM 510 Meta (Zeiss, Oberkochen, Germany) was used. Figure II.8 represents schematically the beam path of this confocal laser scanning microscope. The excitation light is reflected by a main dichroic beamsplitter and focused into the specimen by the objective. The focused excitation light is scanned through the specimen point by point. The light returned or the fluorescent radiation emitted by the specimen is collected by the objective and focused on to a confocal pinhole which allows only the in-focus portion of the light to be imaged.

Light passing through the image pinhole is detected by a photodetector while out-of-focus interference is rejected.

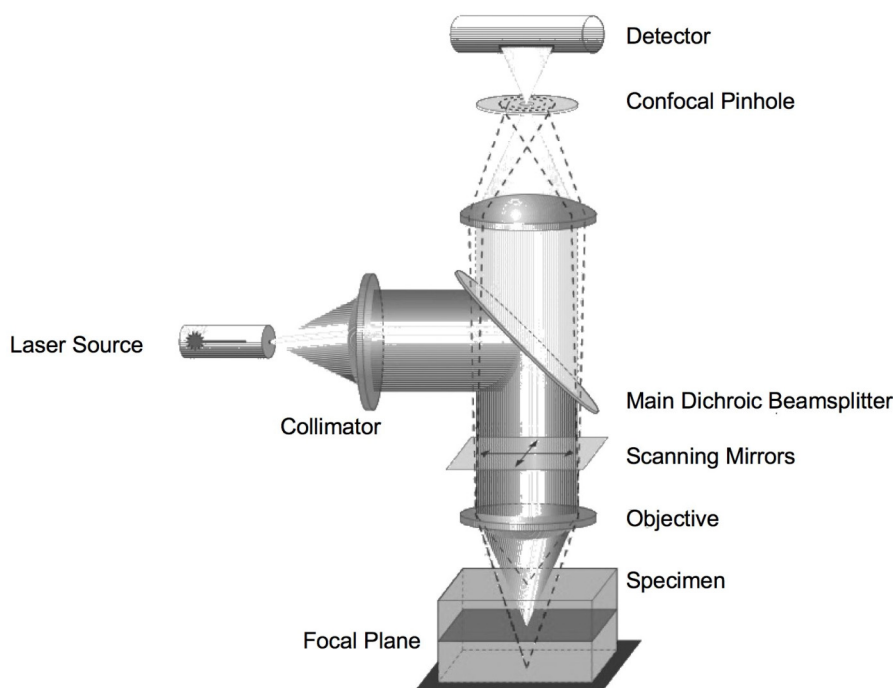


**Figure II.8: LSM 510 Meta beam path (adapted from [119]).**

In order to study the localization of Omi/HtrA2, AIF and EndoG during apoptosis, MCF-7 cells were seeded on glass coverslips coated with collagen A (10% in PBS) in 24-well plates. 1 hour prior to the end of stimulation cells were stained with 100 nM Mitotracker Red 580 (Molecular Probes, Karlsruhe, Germany). After three wash steps with PBS, cells were fixed with 4% paraformaldehyde in PBS for 15 min at room temperature, followed by permeabilization through incubation with 0.2% Triton X-100 in PBS for 2 min. Cells were blocked with 0.2% BSA and incubated with specific antibodies against Omi/HtrA2, AIF and EndoG (Table II.4). The proteins were visualized by secondary antibodies directly labeled with Alexa Fluor® 488 (Table II.5). Nuclei were stained with the fluorescent dye Hoechst 33342 (final concentration 5  $\mu\text{g}/\text{ml}$ ). Upon washing with PBS, glass coverslips were covered with one drop of aqueous mounting medium (Immunotech, Marseille, France) and mounted on a microscope slide. Dual-channel images were taken using a confocal laser scanning microscope.

Investigating the depolymerization of tubulin by spongistatin 1, MCF-7 cells were transiently transfected with an expression plasmid for EGFP-C1-tubulin (a gift from Linder, University of Munich, Germany) using the Nucleofector™ II (Amaxa, Cologne, Germany) according to manufacturer's instructions. The transfected cells were seeded on glass coverslips coated with collagen A (10% in PBS) for overnight culture. After

stimulation, cells were fixed with 4% paraformaldehyde in PBS for 15 min, washed three times, and glass coverslips were mounted in aqueous mounting medium (Immunotech, Marseille, France). Images were taken using a confocal laser scanning microscope.

## 8 WESTERN BLOT

Western Blot is a method extensively used by investigators to identify specific proteins present in a given sample usually prepared from cell lysates. Denatured proteins are first separated by mass utilizing gel electrophoresis, transferred ("blotted") onto a membrane and finally visualized by immunodetection using specific antibodies.

### 8.1 SAMPLE PREPARATION

#### 8.1.1 WHOLE CELL LYSATES

##### General lysis buffer

---

Tris-HCl, pH 7.5	30 mM
NaCl	150 mM
EDTA	2 mM
Triton X-100	1 %
Complete™	

##### Lysis buffer for phosphorylated proteins

---

Tris-HCl, pH 7.5	20 mM
NaCl	137 mM
Na <sub>4</sub> P <sub>2</sub> O <sub>7</sub>	2 mM
EDTA	2 mM
C <sub>3</sub> H <sub>7</sub> Na <sub>2</sub> O <sub>6</sub> P (Na glycerolphosphate)	20 mM
NaF	10 mM
Na <sub>3</sub> VO <sub>4</sub>	2 mM
PMSF	1 mM
Triton X-100	1 %
Glycerol	10 %
Complete™	

##### Sample buffer (5x)

---

Tris-HCl 3.125 M, pH 6.8	100 µl
Glycerol	500 µl
SDS 20 %	250 µl
DTT 16 %	125 µl
Pyronin Y 5%	5 µl
H <sub>2</sub> O	ad 1 ml

Cells were seeded (see II.2.3) and left either untreated or stimulated with spongistatin 1 or the respective positive controls. After the required incubation times cells were harvested by detachment with T/E as described in II.2.2, collected by centrifugation (1500 rpm, 10 min, 4°C) and washed with ice-cold phosphate-buffered saline (PBS). Pellets were resuspended in the appropriate lysis buffer (100  $\mu$ l for three wells) and incubated on ice for 30 min or stored at -20°C. PMSF, Na<sub>3</sub>VO<sub>4</sub> and Complete™ were added to the lysis buffer immediately before use. Lysates were centrifuged at 10,000 x g for 10 min at 4°C. Supernatants were transferred to new tubes and the protein concentration was determined by the Bradford method as described in II.8.2. Lysates were diluted 1:5 with 5 x sample buffer, boiled at 95°C for 5 min and stored at -20°C or used immediately for Western Blot analysis.

### 8.1.2 CYTOSOLIC AND MITOCHONDRIA CONTAINING FRACTIONS

The release of mitochondrial intermembrane space proteins to the cytosol is a key event during apoptosis [120, 121]. Either they are part of the activation complexes for caspases in the cytosol (cytochrome c, Smac/DIABLO, Omi/HtrA2) or they translocate into the nucleus mediating DNA fragmentation (AIF, EndoG). To analyze these proteins, the cytosol has to be separated from the mitochondria. This is accomplished by a permeabilization buffer containing a low concentration of digitonin forming complexes with cholesterol in the cell membrane. Thus, small pores are generated through which the cytosol is eluted into the iso-osmotic buffer while organelles are retained inside the cell.

#### Permeabilization buffer

Mannitol	210 mM
Sucrose	70 mM
Hepes pH 7.2	10 mM
EGTA	0.2 mM
Succinate	5 mM
BSA	0.15 % (w/v)
Digitonin	60 $\mu$ g/ml

The release of cytochrome c, Smac/DIABLO and Omi/HtrA2 from mitochondria was analyzed as described previously [122]. Briefly, cells were seeded and stimulated as for whole cell lysate preparation. Three wells for each sample were collected by centrifugation (360 x g, 10 min, 4°C) and washed with PBS. Cell pellets were resuspended in 100  $\mu$ l permeabilization buffer and incubated on ice for 20 min. The cytosolic fraction was obtained by centrifugation (360 x g, 10 min, 4°C) of the permeabilized cell suspension and the supernatant was cleared of any remaining cell fragments by centrifugation at 13,000 x g (10 min, 4°C). The remaining pellet of permeabilized cells containing the mitochondria, other organelles and membranes was resuspended in 0.1% Triton X-100 in PBS (100  $\mu$ l)

and lysed for 15 min on ice. The supernatant of the subsequent centrifugation (13,000 × g 10 min, 4°C) constitutes the mitochondria-enriched fraction. Determination of protein concentration was carried out with the Bradford method (see II.8.2). Lysates were diluted 1:5 with 5 × sample buffer and boiled at 95°C for 5 min. Afterwards samples were stored at -20°C or used immediately for Western Blot analysis.

### 8.1.3 NUCLEI ISOLATION

Translocation of Omi/HtrA2, AIF and EndoG to the nucleus was analyzed using the Nuclear Extract Kit (Active Motif, Rixensart, Belgium) according to manufacturer's protocol. Briefly, cells were seeded and stimulated as for whole cell lysate preparation, collected by centrifugation (360 × g, 10 min, 4°C) and washed with ice-cold PBS. Cell pellets were resuspended in hypotonic buffer and incubated for 15 min at 4°C to swell the membranes and make them fragile. Addition of detergent caused leakage of the cytoplasmic proteins into the supernatant. The permeabilized cells were centrifuged at 13,000 × g (1 min, 4°C), the supernatants contained the nonnucleic fraction. To obtain the nuclear proteins, pellets were resuspended in lysis buffer, incubated for 30 min at 4°C and centrifuged at 13,000 × g (10 min, 4°C). The supernatants contained the nuclear protein fraction. Determination of protein concentration was carried out with the Bradford method. Lysates were diluted 1:5 with 5 × sample buffer and boiled at 95°C for 5 min. Samples were stored at -80°C or used immediately for Western Blot analysis.

### 8.1.4 TUBULIN FRACTIONATION

Separation of soluble and insoluble tubulin fractions were analyzed according to Puthalakath et al. [123] with modifications. Briefly, cells were seeded and stimulated as for whole cell lysate preparation. Subsequently, cells were fixed with 10% Cytoskelfix™ (Cytoskeleton, Offenbach, Germany) in PBS (4 min, -20°C) retaining both actin and tubulin based structures, collected by centrifugation (360 × g, 10 min, 4°C) and washed with PBS. Cell pellets were resuspended in lysis buffer (see below) and incubated for 20 min at room temperature. The soluble fraction was obtained by centrifugation (100,000 × g, 45 min, 4°C). The supernatant represented the soluble fraction. Pellets were resuspended in disassembling buffer, incubated for 30 min at 4°C and centrifuged (1,500 × g, 10 min, 4°C). The supernatants contained the insoluble fractions. The obtained protein fractions were analyzed by Western Blot analysis or stored at -20°C.

---

**Lysis buffer**

---

PIPES, pH 6.9	100 mM
Glycerin	2 M
Triton X-100	0.5 %
MgCl <sub>2</sub>	2 mM
EGTA	2 mM
GTP	1 mM
Taxol	5 μM
PMSF	50 mM
Complete™	

---

**Disassembling buffer**

---

Tris/HCl pH 6.8	100 mM
MgCl <sub>2</sub>	1 mM
CaCl <sub>2</sub>	10 mM

## 8.2 PROTEIN QUANTIFICATION

The protein concentration in samples was quantified by the Bradford [124] method based on binding of the dye Coomassie Brilliant Blue G-250 to hydrophobic parts of proteins. After binding to proteins, the absorption maximum of this dye shifts from 465 to 595 nm and absorbance is measured at 595 nm.

To determine the protein content of the samples, first 10 μl of a calibration curve containing increasing concentrations of BSA in H<sub>2</sub>O (0 up to 25 mg/ml BSA) and 10 μl of 1:10 in H<sub>2</sub>O diluted cell lysates were incubated with 190 μl Bradford solution (Bio-Rad, Munich, Germany, diluted 1:5 in H<sub>2</sub>O) in 96-well plates for 5-10 min. Absorbance of the samples at 595 nm was measured in a microplate absorbance reader (Sunrise™, Tecan, Crailsheim, Germany). Before electrophoresis, the required volumes of 1 x sample buffer were added to the protein solutions in order to achieve the same protein concentration in all samples.

## 8.3 SDS-PAGE

Equal amounts of the protein samples described above were separated by discontinuous denaturing SDS-polyacrylamide gel electrophoresis (SDS-PAGE) according to Laemmli [125].

In order to ensure reproducibility of the technique, proteins are solubilized and denatured by the anionic detergent sodium dodecyl sulphate (SDS) binding to the hydrophobic parts of the proteins. Thereby, the negative charges of SDS destroy the

secondary and tertiary structure of the proteins. Further unfolding is achieved by the reducing agent dithiothreitol (DTT) included in the sample buffer, cleaving disulfide bonds inside the proteins. Denatured and negatively charged proteins are though drawn towards the anode in an electric field. Therefore, the final separation of the proteins in the polyacrylamide gel depends solely on their differences in the molecular weight of the polypeptides. The discontinuous electrophoresis system consists of two layers. First, proteins are concentrated in the stacking gel in order to get thin bands, directly corresponding to a better resolution and secondly are separated by their size in the separating gel. Depending on the molecular weight of the proteins to be analyzed, the polyacrylamide (PAA) (Rotiphorese™ Gel 30, Roth, Karlsruhe, Germany) concentration was adjusted to yield an optimal separation (Table II.3). Molecular weight of proteins is estimated by comparison with prestained broad range molecular weight markers (precision All Blue®, Bio-Rad, Munich, Germany; MBI-Fermentas, St. Leon-Rot, Germany).

#### Stacking gel

PAA solution 30 %	1.7 ml
Tris-HCl 1.25 M, pH 6.8	1.0 ml
SDS 10 %	100 µl
H <sub>2</sub> O	7.0 ml
TEMED	20 µl
APS 10%	100 µl

#### Separating gel

PAA solution 30 %	5.0 ml
Tris-HCl 1.5 M, pH 8.8	3.75 ml
SDS 10 %	150 µl
H <sub>2</sub> O	6.1 ml
TEMED	15 µl
APS 10 %	75 µl

**Table II.3 PAA-concentration in the separating gel.**

Protein	Acrylamide concentration
AIF, caspase-9, FAK	10 %
Bax, Bcl-2, Bcl-x <sub>L</sub> , Bid, Bim, caspase-2, -6, -7, -8, EndoG, Mcl-1, Omi/HtrA2, β-tubulin	12 %
cytochrome c, Smac	15 %

Electrophoresis was performed using a vertical Mini Protean III system (Bio-Rad, Munich, Germany) connected to a power supply (Biometra, Göttingen, Germany). Electrophoresis was run at 100 V for 21 min for stacking proteins and at 200 V for 40-42 min for the separation of proteins.

---

 Electrophoresis buffer
 

---

Tris base	3.0 g
Glycine	14.4 g
SDS	1.0 g
H <sub>2</sub> O	ad 1,000 ml

## 8.4 WESTERN BLOTTING AND DETECTION

After separation of the protein mixture by electrophoresis, proteins are transferred onto blotting membranes binding proteins with high affinity. The membranes are better to handle than the gels and the blotting process concentrates proteins, thus increasing sensitivity of the subsequent detection of proteins by binding to specific antibodies and visualization by chemiluminescence or fluorescence.

The Western Blot analysis was carried out by the tank blotting technique. Nitrocellulose membranes (Hybond<sup>TM</sup>-ECL<sup>TM</sup>, Amersham Biosciences, Freiburg, Germany) were activated by soaking in freshly prepared 1 x tank buffer for at least 15 minutes. Transfer sandwiches were assembled in a box containing 1 x tank buffer as follows:

---

 Sandwich holder cathode side (black)
 

---

Wetted pad  
 Soaked blotting paper  
 Gel  
 Membrane  
 Soaked blotting paper  
 Wetted pad

---

 Sandwich holder anode side (white)
 

---

Sandwiches were mounted in a transfer device (Mini Trans-Blot®, Bio-Rad, Munich, Germany), the electrophoresis chamber was filled with 1 x tank buffer and transfer was performed at 4°C at 100 V for 90 min or at 23 V overnight, with magnetic stirring.

---

 Tank buffer (5x)
 

---

Tris base	15.2 g
Glycine	72.9 g
H <sub>2</sub> O	ad 1,000 ml

---

 Tank buffer (1x)
 

---

Tank buffer (5x)	200 ml
Methanol	200 ml
H <sub>2</sub> O	ad 1,000 ml

Prior to the immunological detection of the relevant proteins, unspecific protein binding sites were blocked by incubating the membranes in 5% non-fat dry milk in Tris-buffered saline with Tween 20 (TBS-T) for 1 h at room temperature. The membranes were washed shortly in TBS-T and incubated in the respective primary antibody solutions in 5% BSA in TBS-T (Table II.4) either overnight at 4°C or for 3 h at room temperature. After three wash steps in TBS-T for 10 minutes respectively, membranes were incubated with the secondary antibodies (Table II.5) either conjugated to horseradish peroxidase or fluorophores, in 1% non-fat dry milk in TBS-T for 1 h at room temperature. The membranes were washed 3 times as described above. All steps regarding the incubation of the membrane were performed under gentle agitation.

**Table II.4: Primary antibodies.**

Primary antibody	Isotype	Dilution	Company
AIF	rabbit IgG	1:1,000	Upstate, Lake Placid, USA
Bax	rabbit IgG	1:1,000	Santa Cruz Biotechnology, Heidelberg, Germany
Bax 6A7	mouse IgG <sub>1</sub>	1:1,000	BD Transduction Laboratories, Heidelberg, Germany
Bcl-2	mouse IgG <sub>1</sub>	1:1,000	Merck Biosciences, Darmstadt, Germany
Bcl-x <sub>L</sub>	rabbit IgG	1:1,000	Cell Signaling, Frankfurt, Germany
Bid	rabbit IgG	1:1,000	Cell Signaling, Frankfurt, Germany
Bim	rabbit IgG	1:1,000	Merck Biosciences, Darmstadt, Germany
caspase-2	mouse IgG <sub>1</sub>	1:1,000	BD Biosciences, Heidelberg, Germany
caspase-6	rabbit IgG	1:1,000	Cell Signaling, Frankfurt, Germany
caspase-7	mouse IgG <sub>1</sub>	1:1,000	BD PharMingen, Heidelberg, Germany
caspase-8	rabbit IgG	1:1,000	Upstate, Lake Placid, USA
caspase-9	rabbit IgG	1:1,000	Cell Signaling, Frankfurt, Germany
cytochrome c	mouse IgG <sub>2b</sub>	1:1,000	BD PharMingen, Heidelberg, Germany
cytochrome c oxidase	mouse IgG <sub>2a</sub>	1:1,000	Molecular Probes Invitrogen, Carlsbad, USA
EndoG	rabbit IgG	1:1,000	Prosci incorporated, Poway, USA
FAK-tot	mouse IgG	1:1,000	Santa Cruz Biotechnology, Heidelberg, Germany
FAK-Tyr397	rabbit IgG	1:1,000	Santa Cruz Biotechnology, Heidelberg, Germany
Mcl-1	rabbit IgG	1:1,000	Cell Signaling, Frankfurt, Germany
Omi/HtrA2	rabbit IgG	1:1,000	R&D Systems, Minneapolis, USA
Smac/DIABLO	rabbit IgG	1:1,000	Biozol, Eching, Germany
β-tubulin	mouse IgG <sub>2b</sub>	1:1,000	Santa Cruz Biotechnology, Heidelberg, Germany

**Table II.5: Secondary antibodies.**

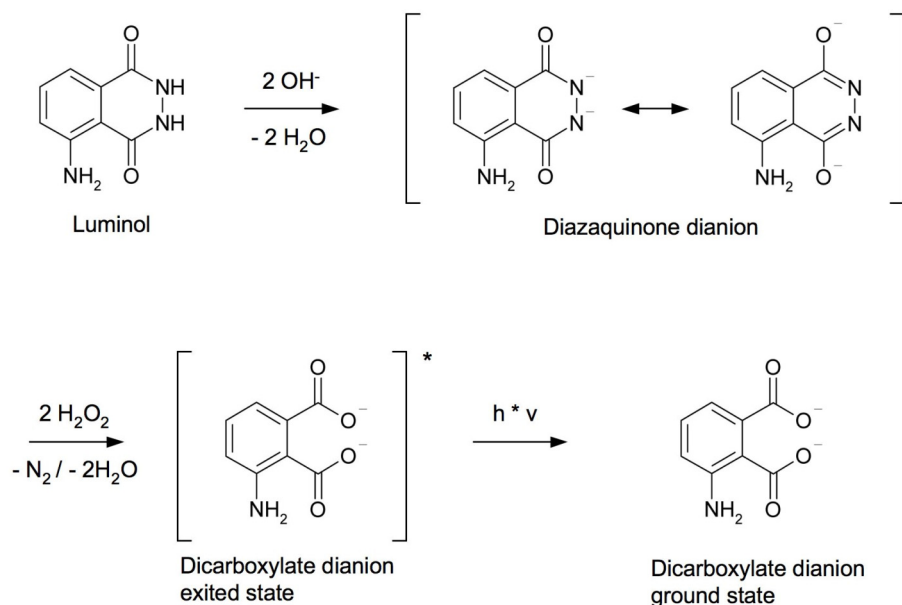
Secondary antibody	Dilution	Company
goat anti mouse IgG <sub>1</sub> :HRP	1:1,000	Biozol, Eching, Germany
goat anti rabbit:HRP	1:10,000	Dianova, Hamburg, Germany
goat anti mouse IgG <sub>2A</sub> :HRP	1:1,000	Biozol, Eching, Germany
Alexa Fluor <sup>®</sup> 680 goat anti rabbit IgG	1:10,000	Molecular Probes/Invitrogen, Karlsruhe, Germany
Alexa Fluor <sup>®</sup> 680 goat anti mouse IgG	1:10,000	Molecular Probes/Invitrogen, Karlsruhe, Germany
TrueBlot anti rabbit:HRP	1:1,000	NatuTec, Frankfurt, Germany

TBS-T (pH 8.0)

Tris base	3.0 g
NaCl	11.1 g
Tween 20	1 ml
H <sub>2</sub> O	ad 1,000 ml

In order to visualize the proteins, two different methods have been used depending on the labels of secondary antibodies.

On the one hand, luminol was utilized as a substrate for horseradish peroxidase (HRP)-coupled secondary antibodies. To visualize the proteins of interest, membranes were incubated in ECL Plus<sup>™</sup> Western Blotting detection reagent (Amersham Biosciences, Freiburg, Germany). The enzyme HRP catalyzes the oxidation of luminol in the presence of H<sub>2</sub>O<sub>2</sub> (Figure II.9). The appearing luminescence was detected by exposure of the membrane to an X-ray film (Super RX, Fuji, Düsseldorf, Germany) for the appropriate time periods and subsequently developed in a tabletop film processor (Curix 60, Agfa, Cologne, Germany).

**Figure II.9: HRP-luminol reaction.**

On the other hand, antibodies directly labeled with the fluorophor Alexa Fluor® 680 exhibiting an emission at 680 nm were used to detect proteins of interest by the Odyssey imaging system (Li-Cor Biosciences, Lincoln, NE).

## 8.5 MEMBRANE STRIPPING

After carrying out a Western Blot experiment membranes can be re-used for the detection of different proteins. Bound antibodies resulting from the previous experiment must be removed to avoid cross reactions and mistaken results. For this purpose, after development membranes were washed three times for 10 minutes in TBS-T and incubated in stripping buffer for 30 min at 50°C on a shaking platform. Afterwards membranes were thoroughly washed (6 x 5 minutes) to remove any remnants of stripping buffer and developed with ECL Plus™ solution to confirm stripping effectiveness. Membranes were washed one time, blocked in 5% non-fat dry milk in TBS-T for 1 h at room temperature and incubated with primary and secondary antibodies as described in II.8.4.

### Stripping buffer

---

Tris-HCl	62.5 mM
SDS	2 %
2-Mercaptoethanol	100 mM

2-Mercaptoethanol was added to the stripping buffer immediately before use.

## 8.6 STAINING OF GELS AND MEMBRANES

Equal protein loading and blotting of samples was checked by staining of gels and membranes after Western Blot experiments. A commonly used dye for detecting proteins in polyacrylamide gels is Coomassie blue, which penetrates the gel and sticks permanently to the proteins. Excess dye is washed out by destaining solution. The transfer of proteins to the membranes was checked incubating the membranes with the dye Ponceau S, directly staining the proteins reversibly in contrast to Coomassie blue.

After the tank blot procedure gels were stained with the Coomassie blue solution for 15 minutes at room temperature. Afterwards gels were washed several times in destaining solution until the proteins appeared as blue bands against a clear background.

### Coomassie staining solution

---

Coomassie Blue	3 g
Glacial acetic acid	100 ml
Ethanol	450 ml
H <sub>2</sub> O	ad 1,000 ml

---

**Destaining solution**

---

Glacial acetic acid	100 ml
Ethanol	300 ml
H <sub>2</sub> O	ad 1,000 ml

After development membranes were stained in Ponceau S staining solution (0.2% Ponceau S in 5% acetic acid) for 5 minutes on a shaking platform. Membranes were washed in H<sub>2</sub>O until the background disappeared. To remove the Ponceau S staining completely, membranes were washed several times in TBS-T.

## 9 IMMUNOPRECIPITATION

Immunoprecipitation is a method used for the enrichment of proteins of interest out of a multitude of proteins. Therefore, a specific antibody is incubated with the cell lysate to form an antigen-antibody complex. This complex can be precipitated e.g. by addition of Protein G or Protein A, which have a high affinity to the Fc-part of immunoglobulins. After dissociation and denaturation of proteins by boiling, the precipitate can be analyzed by Western Blot analysis.

Cells were seeded and stimulated as for whole cell lysate preparation. 50  $\mu$ l Protein A sepharose beads (Sigma, Deisenhofen, Germany) for each sample were centrifuged, washed and resuspended in lysis buffer. 2.5  $\mu$ l of the respective primary antibody was added per 50  $\mu$ l Protein A solution and gently inverted overnight at 4°C. Cells were collected by centrifugation (360 x g, 10 min, 4°C), washed with ice-cold PBS and lysed in general lysis buffer. The content of protein was determined by the Bradford method (described in II.8.2). Simultaneously, the Protein A-antibody solution was centrifuged (3,000 x g, 2 min, 4°C) and carefully washed three times with lysis buffer. Equal amounts of protein (300-400  $\mu$ g) were filled up to a volume of 250  $\mu$ l with lysis buffer and added to the antibody beads mixture. To allow the immune complex to form, the samples were gently shaken for 3 hours at 4°C by end over end rocking. Next, the precipitated proteins were harvested by centrifugation (14,000 rpm, 10 min, 4°C). 40  $\mu$ l of the supernatant were kept as a binding control. The remaining pellet was carefully washed three times with 500  $\mu$ l lysis buffer. After completely removing the last wash solution, samples were mixed with Laemmli sample buffer (see below) containing 2-mercaptoethanol, boiled at 95°C for 5 minutes and analyzed by Western Blot.

The immunoprecipitation and detection of proteins with antibodies from the same species is often associated with antibody cross-reactivities and hindrance by interfering with the immunoprecipitating immunoglobulin heavy and light chains. Rabbit IgG TrueBlot™

(NatuTec, Frankfurt, Germany) enables the detection of immunoblotted target protein bands without this hindrance. TrueBlot™ preferentially detects the non-reduced form of rabbit IgG over the reduced, SDS-denatured form of IgG. When the immunoprecipitate is fully reduced, immediately prior to SDS-gel electrophoresis, the reactivity of Rabbit TrueBlot™ with 55 kDa heavy chains and the 23 kDa light chains of the immunoprecipitating antibody is minimized. Thereby the interference by the heavy and light chains of the immunoprecipitating antibody in immunoblotting applications is eliminated.

Cells were seeded and stimulated as for whole cell lysate preparation (II.8.1.1). Cells were collected by centrifugation (360 x g, 10 min, 4°C), washed with ice-cold PBS and lysed in general lysis buffer. The content of protein was determined by Bradford method. To pre-clear the cell lysate 50 µl of anti-rabbit IgG beads (NatuTec, Frankfurt, Germany) and 500 µl of cell lysate sample were incubated on ice for 30 min. After centrifugation (10,000 x g, 3 min, 4°C), 5 µg of the primary antibodies were added to the supernatant and incubated on ice for one hour. Subsequently 50 µl of anti-rabbit IgG beads were added to the samples and incubated for another hour on a rocking platform at 4°C. Next, the precipitated proteins were harvested by centrifugation (10,000 rpm, 1 min, 4°C) and 40 µl of the supernatant were kept as a binding control. The remaining pellet was carefully washed three times with 500 µl lysis buffer. After completely removing the last wash solution, samples were mixed with Laemmli sample buffer containing 2-mercaptoethanol, boiled at 95°C for 10 minutes and analyzed by Western Blot. As secondary antibody the Rabbit IgG TrueBlot™ (NatuTec, Frankfurt, Germany) at a 1:1,000 dilution in 5% Blotto is used. To visualize the proteins of interest, membranes were incubated in ECL Plus™ Western Blotting detection reagent (Amersham Biosciences, Freiburg, Germany) as described in II.8.4.

#### Laemmli sample buffer (3x)

Tris-HCl	187.5 mM
SDS	6 %
Glycerol	30 %
Bromphenol blue	0.015 %
2-Mercaptoethanol	12.5 %
H <sub>2</sub> O	

2-Mercaptoethanol was added to the buffer immediately before use.

## 10 GENE SILENCING BY RNA INTERFERENCE

The term RNA interference (RNAi) describes the ability of double stranded RNA (dsRNA) to target specific mRNAs for degradation, thereby silencing their expression. For the discovery of this powerful technique that allows highly specific suppression of individual gene function, Craig Mello and Andrew Fire obtained the Nobel Prize in Physiology of Medicine in 2006. Downregulation of the gene of interest can be achieved by introduction of double-stranded short interfering RNAs (siRNAs) into the cells or by producing the silencing RNA within the cells employing expression vectors [126].

The heart of RNA interference is the short interfering RNA, typically consisting of two 21-nucleotide (nt) single-stranded RNAs that form a 19-bp duplex with 2-nt 3' overhangs. Long dsRNA molecules are processed by an enzyme called Dicer to form siRNA. The antisense strand of the siRNA is used by the RNA interference silencing complex (RISC) to guide mRNA cleavage, so promoting RNA degradation (Figure 2.5, modified from [126]). In the present work, post-Dicer cleavage products (siRNAs) are used to initiate RNA interference.

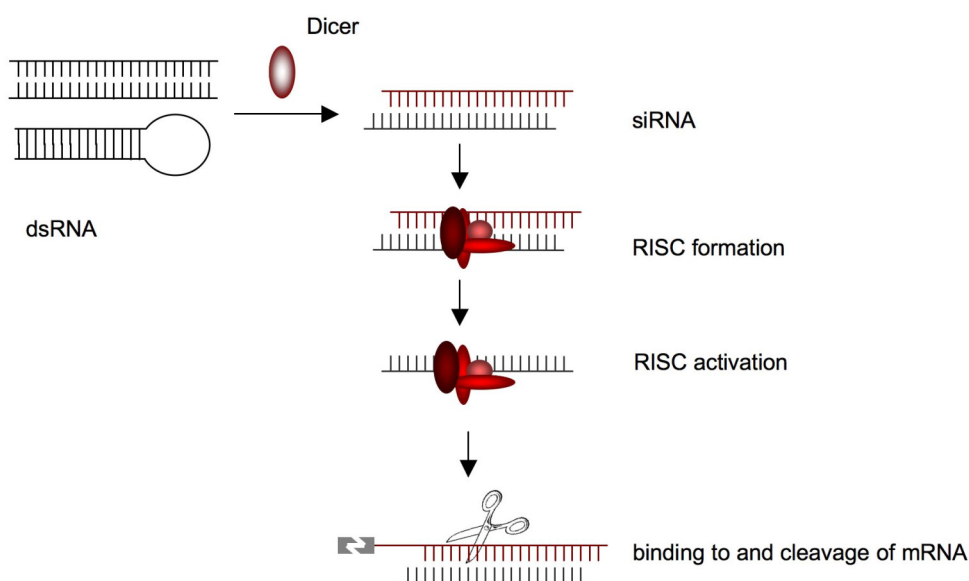


**Figure II.10: Short interfering RNA.**

RNA interference is a powerful method for sequence-specific inhibition of gene function. 21-23 nucleotides long small interfering (si)RNAs are cleaved by DICER out of long dsRNAs. These siRNAs can be also chemically synthesized for laboratory use. The antisense strand is guided to the RNA induced silencing complex (RISC), where the corresponding mRNA strand is bound and degraded, leading to gene silencing.

Sense and antisense siRNA oligonucleotides of Bim (sense: 5'-caauugaccuucucgg(dTdT)-3'; antisense: 5'-ccgagaagguagacaauug(dTdT)-3')[127], sense and antisense siRNA oligonucleotides of EndoG (sense: 5'-augccuggaacaaccugga(dTdT)-3'; antisense: 5'-uccagguuguuccaggcau(dTdT)-3') [128], sense and antisense siRNA oligonucleotides of AIF (sense: 5'-ggaaauaugggaaagauc(dTdT)-3'; antisense: 5'-ggaucuuucccauauuucc(dTdT)-3') [129], sense and antisense siRNA oligonucleotides of Bcl-2 (sense: 5'-caggaccugccgcugcagacc(dTdT)-3'; antisense: 5'-ggucugcagcggcgagguccuggc(dTdT)-3') [130], sense and antisense siRNA oligonucleotides of Bcl-x<sub>L</sub> (sense: 5'-caggacagcauauagag(dTdT)-3'; antisense: 5'-guccugucguauagucuc(dTdT)-3') [131] and oligonucleotides corresponding to a nonsense sequence were purchased from Biomers.net GmbH (Ulm, Germany). Sense and antisense siRNA oligonucleotides of Omi/HtrA2 (sense: 5'-aacggcucaggauucgugg(dTdT)-3'; antisense: 5'-ccacgaauccugagccguu(dTdT)-3') were obtained from Dharmacon (Lafayette, CO, USA).

The single stranded siRNA oligonucleotides were dissolved to 100 μM stock solutions in RNase free water (DEPC H<sub>2</sub>O) and annealed to create the 20 μM double-stranded siRNAs as follows: 15 μl of sense and 15 μl of antisense siRNA were combined with 30 μl RNase free water and 15 μl annealing buffer (Ambion, Hamburg, Germany). This solution was incubated at 90°C for 1 minute and was left to cool down until the temperature reached 37°C. Afterwards, the double stranded siRNA was incubated for further 5 minutes at room temperature and stored at -20°C.

2 × 10<sup>6</sup> cells in the exponential growing phase were transfected with 2.5 μg of nonsense, Bim siRNA, EndoG siRNA, AIF siRNA, Omi/HtrA2 siRNA, Bcl-2 siRNA or Bcl-x<sub>L</sub> siRNA by electroporation using the Nucleofector™ II (Amaxa, Cologne, Germany) according to manufacturer's instructions. Cells were seeded and stimulated 24 h after nucleofection. Efficiency of RNA interference was checked by Western Blot analysis using antibodies against Bim, EndoG, AIF and Omi/HtrA2.

## 11 STATISTICS

All experiments were performed at least three times. Results are expressed as mean value ± S.E. One-way statistical analysis was performed with GraphPad Prism™ version 3.03 for Windows (GraphPad Software, San Diego, CA). Statistical comparisons were made by one-way ANOVA with Bonferroni. P values < 0.05 were considered significant.



## **RESULTS**

### III RESULTS

#### 1 CYTOTOXICITY OF SPONGISTATIN 1

Two major problems in chemotherapy are the metastatic spread of tumor cells to secondary sites and the frequently developed resistance of cancer cells to anticancer agents. Therefore, the cytotoxic effects of spongistatin 1 were examined in different cancer cell lines, some being quite insensitive to many chemotherapeutic agents probably caused by defects in the apoptotic machinery or by being highly invasive. The epithelial breast cancer cell line MCF-7 is characterized by a deficiency in caspase-3 owing to a deletion mutation [132]. SK-Mel-5 is a melanoma cell line derived from a very aggressive form of skin cancer, which is resistant probably due to low Apaf-1 levels [133, 134] to most forms of therapy including combined applications of chemotherapy and immunotherapy [135]. The human ovary adenocarcinoma cell line SK-OV-3 is featured by depletion of the tumor suppressor gene p53, thus making these cells resistant to tumor necrosis factor and several cytotoxic drugs including cisplatin. The human pancreatic cancer cell line Panc-1 is characterized by its aggressive behavior. Bruns et al. [112] generated the highly metastatic human pancreatic cancer cell line L3.6pl by injecting COLO 357 fast-growing cells into the pancreas of nude mice. After the establishment of a tumor, hepatic metastases were harvested and tumor cells were reinjected into the pancreas. This cycle was repeated several times to yield the L3.6pl (pancreas to liver) cell line.

##### 1.1 APOPTOSIS INDUCTION BY SPONGISTATIN 1

###### 1.1.1 CHARACTERISTIC APOPTOTIC FEATURES CAUSED BY SPONGISTATIN 1

As described in I4, apoptotic cells are characterized by typical morphological alterations. Apoptotic cells round up, detach and undergo morphological changes including cell shrinkage and the formation of apoptotic bodies. Besides changes in size and shape of the entire cell, the nucleus of an apoptotic cell is subject of numerous biochemical processes. EndoG and other enzymes condense the chromatin and ultimately the DNA is fragmented by endonucleases.

MCF-7 cells exposed to spongistatin 1 for 48 h revealed a typical morphology of dying cells (Figure III.1A): MCF-7 cells appeared shrunken and rounded with the formation of apoptotic bodies. Furthermore, upon staining the spongistatin 1 treated MCF-7 cells with the vital dye Hoechst 33342, the condensation of DNA, a characteristic feature of apoptotic cell death, was clearly observed. Untreated cells showed faint staining, whereas treated cells appeared bright indicating chromatin condensation (Figure III.1B).

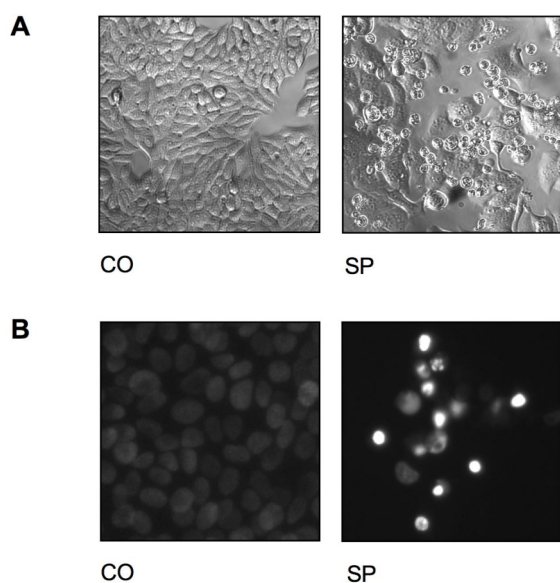


**Figure III.1: Morphological alterations in spongistatin 1-treated MCF-7 cells.**

MCF-7 cells were left untreated (CO) or stimulated with spongistatin 1 (SP; 500 pM) for 48 h. **(A)** Morphological alterations were analyzed by light microscopy. **(B)** Nuclei were stained with Hoechst 33342 and analyzed by fluorescence microscopy. Representative pictures out of three experiments are shown.

### 1.1.2 SPONGISTATIN 1 INHIBITS METABOLIC ACTIVITY

Moreover, the cytotoxic effect of spongistatin 1 was investigated by the MTT assay measuring the metabolic activity as a parameter for cell viability. As shown in Figure III.2, spongistatin 1 reduced the mitochondrial respiratory activity of MCF-7 cells in a concentration- and time-dependent manner. Spongistatin 1 was effective at concentrations as low as 500 pM and with as little as 16 h of exposure to MCF-7 cells.

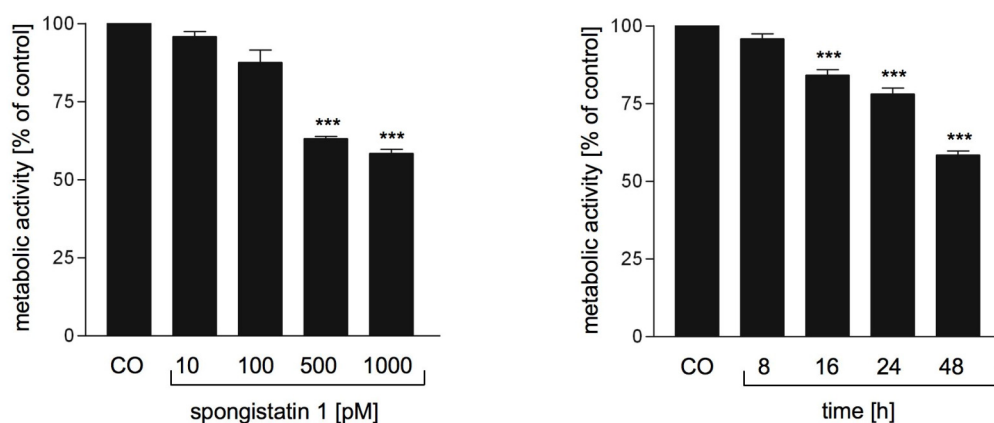


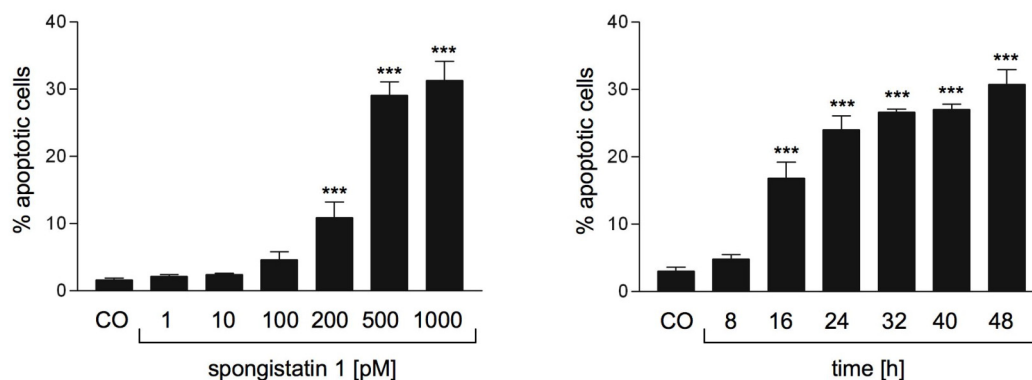
**Figure III.2: Spongistatin 1 induces dose- and time-dependent cell death in MCF-7.**

MCF-7 cells were left untreated (CO) or stimulated with increasing concentrations of spongistatin 1 for 48 h (left panel), or were treated with spongistatin 1 (SP; 500 pM) for the indicated times (right panel). Impairment of metabolic activity was analyzed by MTT assay. *Bars*, the mean  $\pm$  S.E. of three independent experiments performed in triplicate. \*\*\*,  $p < 0.001$  (ANOVA/Bonferroni).

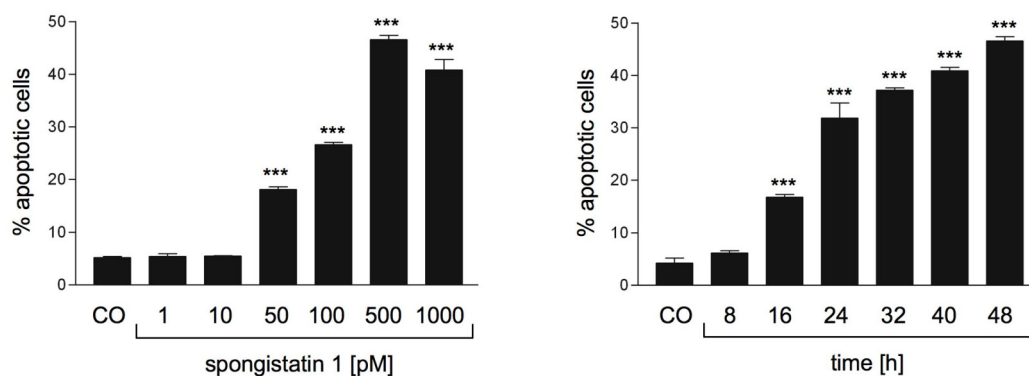
### 1.1.3 DNA FRAGMENTATION IN DIFFERENT CANCER CELL LINES

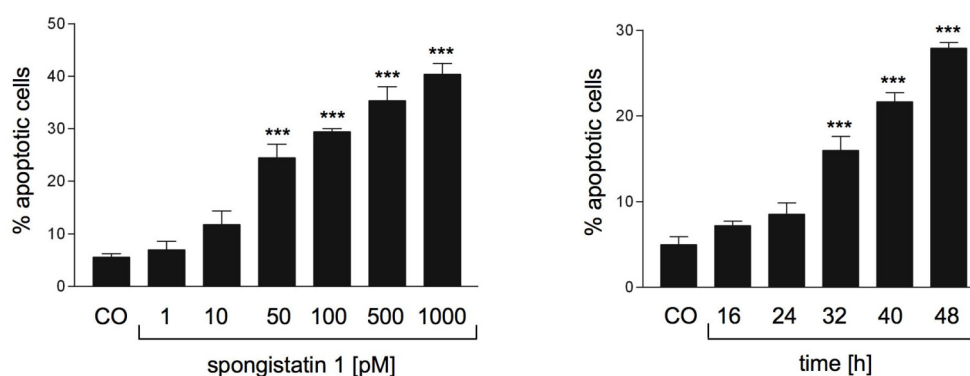
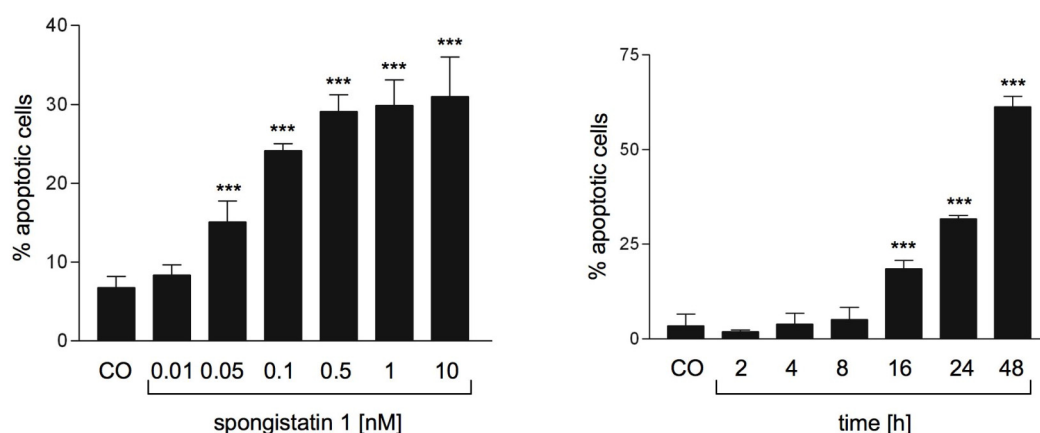
In order to quantify the apoptotic potential of spongistatin 1, a classical feature of apoptosis, DNA fragmentation, was measured by flow cytometry of propidium iodide stained cells according to the Nicoletti method (described in II.3.2). In line with its ability to decrease the metabolic activity, spongistatin 1 induced apoptosis in a time- and dose-dependent manner in MCF-7 cells (Figure III.3A). The appearance of apoptotic cells was significant at a concentration as low as 200 pM and 16 h upon treatment with spongistatin 1 (500 pM). Importantly, the apoptosis-inducing effect of spongistatin 1 is not limited to MCF-7 cells. Additionally, spongistatin 1 potently induced DNA fragmentation in the chemoresistant cell lines SK-Mel-5 and SK-OV-3 as well as in the highly invasive pancreatic cancer cell line L3.6pl. In SK-Mel-5 melanoma cells apoptosis was already significantly induced at a concentration of 50 pM and 16 h exposure of spongistatin 1, whereas a significant onset of DNA-fragmentation in SK-OV-3 started at 32 h. In the pancreatic cancer cell line L3.6pl apoptotic cells became significant after 16 h and at a concentration as low as 50 pM.

#### A MCF-7



#### B SK-Mel-5



**C SK-OV 3****D L3.6pl**

**Figure III.3: Spongistatin 1 induces dose- and time-dependent DNA fragmentation.**

MCF-7, SK-Mel-5, SK-OV-3 or L3.6pl cells were left untreated (CO) or stimulated with increasing concentrations of spongistatin 1 for 48 h (left panels), or were treated with 500 pM spongistatin 1 for the indicated times (right panels). SK-OV-3 cells were stimulated with 100 pM spongistatin 1. Apoptotic cells were quantified by flow cytometry. Bars, the mean  $\pm$  S.E. of three independent experiments performed in triplicate. \*\*\*,  $p < 0.001$  (ANOVA/Bonferroni).

#### 1.1.4 SPONGISTATIN 1 INDUCES CELL CYCLE ARREST AT G<sub>2</sub>/M PHASE

Microtubule-interacting agents usually induce a cell cycle arrest at G<sub>2</sub>/M phase followed by apoptosis induction [11]. The cell cycle is the series of events during a cell replication period comprised of the mitosis and interphase, the latter subdividing into G<sub>1</sub>/G<sub>0</sub>, S and G<sub>2</sub> phase depending on the amount of DNA per cell. A major defining characteristic for G<sub>1</sub>/G<sub>0</sub> is a single DNA content, whereas for G<sub>2</sub> a double DNA content. Since spongistatin 1 has been described as a depolymerizing agent of the microtubule network [24], it has been hypothesized to arrest the cell cycle at the G<sub>2</sub>/M phase.

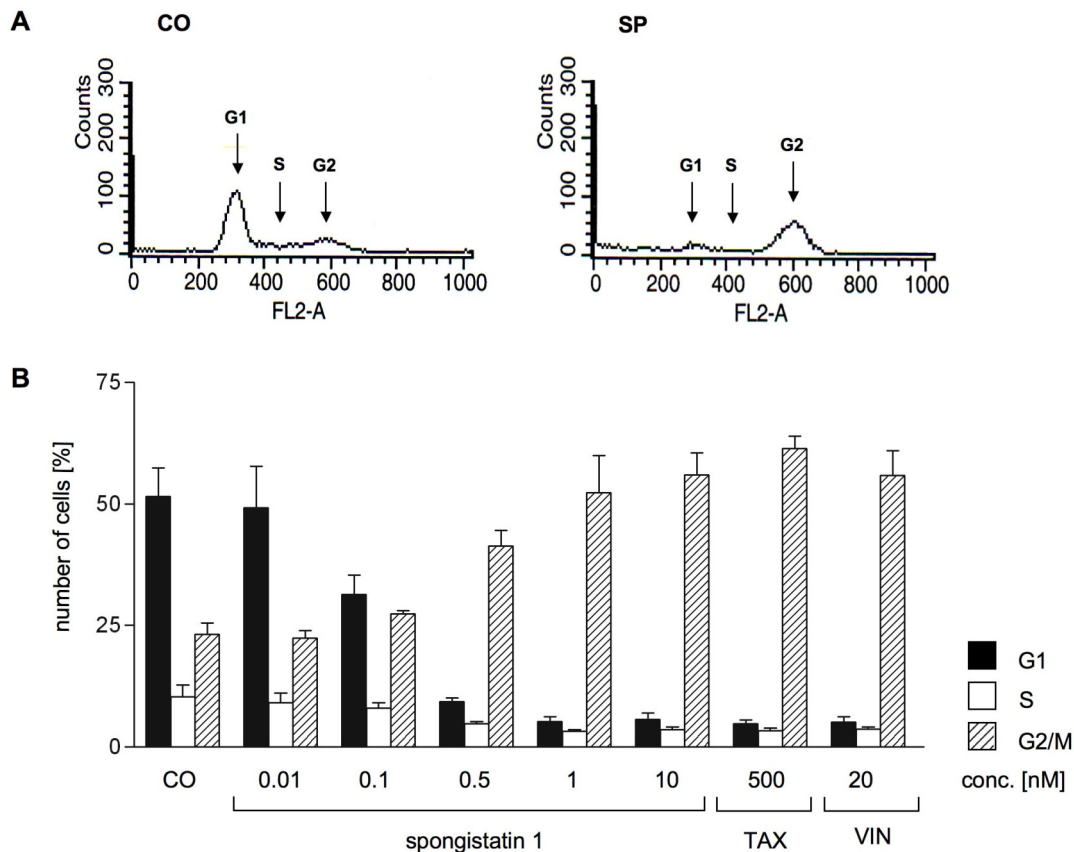


**Figure III.4: Spongistatin 1 induces cell cycle arrest in L3.6pl cells.**

(A) L3.6pl cells were either left untreated (CO) or stimulated with spongistatin 1 (SP; 500 pM) for 24 h. Cells were harvested and stained with PI as for Nicoletti method (described in II.3.2). Cell cycle distribution was quantified by flow cytometry. A representative histogram out of three independent experiments is shown. (B) L3.6pl cells were left untreated (CO) or stimulated with spongistatin 1 in increasing concentrations (SP; 0.01 to 10 nM), taxol (TAX; 500 nM) or vinblastine (VIN; 20 nM) for 24 h. Cells were harvested and stained with PI as for Nicoletti method (described in II.3.2). The distribution of cells in the different cell cycle phases was measured by flow cytometry. For each stimulation three bars are shown corresponding to  $G_1/G_0$ , S and  $G_2$ , respectively. Bars, the mean  $\pm$  S.E. of three independent experiments performed in triplicate.

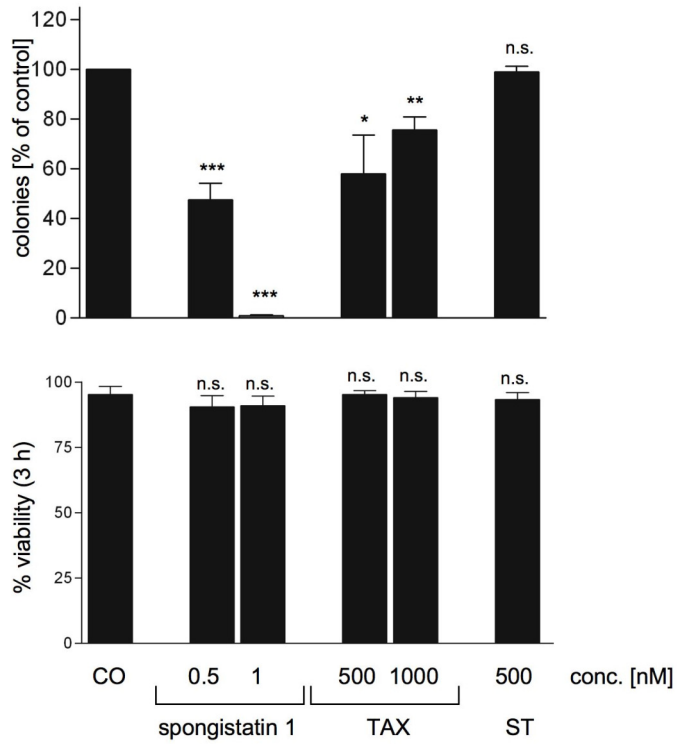
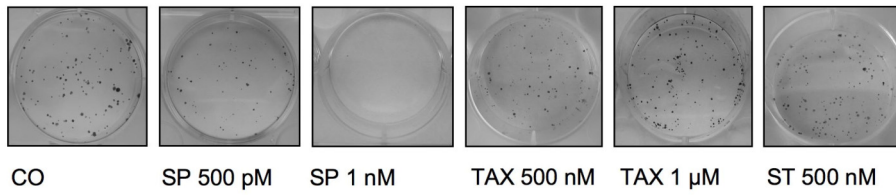
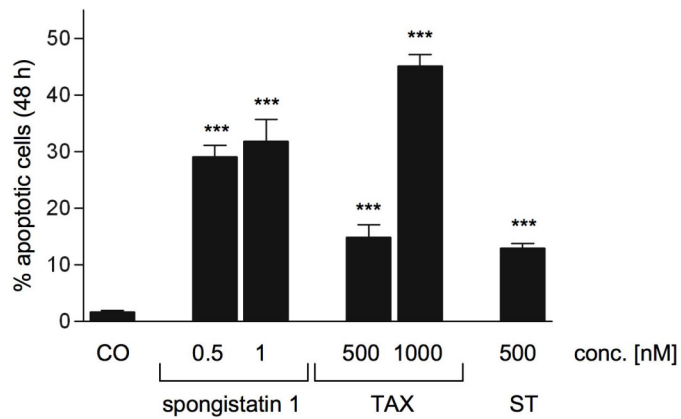
Indeed, treatment of L3.6pl cells with increasing concentrations of spongistatin 1 resulted in a  $G_2/M$  cell cycle arrest in a concentration dependent way, being significant at a concentration of 500 pM. In detail, the number of cells in  $G_1/G_0$  phase was significantly decreased, whereas in contrast the number of cells in  $G_2$  clearly increased (Figure III.4). These results are consistent with the concentration dependent DNA fragmentation upon spongistatin 1 treatment of L3.6pl cells (Figure III.3D). As a positive control, the tubulin interacting agents taxol and vinblastine, which are well known to induce apoptosis by stabilizing or depolymerizing microtubules respectively, were used because they also arrest the cell cycle at  $G_2/M$  phase.

## 1.2 SPONGISTATIN 1 STRONGLY INHIBITS CLONOGENIC SURVIVAL OF TUMOR CELLS

The colony formation assay is an *in vitro* cell survival assay to determine the effectiveness of cytotoxic agents. This assay basically tests every single cell in the population for its ability to undergo unlimited division. In contrast to short term tests, e.g. DNA fragmentation or MTT assay, the cells are allowed to grow over an extended time period of one week following a short period of stimulation of 3 h. This setting is related more closely to *in vivo* conditions in chemotherapy. Thus, it can be determined whether the percentage of cells that do not show DNA fragmentation or are still viable in the MTT assay die later or are able to grow and to form new colonies, a characteristic of chemoresistant and metastatic tumor cells.

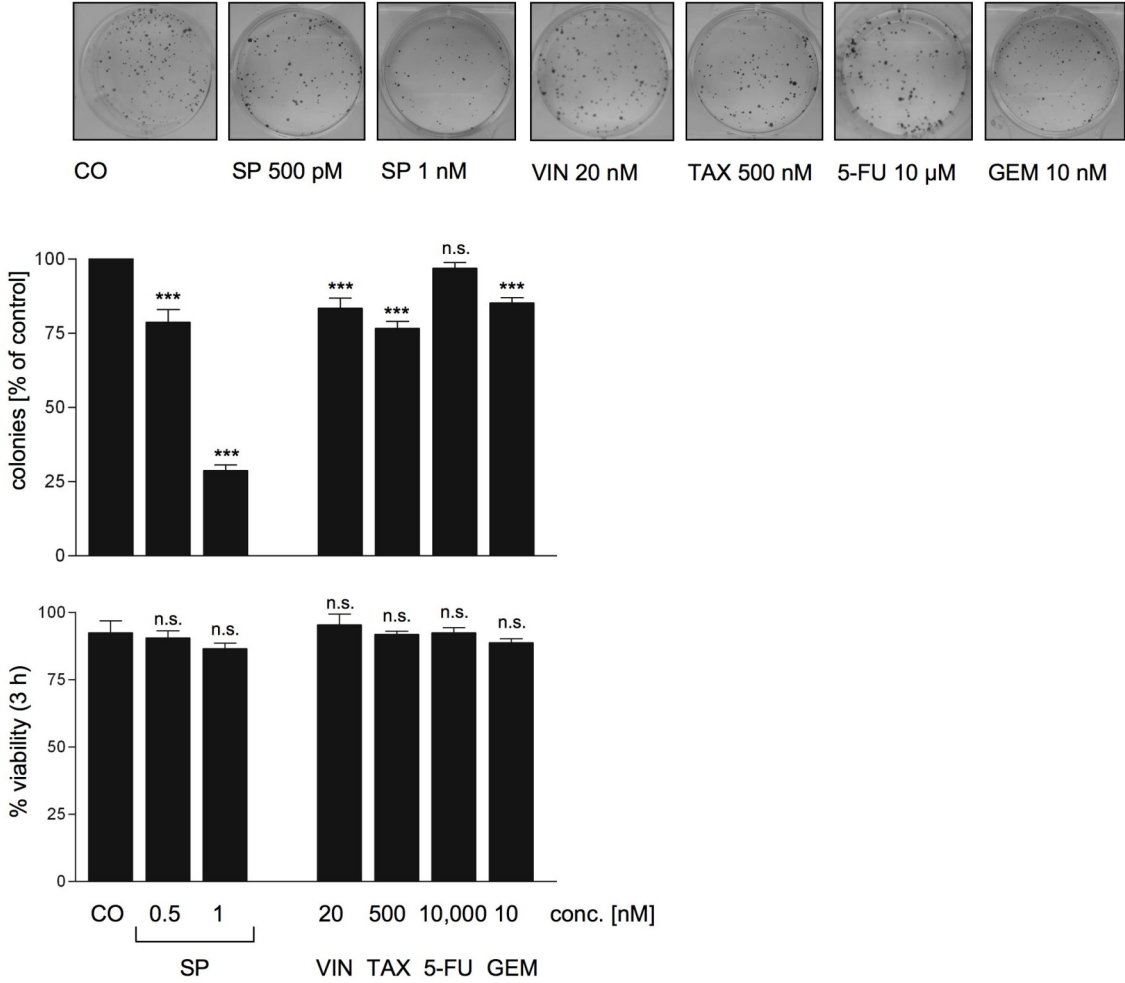
Stimulation of MCF-7 cells with spongistatin 1 (SP; 500 pM) reduced the growth of colonies by approximately 50% in comparison to the untreated cells, whereas a stimulation with a higher concentration of spongistatin 1 (1 nM) eliminated the formation of colonies completely (Figure III.5A). Exposure of cells to staurosporine (500 nM) did not inhibit the survival of MCF-7 cells. Although taxol induced apoptosis in MCF-7 cells in concentration corresponding the apoptosis rate of spongistatin 1 (1 nM) (Figure III.5B), it reduced MCF-7 colony formation by only 40% and 30%, respectively. The lower panel shows the viability of the cells 3 h after treatment, the point at which the cells are seeded to grow in colonies, measured by the trypan blue exclusion assay. In both untreated and treated cells, the viability was about 95%, indicating that the cells did not undergo necrosis to this 3 hours time point. This strong effect of spongistatin 1 on the clonogenic survival was not limited to MCF-7 cells, as this experiment could be repeated using the highly invasive pancreatic cancer cell lines Panc-1 and L3.6pl, with consistent results. In these cell lines vinblastine and taxol as well as the two anticancer compounds used as standard therapy in the treatment of pancreatic cancer, 5-fluoruracil and gemcitabine, just showed marginal effects on the clonogenic survival. The concentrations of these substances were chosen by their potential to induce DNA fragmentation by about 30%, the same range as the DNA fragmentation by spongistatin 1.

In all three cell lines tested, spongistatin 1 treatment resulted in a strong inhibition of clonogenic tumor growth, as shown in Figure III.5A. Most importantly, other chemotherapeutic agents, such as the tubulin-antagonists taxol and vinblastine, which were also able to induce apoptosis to a comparable extent than spongistatin 1 assured by DNA fragmentation, revealed a minor capacity of inhibiting the growth of MCF-7 cells, L3.6pl cells or Panc-1 cells.

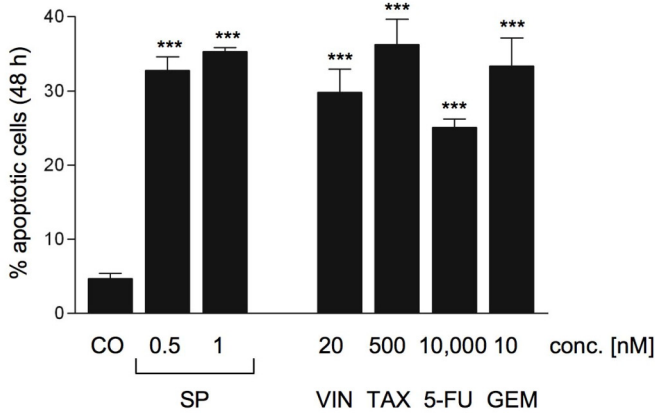
**MCF-7****A long term effects****B short term effects**

**Panc-1**

**A long term effects**

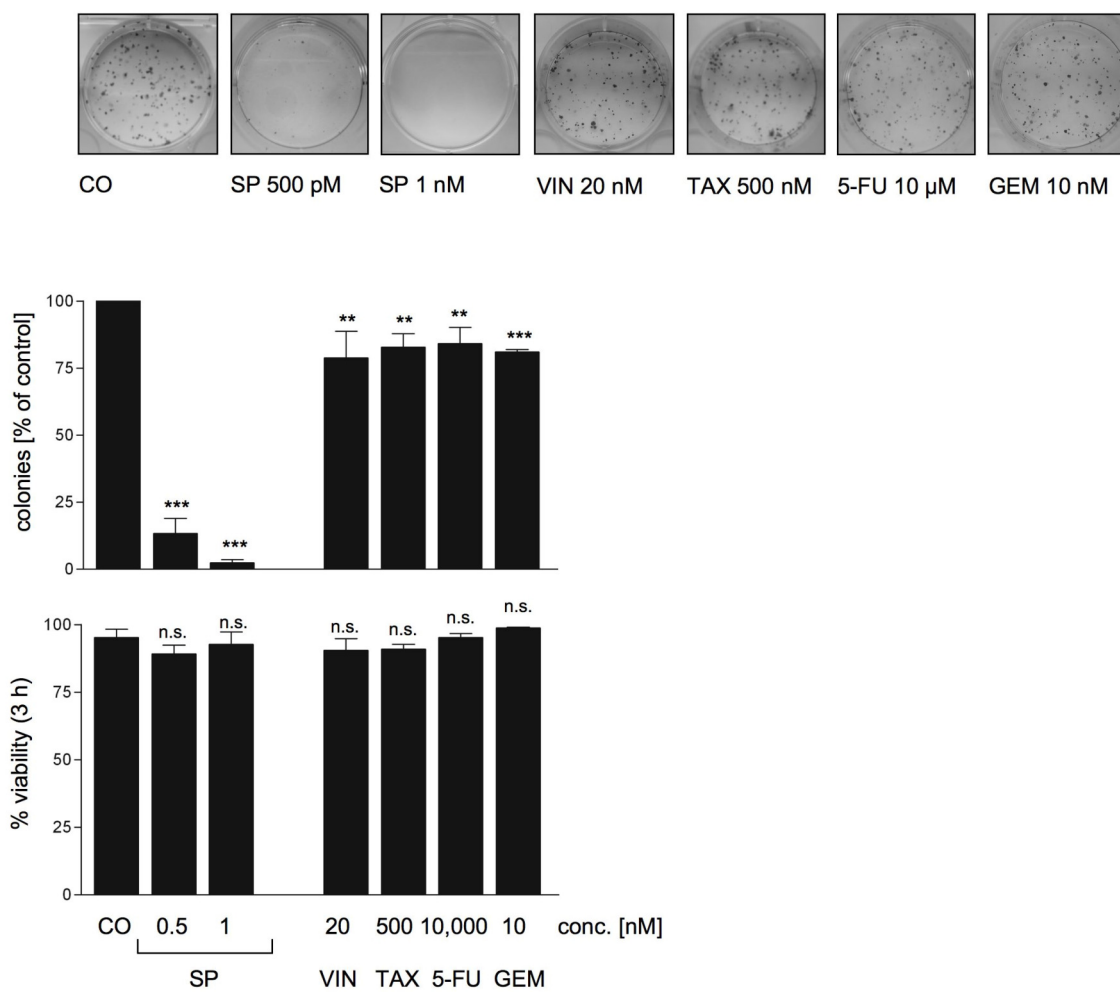


**B short term effects**



### L3.6pl

#### A long term effects



#### B short term effects

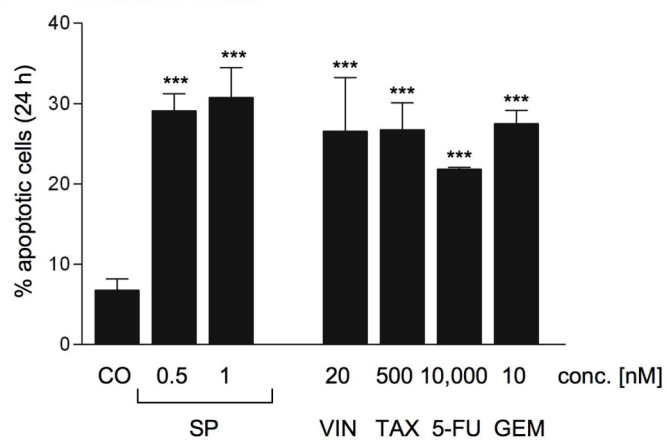


**Figure III.5: Spongistatin 1 shows long term effects on the clonal tumor cell growth.**

MCF-7 cells were left untreated (CO) or stimulated with spongistatin 1 (SP; 500 pM, 1 nM), taxol (TAX; 500 nM, 1  $\mu$ M) or staurosporine (ST; 500 nM). Panc-1 and L3.6pl cells were left untreated (CO) or stimulated with spongistatin 1 (SP; 500 pM, 1 nM), vinblastine (VIN; 20 nM), taxol (TAX; 500 nM), 5-fluoruracil (5-FU; 10  $\mu$ M) or gemcitabine (GEM; 10 nM). **(A)** A clonogenic assay (*upper panel*) was performed as described in “Materials and Methods” (II5), results are represented as the number of colonies in comparison to untreated cells (CO). The images show representative wells of the colonies stained with crystal violet. The viability of the cells 3 h after stimulation, when the cells are seeded to grow as colonies, was determined by the Trypan blue excusion assay (*lower panel*). **(B)** Apoptotic cells were quantified after 24 h or 48 h of stimulation by flow cytometry. *Bars*, the mean  $\pm$  S.E. of three independent experiments performed in triplicate. \*,  $p < 0.01$ ; \*\*,  $p < 0.05$ ; \*\*\*,  $p < 0.001$  (ANOVA/Bonferroni).

Taken together, spongistatin 1 potently induced apoptotic cell death in the picomolar range in a variety of cancer cell lines that are quite insensitive to many chemotherapeutic drugs. Moreover, spongistatin 1 showed strong long term effects on the clonogenic survival of MCF-7 cells as well as on highly invasive human pancreatic cancer cell lines. This clearly points the potential of spongistatin 1 as a chemoresistance combatant and its capability to act as an antimetastatic compound.

These impressive effects of spongistatin 1 were further elucidated in more detail in two separate models. First, spongistatin 1 and its effects in the metastatic process were studied *in vitro* using the highly metastatic human pancreatic cancer cells L3.6pl. Secondly, the underlying apoptotic signaling pathway induced by spongistatin 1 was investigated in the human breast cancer cell line MCF-7.

## 2 ANTIMETASTATIC PROPERTIES OF SPONGISTATIN 1 *IN VITRO*

In the orthotopic pancreatic tumor model, performed by Andrea Rothmeier (Department of Pharmacy, University of Munich, Germany) in cooperation with Ivan Ischenko and Christiane Bruns (Klinikum Großhadern, Munich, Germany), the efficacy of spongistatin 1 on L3.6pl pancreatic tumor metastasis was exhibited *in vivo*. This tumor model bears clinical relation as the L3.6pl cells were injected into the subcapsular region of the pancreas just beneath the spleen of nude mice [136] and allowed to grow and establish a tumor for one week. Seven days after the implantation of tumor cells, the mice were injected daily with spongistatin 1 (10  $\mu$ g/kg/day) or solvent (PBS) over 21 days. Subsequently, the animals were sacrificed and the number of visible liver and lymph node metastases was confirmed with a dissecting microscope. In fact, spongistatin 1 was able to reduce the formation of metastases in an impressive manner. Liver metastases and regional lymph node metastases were detected in all control animals, whereas only a third of spongistatin 1-treated mice developed metastases in liver and lymph nodes (Table III.1).

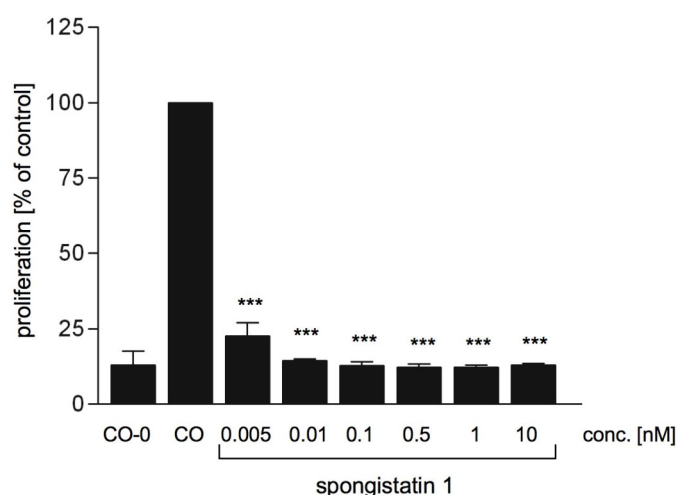
**Table III.1: Orthotopic pancreatic tumor model.**

Treatment group	Incidence of macroscopic tumors		
	Pancreatic tumor	Liver metastasis	Regional lymph node metastasis
CO	100%	90%	100%
SP 10 µg/kg/day	100%	22%	33%

Based on these strong *in vivo* effects of spongistatin 1 on tumor metastasis obtained in the orthotopic tumor model, the impact of spongistatin 1 on several steps of the metastatic process was studied *in vitro* using these highly invasive L3.6pl cells.

## 2.1 SPONGISTATIN 1 REVEALS ANTIPROLIFERATIVE PROPERTIES

Cell proliferation is one of the major steps in tumorigenesis and metastasis. Metastatic tumor cells are characterized by strong proliferation in the primary tumor as well as at a distant site to establish new metastatic foci. Thus, the effect of spongistatin 1 on tumor cell proliferation was assessed using the crystal violet staining assay. As demonstrated in Figure III.6, spongistatin 1 effectively inhibited tumor cell proliferation, even in concentrations as low as 5 pM.

**Figure III.6: Spongistatin 1 significantly inhibits tumor cell proliferation after 72 h.**

L3.6pl cells were seeded in 96-well plates. Cells in a reference plate were stained after 24 h serving as baseline (CO-0). L3.6pl cells in the remaining plates were either kept untreated (CO) or stimulated with increasing concentrations of spongistatin 1 (SP; 5 pM to 10 nM) over a time period of 72 h. Bars, the mean  $\pm$  S.E. of three independent experiments. \*\*\*,  $p < 0.001$  (ANOVA/Bonferroni).

## 2.2 SPONGISTATIN 1 INHIBITS TUMOR CELL MIGRATION

Cell motility and migration are key features of metastatic cells, allowing for the change of position of metastatic cells within tissues and to enter lymphatic and blood vessels for dissemination into the circulation. The “wound healing” assay (described in II.6.2) was performed to study the effects of spongistatin 1 on the cell motility *in vitro*. As shown in Figure III.7, migration of L3.6pl cells as indicated by the ability to close the artificial wound, was significantly inhibited by spongistatin 1, even in nontoxic concentrations. In comparison to untreated cells, the percentage of cell-covered area in relation to the total image area was reduced to 85%, 70% and 59% with 10 pM, 50 pM and 100 pM spongistatin 1, respectively. Taxol, a well-known substance to inhibit cell migration, was used as positive control. The decreased cell migration was not a consequence of apoptotic cells death, as the cells stained with the vital dye Hoechst 33342 showed no chromatin condensation (data not shown).

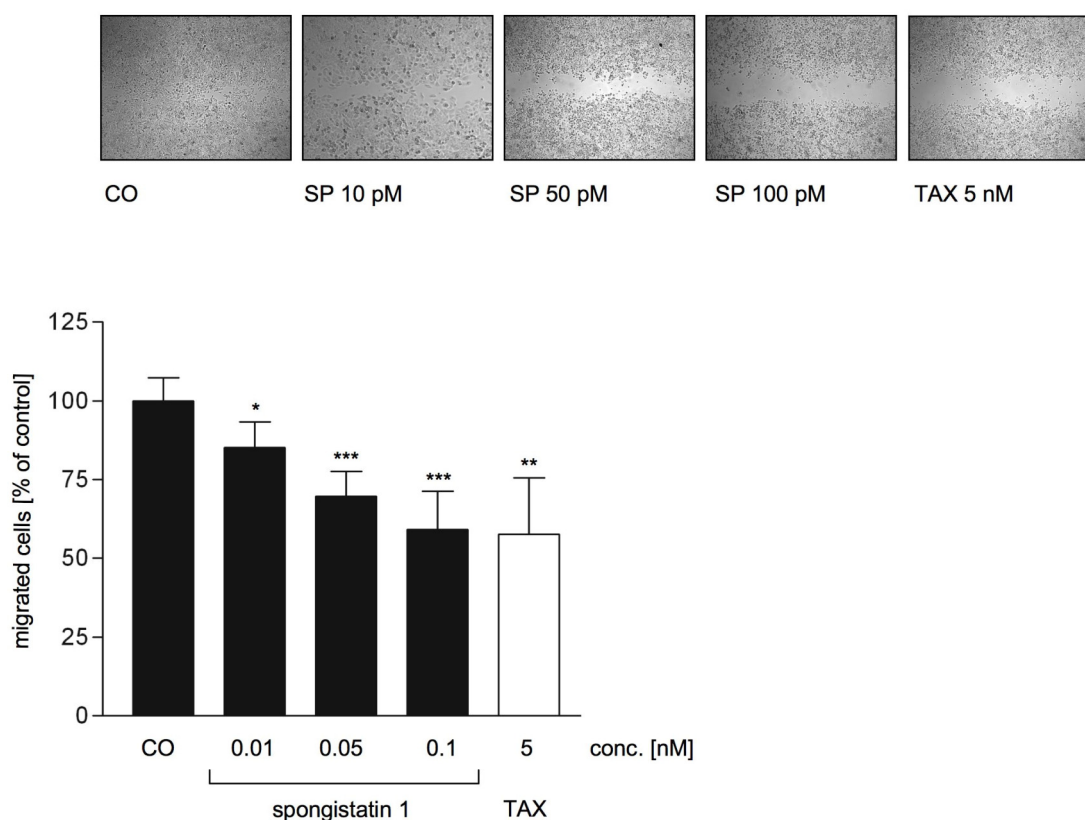


**Figure III.7: Spongistatin 1 reduces tumor cell migration.**

*Upper panel*, a confluent L3.6pl monolayer was scratched and subsequently left untreated or stimulated with spongistatin 1 (SP; 10 pM, 50 pM, 100 pM) or taxol (TAX; 5 nM) for 16 h. One representative image out of three independent experiments is shown. *Lower panel*, the graph displays the ratio of pixels covered by cells and pixels in the wound area. *Bars*, the mean  $\pm$  S.E. of three independent experiments. \*,  $p < 0.01$ ; \*\*,  $p < 0.05$ ; \*\*\*,  $p < 0.001$  (ANOVA/Bonferroni).

### 2.3 EFFECTS OF SPONGISTATIN 1 ON TUMOR CELL INVASION

Invasive and metastatic cells have to cross basement membranes in order to disseminate. The degradation of the membrane by proteolytic enzymes constitutes a critical condition for metastatic cells to penetrate into secondary tissues. In order to evaluate *in vitro* the effect of spongistatin 1 on tumor cell invasion, a transwell assay using Matrigel™ as reconstituted basal membrane and hFGF as chemoattractant was performed (described in II6.3). Treatment of L3.6pl cells with 10 pM spongistatin 1 showed no effect on the tumor cell invasion, whereas a concentration of 100 pM spongistatin 1 reduced the number of invading cells about 25% (Figure III.8). Taxol was again used as a positive control, revealed a 20% decrease in tumor cell invasion.

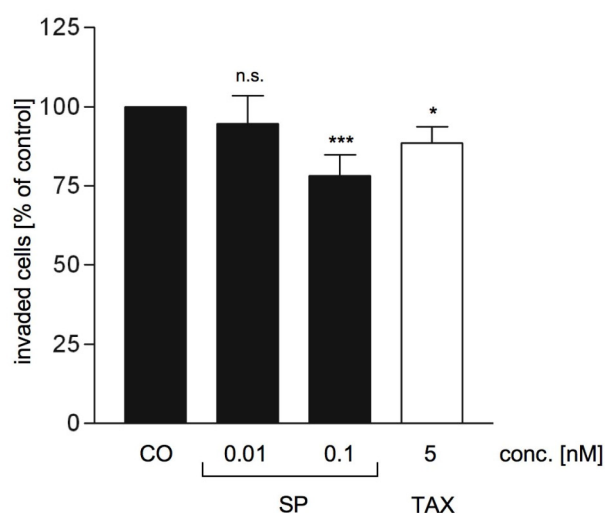


**Figure III.8: Effect of spongistatin 1 on tumor cell invasion.**

A transwell invasion assay was performed as described in II6.3 using Matrigel™ and hFGF as a chemoattractant. L3.6pl cells were seeded in the upper chamber and left either untreated or were stimulated with spongistatin 1 (SP; 10 pM, 100 pM) or taxol (TAX; 5 nM). After 24 h, invaded cells were fixed, stained with crystal violet and the absorbance was measured. Bars, the mean  $\pm$  S.E. of three independent experiments. *n.s.*, non significant; \*,  $p < 0.01$ ; \*\*\*,  $p < 0.001$  (ANOVA/Bonferroni).

### 2.4 SPONGISTATIN 1 INHIBITS THE ADHESION OF CANCER CELLS

The significance of aberrant cellular adhesion for cancer metastasis is widely recognized. Cell adhesion plays an important role at two different steps in the metastatic process. First, tumor cell motility is essential for migration and invasion and is a dynamic process involving adhesion to the extracellular matrix as well as detachment events. Secondly, tumor cell adhesion is critical for the arrest of circulating metastatic cells at a distant site.

In order to investigate the effects of spongistatin 1 on cell adhesion, an *in vitro* adhesion assay was performed, mimicking the conditions of the latter process. L3.6pl cells in confluent conditions were treated with spongistatin 1 over a period of three hours.

Subsequently, the cells were detached and allowed to adhere for 16 h. In contrast to vinblastine, gemcitabine and 5-FU, spongistatin 1 was able to reduce the adherence of detached tumor cells in a concentration-dependent manner with a decrease of adhered cells to about 50% at a concentration of spongistatin 1 as low as 1 nM (Figure III.9).

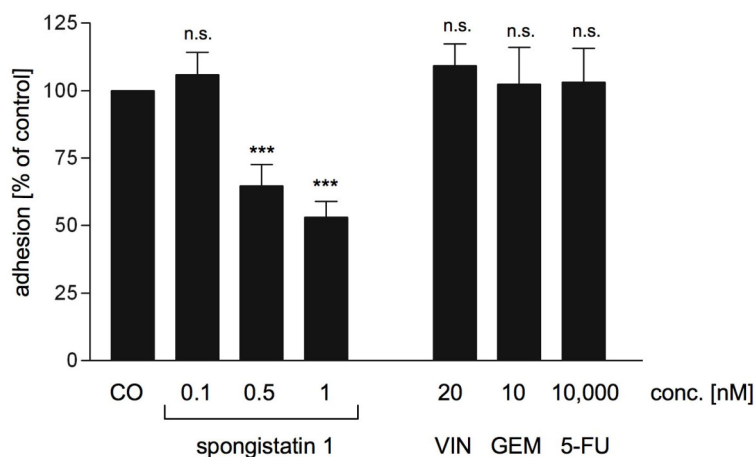


**Figure III.9: Spongistatin 1 inhibits adhesion of L3.6pl cells.**

L3.6pl cells were either left untreated (CO) or stimulated with spongistatin 1 (SP; 0.1 nM, 0.5 nM, 1 nM), vinblastine (VIN; 20 nM), gemcitabine (GEM; 10 nM) or 5-fluoruracil (5-FU; 10  $\mu$ M) for 3 h. Subsequently, cells were harvest with T/E, seeded on Collagen G-coated plates and allowed to adhere for 16 h. Adhered cells were stained with crystal violet and absorbance was measured. Bars, the mean  $\pm$  S.E. of three independent experiments. *n.s.*, non significant; *\*\*\**,  $p < 0.001$  (ANOVA/Bonferroni).

## 2.5 FAK IS DEPHOSPHORYLATED BY SPONGISTATIN 1

Proteins involved in the integrin signaling, such as the focal adhesion kinases (FAK), are central players in the metastatic process. The activation of FAK leads to a number of cell biological processes including cell attachment, proliferation, migration, invasion and survival. The activity of FAK is regulated at the post-translational level by phosphorylation. Autophosphorylation of FAK on a particular tyrosine residue, Tyr397, occurs in response to many stimuli, e.g. attachment to the extracellular matrix, resulting in the enzymatic activity of FAK. Phosphorylation of FAK at Tyr397 reflects its kinase activity and is frequently found in invasive tumors.

As shown in Figure III.10, FAK is constitutively activated by phosphorylation at Tyr397 in L3.6pl cells. As soon as 30 min upon spongistatin 1 exposure, FAK was dephosphorylated and thereby hypothetically inactivated. The total protein level stayed equal during the time of the experiment. Interestingly, treatment with taxol or gemcitabine FAK did not induce a dephosphorylation at this residue.

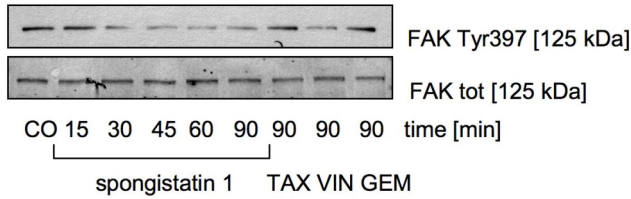


**Figure III.10: Spongistatin 1 dephosphorylates FAK at Tyr397.**

L3.6pl cells were left untreated (CO) or stimulated with spongistatin 1 (SP; 500 pM), taxol (TAX; 500 nM), vinblastine (VIN; 20 nM) or gemcitabine (GEM; 10 nM) for the indicated times. Total FAK level and phosphorylation of FAK on Tyr397 was analyzed by Western blot. All experiments were carried out three times.

## 2.6 SPONGISTATIN 1 INDUCES APOPTOSIS IN ANOIKIS - RESISTANT CELLS

Metastatic cells are characterized by their resistance to anoikis, apoptosis caused by detachment from the extracellular matrix. During migration and intravasation into the circulation metastatic cells are either deprived of extracellular matrix or exposed to foreign matrix components. Therefore, the ability to survive in the absence of normal matrix components represents a crucial property of metastatic cells.

In order to investigate if the selected cancer cell line is resistant to anoikis, L3.6pl cells were seeded on plates coated with poly-HEMA to prevent cell adhesion. Indeed, L3.6pl cells did not undergo apoptosis when they were kept in suspension over 24 h as DNA fragmentation did not exceed 12%. However, spongistatin 1 was able to overcome this resistance to anoikis and to induce DNA fragmentation, being significant 24 h after stimulation with spongistatin 1 (Figure III.11).

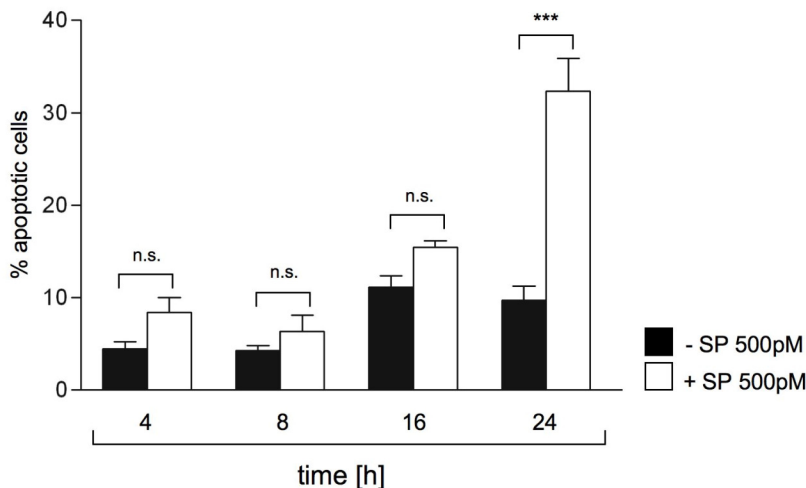


### Figure III.11: Spongistatin 1 induces apoptosis in anoikis-resistant tumor cells.

L3.6pl cells were seeded in 24-well plates coated with poly-HEMA to prevent cell adhesion. Subsequently, cells were left untreated or stimulated with spongistatin 1 (SP; 500 pM) for the indicated times. Apoptotic cells were quantified by flow cytometry. *Bars*, the mean  $\pm$  S.E. of three independent experiments. *n.s.*, non significant; \*\*\*,  $p < 0.001$  (ANOVA/Bonferroni).

Based on a variety of previous experiments by several groups, there is evidence indicating that higher resistance to apoptosis of metastatic cancer cells is associated with dysregulation of proteins involved in the regulation of the apoptotic cascade. Among them, expression and activity of Bcl-2 family proteins, especially Bcl-2 and Bcl-x<sub>L</sub>, seem to be associated with both metastasis and resistance to apoptosis.

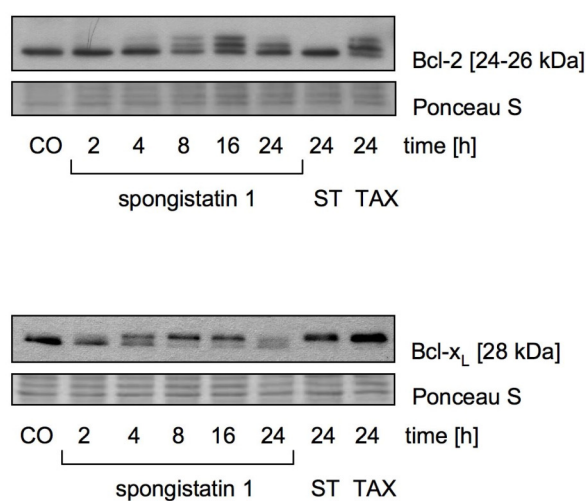


### Figure III.12: Inactivation of antiapoptotic Bcl-2 family proteins.

L3.6pl cells were left untreated (CO) or stimulated with spongistatin 1 (SP; 500 pM), staurosporine (ST; 500 nM) or taxol (TAX; 500 nM) for the indicated times. Western Blot analysis was performed using antibodies against the inactive phosphorylated forms of Bcl-2 and Bcl-x<sub>L</sub>. Equal protein loading was controlled by staining membranes with Ponceau S (a representative section of the stained membrane is shown). All experiments were carried out three times.

In fact, spongistatin 1 influences the activity of antiapoptotic Bcl-2 proteins. As shown in Figure III.12, Bcl-2 was phosphorylated and thereby inactivated upon treatment with spongistatin 1 for 8 h. In addition, spongistatin 1-treatment induced both downregulation or degradation and phosphorylation of Bcl-x<sub>L</sub>, whereas the protein levels upon stimulation with staurosporine or taxol were not affected.

## 2.7 INVOLVEMENT OF BCL-2 AND BCL-x<sub>L</sub> IN METASTSIS

In order to elucidate the functional involvement of these two antiapoptotic Bcl-2 proteins in anoikis-resistance and metastasis, the expression of Bcl-2 and Bcl-x<sub>L</sub> was silenced by siRNA. Interestingly, downregulation of Bcl-2 as well as Bcl-x<sub>L</sub> sensitized L3.6pl cells to anoikis. Whereas L3.6pl cells transfected with a nonsense sequence showed a DNA fragmentation by about 30% upon culturing in suspension for 24 h, silencing of Bcl-2 and Bcl-x<sub>L</sub> led to an increased apoptosis induction by about 50% (Figure III.13).

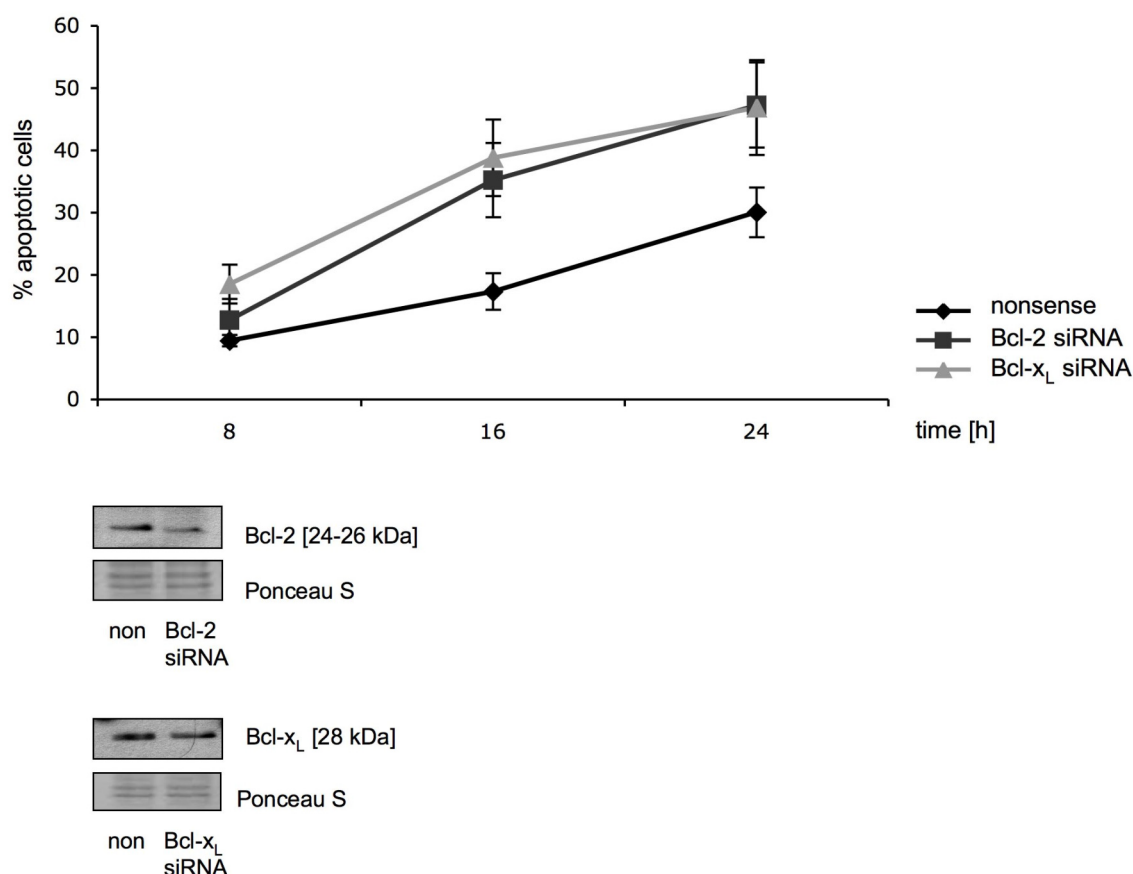


**Figure III.13: Bcl-2 and Bcl-x<sub>L</sub> knockdown sensitizes L3.6pl cells to anoikis.**

*Upper panel*, L3.6pl cells were transfected with oligonucleotides encoding for either Bcl-2 siRNA, Bcl-x<sub>L</sub> siRNA or a nonsense sequence. Cells were cultured in plates coated with poly-HEMA to prevent cell adhesion for the indicated times. Apoptotic cells were quantified by flow cytometry. Represented are the mean  $\pm$  S.E. of two independent experiments. *Lower panel*, downregulations of Bcl-2 and Bcl-x<sub>L</sub> protein levels were verified by Western Blot. Equal protein loading was controlled by staining membranes with Ponceau S (a representative section of the stained membrane is shown).

In addition, the influence of Bcl-2 and Bcl-x<sub>L</sub> on the metastatic cascade was investigated. Since cell motility and migration are essential features in this process, a “wound healing” assay was performed using L3.6pl cells silenced by Bcl-2 siRNA and Bcl-x<sub>L</sub> siRNA. Indeed, both Bcl-2 and Bcl-x<sub>L</sub> are sufficient for cell motility as the migration of L3.6pl cells was inhibited both after Bcl-2 and Bcl-x<sub>L</sub> downregulation. As shown in Figure III.14, L3.6pl cells

transfected with a nonsense sequence were able to migrate and to close the artificial wound, whereas the scratch stayed open upon silencing L3.6pl cells with Bcl-2 siRNA and Bcl-x<sub>L</sub> siRNA, respectively.

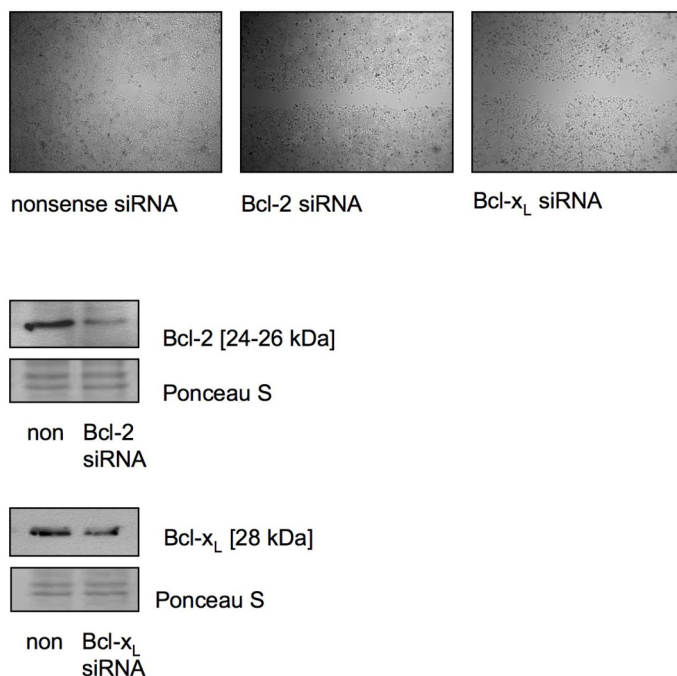


**Figure III.14: Involvement of Bcl-2 and Bcl-x<sub>L</sub> in cell migration.**

*Upper panel*, L3.6pl cells were transfected with oligonucleotides encoding for either Bcl-2 siRNA, Bcl-x<sub>L</sub> siRNA or a nonsense sequence. A confluent cell monolayer was scratched and cell migration was monitored after 16 h. One representative image out of three is shown. *Lower panel*, downregulations of Bcl-2 and Bcl-x<sub>L</sub> protein levels were verified by Western Blot. Equal protein loading was controlled by staining membranes with Ponceau S (a representative section of the stained membrane is shown).

### 3 SIGNAL TRANSDUCTION PATHWAYS IN SPONGISTATIN 1-INDUCED APOPTOSIS

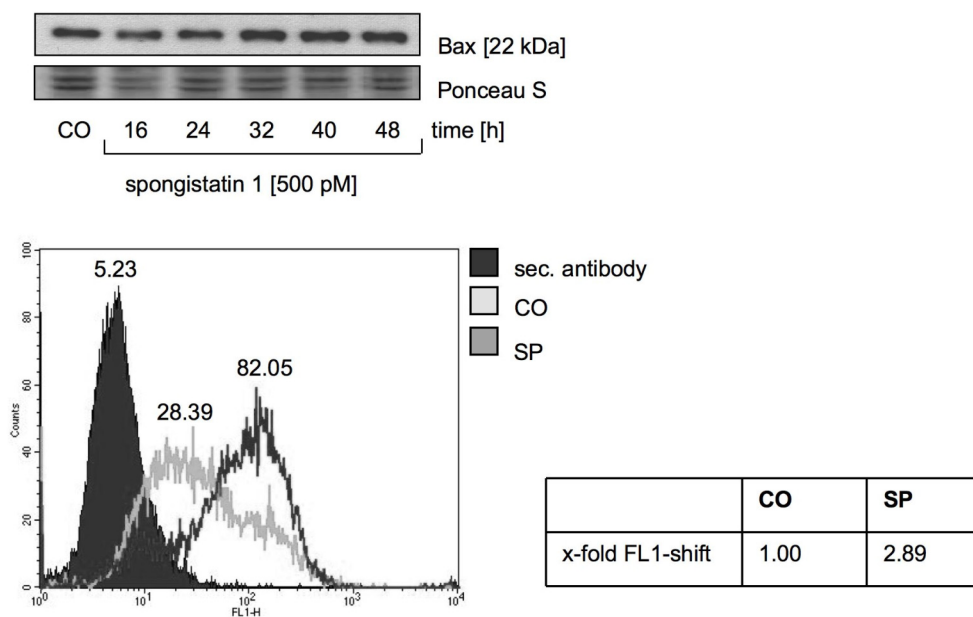
Caused by the deficiency in caspase-3, the human breast cancer cell line MCF-7 is an interesting model to study the underlying apoptotic mechanisms caused by spongistatin 1 to overcome chemoresistance. For all experiments in MCF-7 cells, a concentration of 500 pM spongistatin 1 was applied, which induced about 30% DNA-fragmentation after 48 h of treatment (Figure III.3).

### 3.1 RELEASE OF PROAPOPTOTIC PROTEINS FROM MITOCHONDRIA

A majority of chemotherapeutic agents mediate apoptosis via the intrinsic pathway [6]. Based on this knowledge, we initially monitored the mitochondrial events upon spongistatin 1 treatment. Members of the Bcl-2 protein family are the major regulators of the intrinsic apoptotic pathway. Proapoptotic Bcl-2 proteins like Bax form pores in the outer mitochondrial membrane after their activation followed by a release of proapoptotic factors into the cytosol. The proapoptotic Bcl-2 proteins are antagonized by the antiapoptotic Bcl-2 family members including Bcl-2 and Bcl-x<sub>L</sub>. Anticancer agents causing a mitotic arrest are demonstrated to inactivate Bcl-2 by phosphorylation [83], thereby activating Bax and promoting apoptosis.

As shown in Figure III.15A in the upper panel, treatment with spongistatin 1 did not provoke an upregulation of Bax protein over an extended time period. However, upon spongistatin 1 treatment Bax underwent a N-terminal conformational change resulting in oligomerization of the protein and formation of pores in the outer mitochondrial membrane. This conformational change could be analyzed using specific antibodies against the normally occluded N-terminus. FACS analysis of MCF-7 cells with such antibodies revealed an activation of Bax as early as 8 h, evidenced by a shift in the FL1 channel (Figure III.15A, lower panel). In addition, the antiapoptotic proteins Bcl-2 and Bcl-x<sub>L</sub> were phosphorylated and thereby inactivated upon stimulation with spongistatin 1 for 4 h (Figure III.15B).

**A**



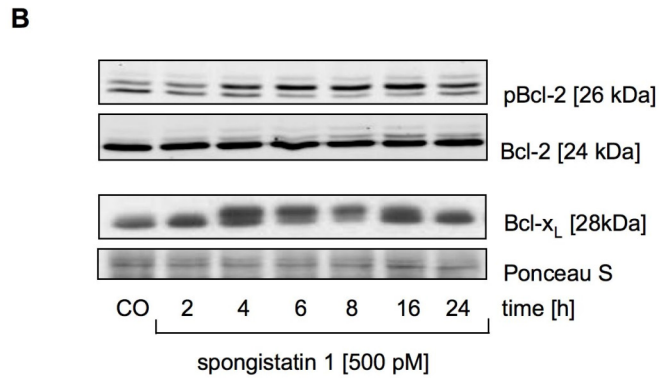


**Figure III.15: Spongistatin 1 induces the intrinsic apoptotic pathway by activation of Bax and inactivation of Bcl-2 and Bcl-x<sub>L</sub>.**

(A) *Upper panel*, MCF-7 cells were left untreated (CO) or stimulated with spongistatin 1 (SP; 500 pM) for the indicated times. Western Blot analysis was performed using antibodies against Bax. *Lower panel*, MCF-7 cells were either left untreated (CO) or incubated with spongistatin 1 (SP; 500 pM) for 8 h. The conformational change was measured by flow cytometry using activation-specific antibodies against Bax. The filled histogram shows the staining of untreated cells with secondary antibody and the gray lines indicate the specific staining for active forms of Bax. The numbers describe the median. The table indicates the x-fold FL1-shift upon treatment with spongistatin 1 (SP; 500 pM, 8 h). (B) MCF-7 cells were left untreated (CO) or stimulated with spongistatin 1 (SP; 500 pM) for the indicated times. Western Blot analysis was performed using antibodies against Bcl-2 and the inactive phosphorylated forms of Bcl-2 and Bcl-x<sub>L</sub>. Equal protein loading was controlled by staining membranes with Ponceau S. One representative blot of three is shown.

As a consequence of both Bax activation and inactivation of Bcl-2 and Bcl-x<sub>L</sub>, spongistatin 1 triggered the release of cytochrome c, Smac and Omi/HtrA2 from the mitochondria to the cytosol starting 8 h after stimulation and becoming significant 16 h upon treatment with spongistatin 1 (Figure III.16).

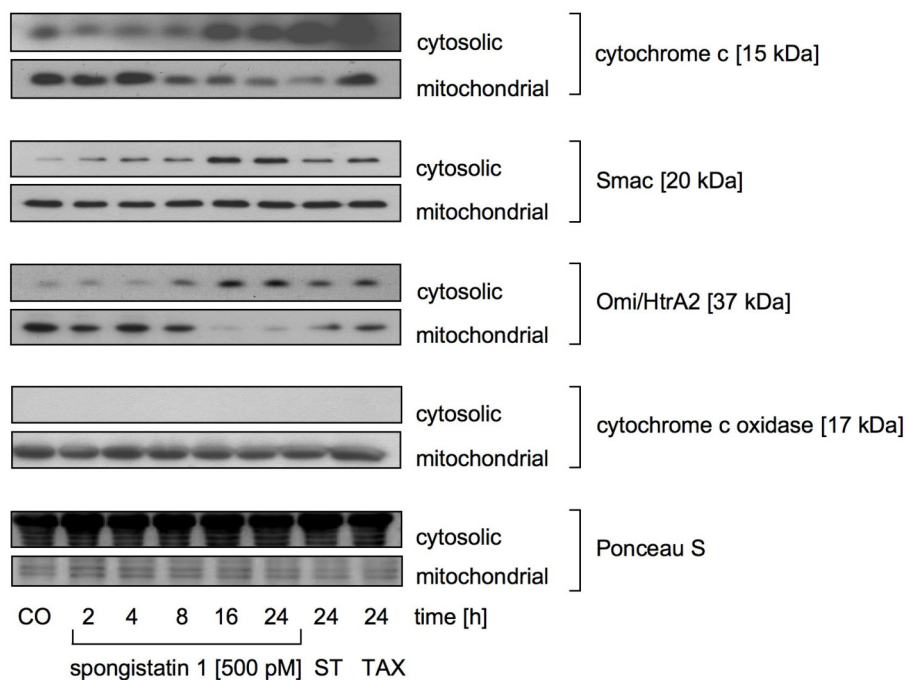
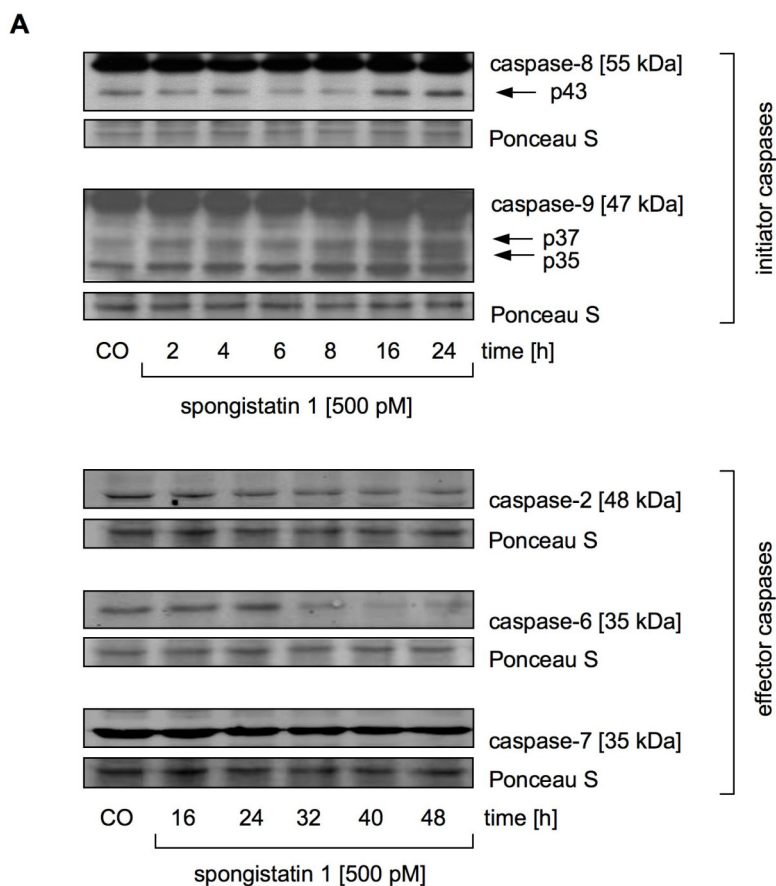


**Figure III.16: Spongistatin 1 induces the release of proapoptotic proteins from mitochondria.**

Cells were left untreated (CO) or treated with spongistatin 1 (SP; 500 pM) or as positive control with staurosporine (ST; 500 nM) and taxol (TAX; 500 nM) for the indicated times. Cytosol and mitochondrial protein fractions were prepared and cytochrome c, Smac/DIABLO, Omi/HtrA2 were detected by specific antibodies using Western Blot analysis. Cytochrome c oxidase served as control for the quality of the extraction procedure. Equal protein loading was controlled by staining membranes with Ponceau S (a representative section of the stained membrane is shown). One representative blot of three is shown.

**3.2 MINOR ROLE OF CASPASES IN SPONGISTATIN 1-INDUCED****APOPTOSIS**

Caspases are described as the major executioners of classical apoptotic morphology induced by various stimuli. But there is growing evidence that apoptotic cell death can also be mediated independent of caspases by other factors like AIF and EndoG. The activation of initiator and effector caspases was elucidated by Western Blot analysis (Figure III.17A). A weak appearance of cleavage products 16 h after stimulation suggests a rather poor activation of the initiator caspases-8 and -9. Even though cleavage products of the effector caspases-2, -6 and -7 were difficult to detect in MCF-7 cells, a slight decrease of the proform could be observed after 32 h of spongistatin 1 treatment.



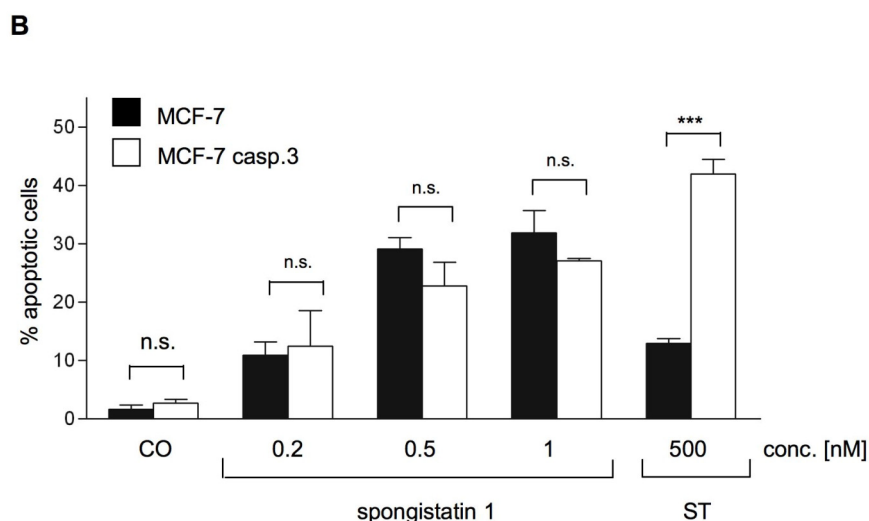


**Figure III.17: Marginal participation of the caspases in spongistatin 1-induced cell death.**

(A) MCF-7 cells were left untreated (CO) or stimulated with spongistatin 1 (SP; 500 pM) for the indicated times. Expression of caspase-8, -9, -2, -6 and -7 was assessed by Western Blot analysis. Cleavage products are indicated by arrows. Equal protein loading was controlled by staining membranes with Ponceau S (a representative section of the stained membrane is shown). All experiments were carried out three times. (B) MCF-7 cells and caspase-3 reconstituted MCF-7 cells (MCF-7 casp.3) were left untreated (CO) or stimulated with increasing concentrations of spongistatin 1 for 48 h. Staurosporine (ST; 500nM) was used as a positive control. Apoptotic cells were quantified by flow cytometry. Bars, the mean  $\pm$  S.E. of three independent experiments performed in triplicate. *n.s.*, non significant; \*\*\*,  $p < 0.001$  (ANOVA/Bonferroni).

Moreover, MCF-7 cells reconstituted with caspase-3 acquired no greater sensitivity to spongistatin 1. In contrast, stimulation with staurosporine (ST) showed clear caspase-3-dependent DNA fragmentation, indicating a marginal impact of caspase-3 in the apoptotic signaling of spongistatin 1 in MCF-7 cells (Figure III.17B). Due to this weak activation of the caspases occurring very late in the apoptotic process induced by spongistatin 1, an inferior participation of the caspases is supposed. To exclude a functional involvement of the caspases, their actual role in the spongistatin 1-evoked cell death was examined using the broad-range caspase inhibitor N-(2-quinoly)valyl-aspartyl-(2,6-difluorophenoxy)-methylketone (Q-VD-OPh) (Figure III.18). Presence of Q-VD-OPh only led to a moderate decrease in the apoptosis rate of spongistatin 1 (21.4%), whereas a more pronounced reduction was seen when cells were treated with taxol (69.5%). To ensure that the effect of spongistatin 1 is not a unique property of MCF-7 cells, this experiment was repeated with comparable results in four additional cell lines derived from different tumors, the melanoma cell line SK-Mel-5, the prostate cancer cell line LNCaP and the pancreatic cell lines Panc-1 and L3.6pl. In the L3.6pl cell line the experiment was performed after 24 h and 48 h treatment of spongistatin 1. Pretreatment with the caspase-inhibitor Q-VD-OPh led only to a protection from DNA fragmentation about 6% when the cells are stimulated for 24 h, whereas after 48 h a protection about 34 % was detectable, confirming that the caspases are activated to a small extent and very late in the apoptotic process.

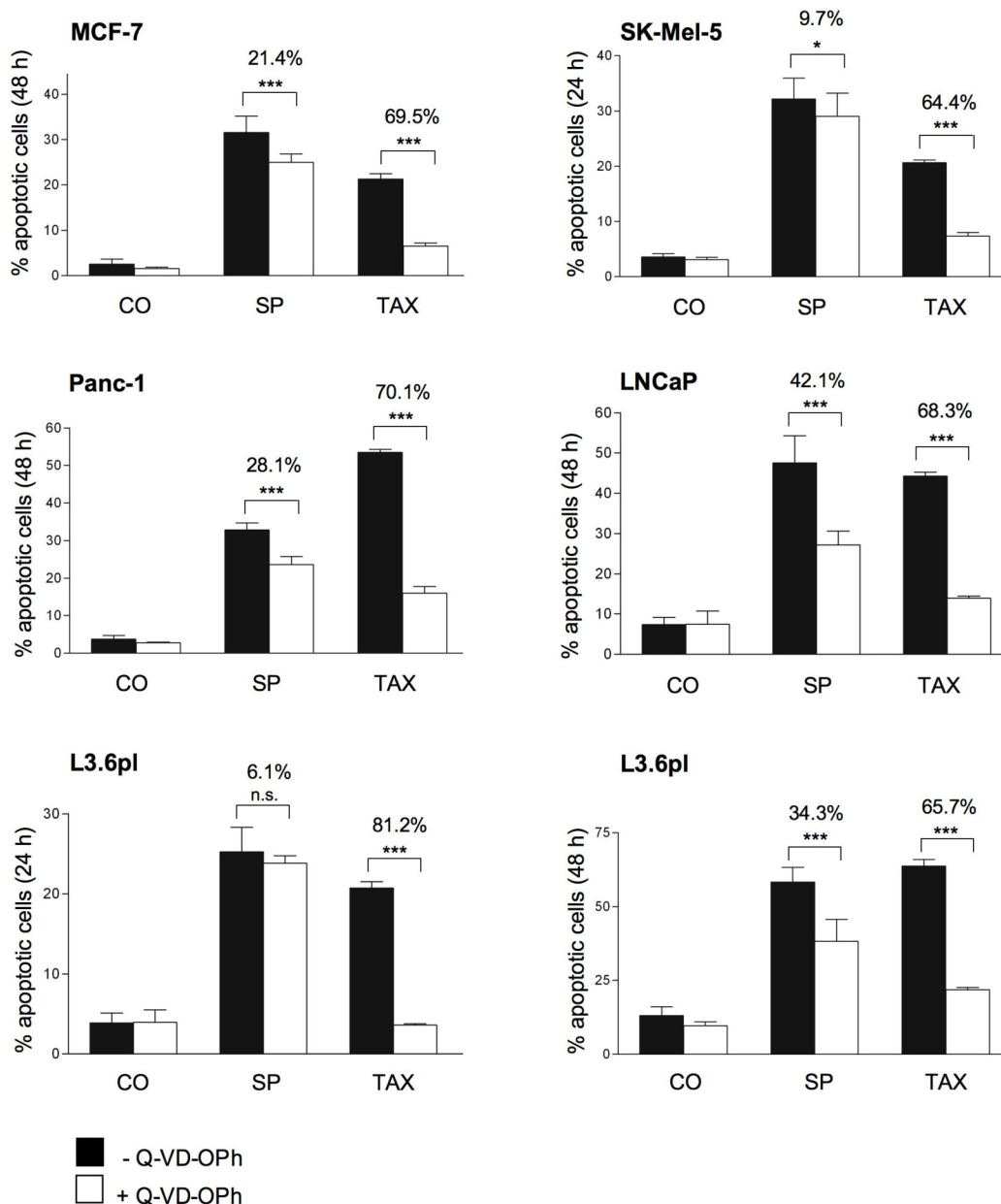


**Figure III.18: Spongistatin 1 induces cell death mainly independent of caspases in several cancer cell lines.**

MCF-7 cells, SK-Mel-5, Panc-1, LNCaP and L3.6pl cells were left untreated (CO), incubated with spongistatin 1 (SP; 500 pM) or taxol (TAX; 500 nM) for the indicated times or pretreated with Q-VD-OPh (10  $\mu$ M, 1 h) and then stimulated with spongistatin 1 (SP; 500 pM) or taxol (TAX; 500 nM) for the indicated times. Apoptotic cells were quantified by flow cytometry. Bars, the mean  $\pm$  S.E. of three independent experiments performed in triplicate. *n.s.*, non significant; \*,  $p < 0.01$ ; \*\*\*,  $p < 0.001$  (ANOVA/Bonferroni). The numbers describe the percental inhibition of apoptosis by Q-VD-OPh.

To verify the effects of spongistatin 1 on caspase activation with the broad-range caspase-inhibitor N-(2-quinolyl)valyl-aspartyl-(2,6-difluorophenoxy)-methylketone (Q-VD-OPh), the experiment was repeated in MCF-7 cells using a further pan-caspase-inhibitor, namely the N-benzyloxycarbonyl-Val-Ala-Asp(OMe)-fluoromethylketone (zVAD.fmk). As shown

in Figure III.19, the same results were obtained with these both caspase inhibitors, establishing the marginal role of caspases in the spongistatin 1-induced cell death.

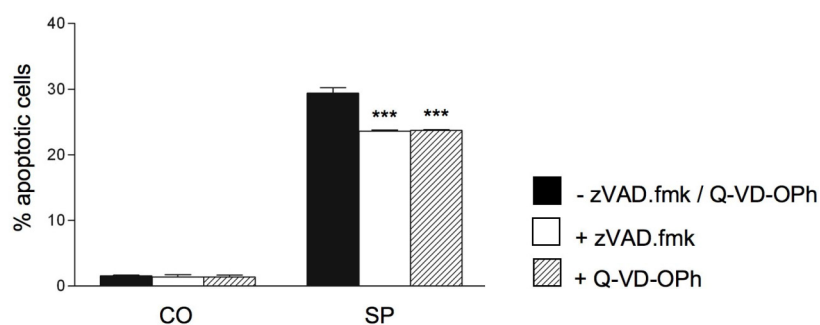


**Figure III.19: The pan-caspase-inhibitors zVAD.fmk and Q-VD-Oph exhibit equal effects in MCF-7 cells.**

MCF-7 cells were left untreated (CO), incubated with spongistatin 1 (SP; 500 pM, 48 h) or pretreated with zVAD.fmk (25  $\mu$ M, 1 h) or Q-VD-Oph (10  $\mu$ M, 1 h) and then stimulated with spongistatin 1 (SP; 500 pM, 48 h). Apoptotic cells were quantified by flow cytometry. *Bars*, the mean  $\pm$  S.E. of two independent experiments performed in triplicate; \*\*\*,  $p < 0.001$  (ANOVA/Bonferroni).

These data suggest that caspases are not central in spongistatin 1-induced cell death, which clearly suggests the involvement of caspase-independent apoptotic pathways.

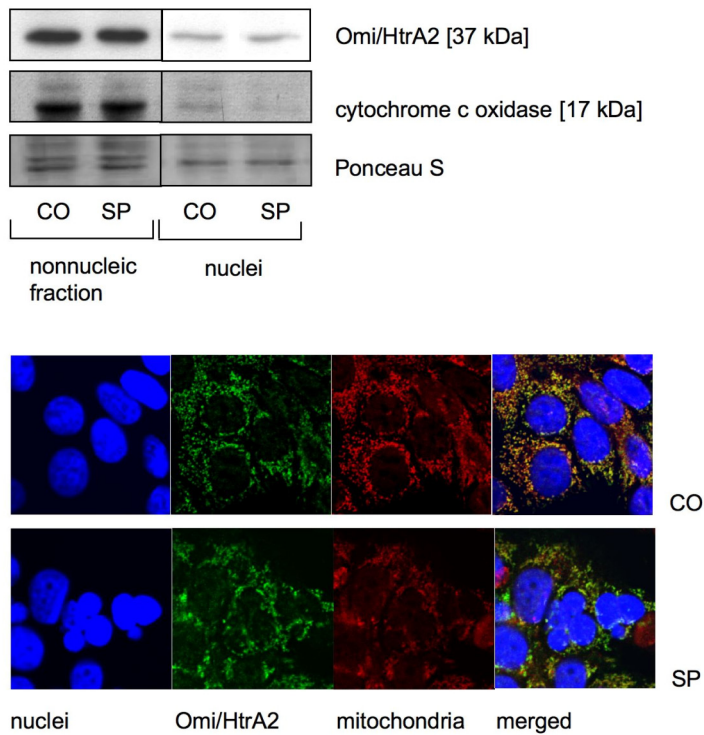
### 3.3 SPONGISTATIN 1-INDUCED APOPTOSIS INVOLVES AIF AND ENDO G, BUT NOT OMI/HTRA2

In search for apoptotic factors working independently of caspases, spongistatin 1 was hypothesized to induce the translocation of Omi/HtrA2, AIF and EndoG to the nucleus. Besides its caspase-dependent cytotoxicity, Omi/HtrA2 is reported to induce apoptosis in a caspase-independent way based on its serine protease activity. The proapoptotic mitochondrial proteins AIF (apoptosis inducing factor) and endonuclease G are well described death effectors working independently of caspases during cell death. Upon apoptotic stimuli, AIF and EndoG translocate from mitochondria to the nucleus inducing chromatin condensation and DNA fragmentation.

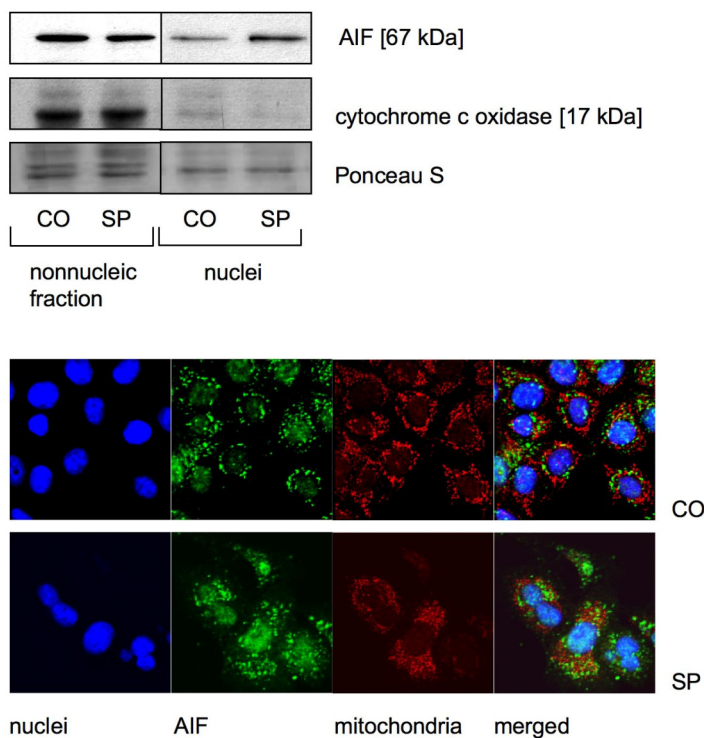
As shown in Figure III.20A by both Western Blot analysis and confocal microscopy, no translocation of Omi/HtrA2 from the mitochondria to the nucleus was detectable. However, spongistatin 1 caused a translocation of AIF and EndoG to the nucleus, observed by an increase of these proteins in the nuclear fraction (Figure III.20B, C). These results were further supported by confocal microscopy studies. Untreated control cells show the co-localization of these proteins with a mitochondrial dye, proving the mitochondrial

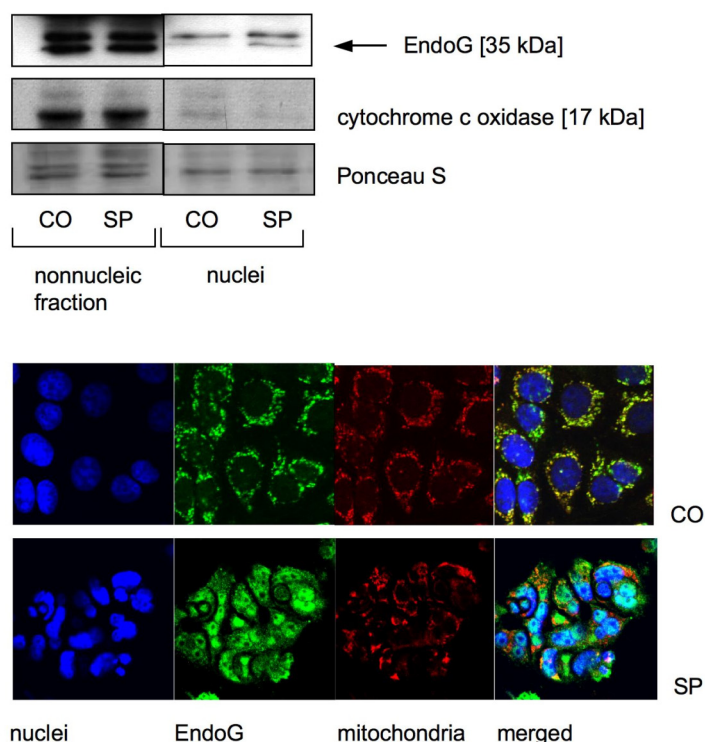
localization of these proteins. Upon treatment with spongistatin 1, AIF and EndoG were found in the nucleus demonstrated by co-localization of these proteins with the nuclei.

### A Omi /HtrA2



### B AIF



**C EndoG**

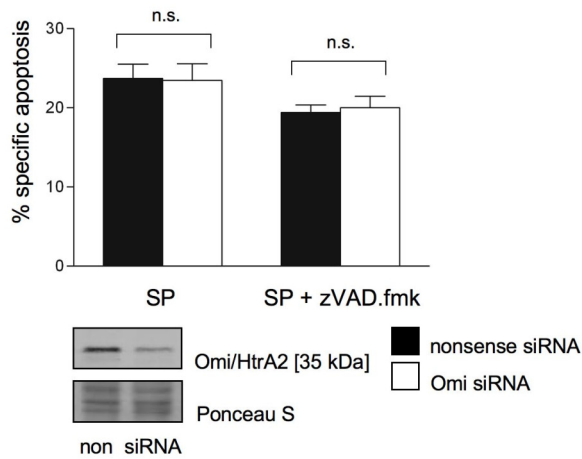
**Figure III.20: Spongistatin 1 induces the translocation of AIF and EndoG to the nucleus.**

*Upper panel*, cells were left untreated (CO) or treated with spongistatin 1 (SP; 500 pM) for 24 h. Nonnucleic and nuclear protein fractions were prepared and Omi/HtrA2 (A), AIF (B) and EndoG (C) were detected by specific antibodies using Western Blot analysis. Cytochrome c oxidase served as a control for the quality of the extraction procedure. *Lower panel*, cells were left untreated (CO) or treated with spongistatin 1 (SP; 500 pM) for 24 h. The translocation of Omi/HtrA2 (A), AIF (B) and EndoG (C) from mitochondria to the nucleus was analyzed by confocal microscopy. Nuclei are shown blue, mitochondria red and Omi/HtrA2, AIF and EndoG green, respectively. All experiments were performed three times with consistent results.

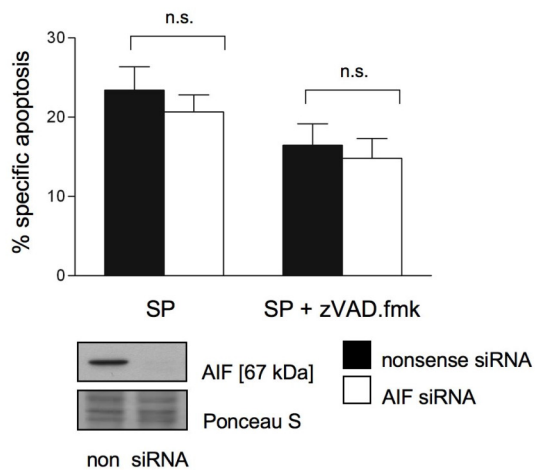
In order to elucidate the impact of these factors on the spongistatin 1-induced cell death, the expression of these proteins was silenced by siRNA. As no translocation of Omi/HtrA2 to the nucleus was detectable (Figure III.20A), downregulation of this protein did not protect cells against DNA fragmentation upon stimulation with spongistatin 1 even when caspases were inhibited with zVAD.fmk (Figure III.21A). Therefore, Omi/HtrA2 was considered not to be involved in the cell death pathway initiated by spongistatin 1. Interestingly, downregulation of AIF did not lead to a significant reduction in DNA fragmentation upon stimulation with spongistatin 1 despite its translocation to the nucleus. In contrast, silencing of EndoG by siRNA induced a marked decrease in the apoptosis rate. Moreover, these two factors were shown to act independently of caspases, as preincubation with the pan-caspase inhibitor zVAD.fmk had no effect on the DNA fragmentation (Figure III.21A). Previous *in vitro* studies using recombinant AIF [71, 74], demonstrated, that AIF is not able to cleave DNA by itself, but needs the interplay with endonucleases to facilitate DNA fragmentation and chromatin condensation [75, 76].

Therefore, AIF was hypothesized to collaborate with EndoG in the apoptotic signaling induced by spongistatin 1. In fact, cotransfection of MCF-7 cells with AIF and EndoG siRNA showed an advanced reduction in DNA fragmentation in response to spongistatin 1 indicating the functional role of these factors collaborating in the apoptotic process induced by spongistatin 1 (Figure III.21B).

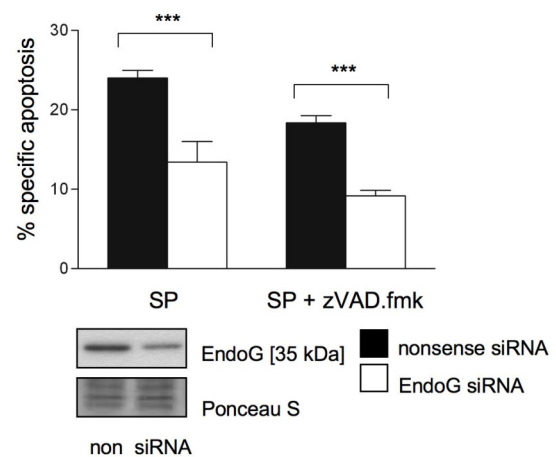
### A Omi / HtrA2



### AIF



### EndoG



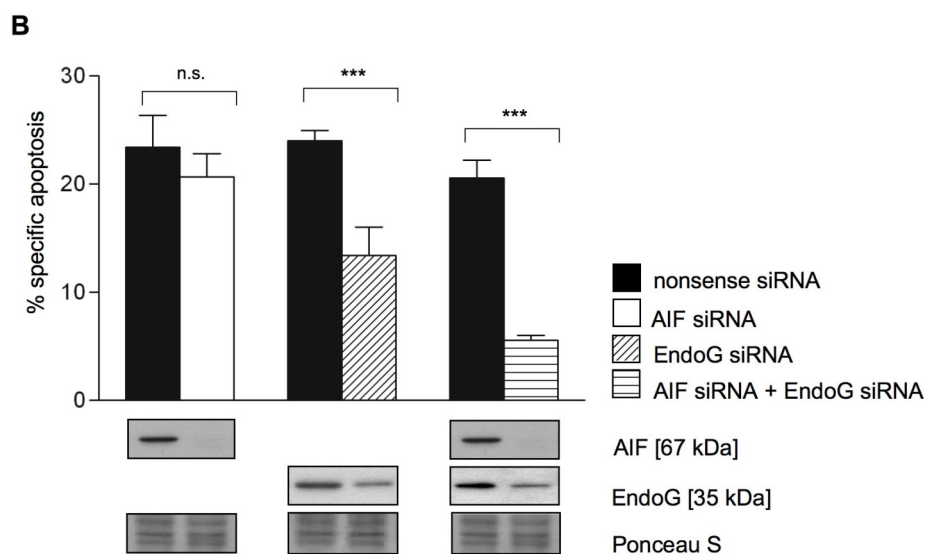


**Figure III.21: AIF and EndoG, but not Omi/HtrA2, assume a functional role in spongistatin 1-induced apoptosis.**

(A) MCF-7 cells were transfected with oligonucleotids encoding for either Omi/HtrA2 siRNA, AIF siRNA, EndoG siRNA or a nonsense sequence. Cells were left untreated (CO), incubated with spongistatin 1 (SP; 500 pM, 48 h) or pretreated with zVAD.fmk (25  $\mu$ M, 1 h) and then stimulated with spongistatin 1 (SP; 500 pM, 48 h). Apoptotic cells were quantified by flow cytometry. Results are represented as the percental specific apoptosis. (B) MCF-7 cells were transfected or cotransfected with oligonucleotids encoding for either AIF siRNA and EndoG siRNA or a nonsense sequence. Cells were left untreated (CO) or treated with spongistatin 1 (SP; 500 pM) for 48 h. Apoptotic cells were quantified by flow cytometry. Results are represented as the percental specific apoptosis. Bars, the mean  $\pm$  S.E. of three independent experiments performed in triplicate. *n.s.*, non significant; \*\*\*,  $p < 0.001$  (ANOVA/Bonferroni). Downregulations of Omi/HtrA2, AIF and EndoG protein levels were verified by Western Blot. Equal protein loading was controlled by staining membranes with Ponceau S (a representative section of the stained membrane is shown).

### 3.4 BID IS NOT ENGAGED IN SPONGISTATIN 1-MEDIATED CELL DEATH

The next step was to identify upstream effectors in spongistatin 1-induced apoptosis. Multiple evidence demonstrates that the balance of pro- and antiapoptotic Bcl-2 protein family members is crucial for the regulation of mitochondrial integrity and function. In this range, the BH3-only proteins play a key role in the regulation of the intrinsic apoptotic pathway by either activating the proapoptotic Bcl-2 family members or inhibiting the antiapoptotic Bcl-2 proteins. Since the BH3-only proteins Bid and Bim execute a highly proapoptotic function by acting as direct agonists of Bax or Bak, they were considered to be central factors regulating the release of AIF and EndoG from the mitochondria.

First, the involvement of Bid was examined. Under physiological conditions, inactive full-length Bid resides in the cytosol and removal of the N-terminal repressor of the membrane-anchoring segment by proteolytic cleavage is necessary to activate the

proapoptotic function of Bid. Western Blot analysis of total protein cell lysate with an antibody detecting Bid and truncated Bid (tBid) revealed that no cleavage of Bid occurred during spongistatin 1-induced apoptosis, whereas upon treatment with staurosporine the active truncated form of Bid was detectable (Figure III.22).

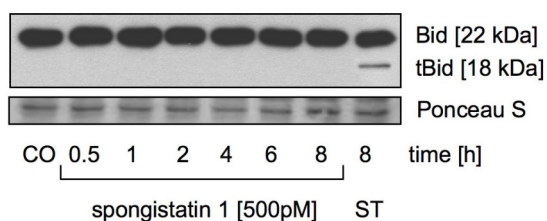


**Figure III.22: Bid is not cleaved to its active form tBid upon spongistatin 1 treatment.**

MCF-7 cells were left untreated (CO) or stimulated with spongistatin 1 (SP; 500 pM) or staurosporine (ST; 500 nM) for the indicated times. Activation of Bid was analyzed by Western Blot. Equal protein loading was controlled by staining membranes with Ponceau S (a representative section of the stained membrane is shown). One representative blot of three is shown.

The necessity of Bid cleavage to its active proapoptotic form tBid was recently challenged by the fact that full-length Bid was also able to translocate to the mitochondria resulting in a breakdown of the mitochondrial membrane potential and subsequent induction of apoptosis [137]. Thus, the actual role of Bid in the spongistatin 1-induced apoptosis was further elucidated using the Bid-inhibitor BI-6C9 [138].

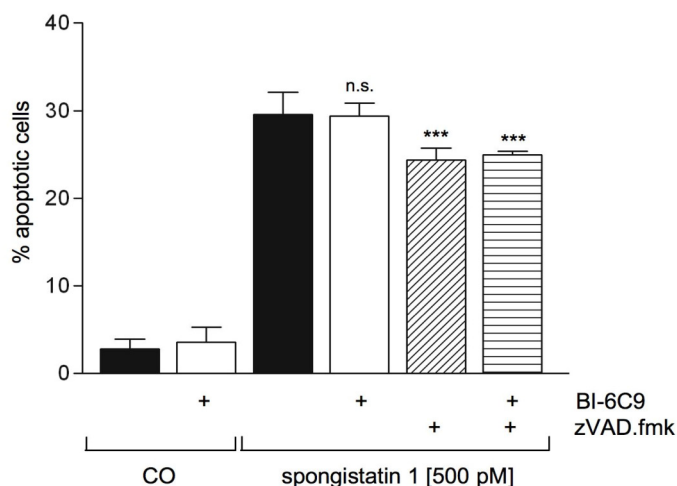


**Figure III.23: Bid is not involved in spongistatin 1-induced cell death.**

MCF-7 cells were left untreated (CO), incubated with spongistatin 1 (SP; 500 pM, 48 h) or pretreated with zVAD.fmk (25  $\mu$ M, 1 h) or BI-6C9 (20  $\mu$ M, 1 h) and then stimulated with spongistatin 1 (SP; 500 pM, 48 h). Apoptotic cells were quantified by flow cytometry. Bars, the mean  $\pm$  S.E. of three independent experiments performed in triplicate. *n.s.*, non significant; \*\*\*,  $p < 0.001$  (ANOVA/Bonferroni).

As shown in Figure III.23, pre-treatment of MCF-7 cells with BI-6C9 did not protect the cells from DNA fragmentation. Even in combination of BI-6C9 with the pan-caspase-inhibitor zVAD.fmk, there was no difference in the DNA fragmentation observed, supporting the previous finding that Bid is not engaged in the apoptotic signaling mediated by spongistatin 1.

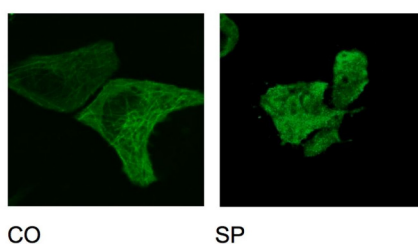
### 3.5 MAJOR ROLE OF BIM IN SPONGISTATIN 1-INDUCED APOPTOSIS

Next, the role of the BH3-only protein Bim as a key regulator in the apoptotic pathway induced by spongistatin 1 was investigated. Spongistatin 1 has been reported to depolymerize the microtubule network by interacting with tubulin [24]. The working hypothesis was that spongistatin 1 releases Bim from its sequestration at the microtubule associated dynein motor complex, thereby activating its proapoptotic function.

#### 3.5.1 SPONGISTATIN 1 FREES BIM FROM ITS SEQUESTRATION BY MICROTUBULES

In order to confirm that spongistatin 1 inhibits microtubule assembly, MCF-7 cells were transfected with GFP-tubulin and exposed to spongistatin 1. As observed in Figure III.24A, the tubulin scaffold in MCF-7 cells transfected with GFP-tubulin was dissolved in 8 h upon treatment with spongistatin 1. In addition to this, the level of  $\beta$ -tubulin decreased in the insoluble fraction and increased in the soluble fraction (Figure III.24B).

**A**



**B**

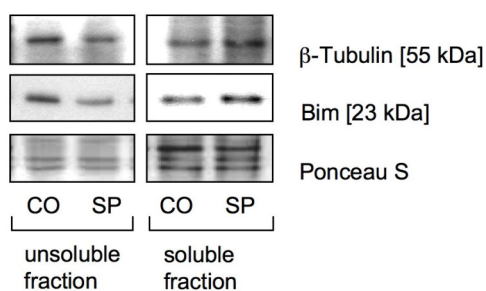


**Figure III.24: Spongistatin 1 depolymerizes tubulin, thereby releasing Bim from its sequestration at microtubules.**

(A) Spongistatin 1 acts as a tubulin depolymerizing agent. MCF-7 cells were transfected with plasmids encoding for GFP-tubulin. Cells were left untreated (CO) or treated with spongistatin 1 (SP; 500 pM) for 8 h. The depolymerization of the tubulin was analyzed by confocal microscopy. GFP-tubulin is shown green. (B) Spongistatin 1 induces the release of Bim from the microtubules. MCF-7 cells were left untreated (CO) or treated with spongistatin 1 (SP; 500 pM) for 8 h. Soluble and insoluble fractions were prepared and  $\beta$ -tubulin and Bim were detected by Western Blot analysis. Equal protein loading was controlled by staining membranes with Ponceau S (a representative section of the stained membrane is shown). One representative blot of three is shown.

Thereby Bim was released from the microtubules shown by a diminished Bim level in the insoluble fraction and an elevation of Bim in the soluble fraction upon stimulation with spongistatin 1. The protein level of Bim in the whole cell lysate stayed equal during the entire process (Figure III.27).

### 3.5.2 SPONGISTATIN 1 DISRUPTS THE MCL-1/BIM COMPLEX

As Bim was originally described as a Bcl-2 interacting protein capable of triggering the mitochondrial pathway by either directly activating Bax or by binding prosurvival Bcl-2 proteins [91], Bim was suggested to block Bcl-2 and/or activate Bax via binding to these factors. However, immunoprecipitation experiments shown in Figure III.25 indicated that Bim is constitutively associated with Bcl-2, Bcl-x<sub>L</sub> and Bax, but did not support the view of Bim translocating to Bcl-2, Bcl-x<sub>L</sub> or Bax during induction of apoptosis by spongistatin 1. No enhanced translocation of Bim to Bcl-2, Bcl-x<sub>L</sub> or Bax was respectively detectable upon treatment with spongistatin 1.

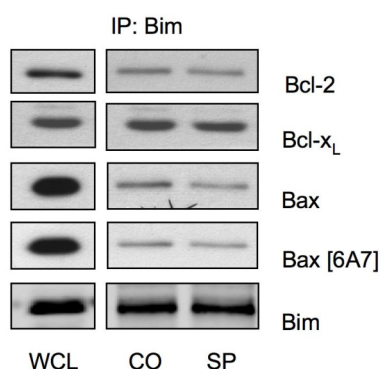


**Figure III.25: Bim is constitutively associated with Bcl-2, Bcl-x<sub>L</sub> and Bax.**

MCF-7 cells were left untreated (CO) or treated with spongistatin 1 (SP; 500 pM) for 8 hours. Bim was precipitated and its interactions with Bcl-2, Bcl-x<sub>L</sub>, Bax and Bax (6A7) were detected by specific antibodies using Western Blot analysis. Equal protein precipitation was controlled by detecting Bim with a specific antibody. The whole cell lysate (WCL) was used as control for protein detection. All experiments were carried out three times.

As Bim and Mcl-1 are well-known binding partners, the sequestration of Bim by the antiapoptotic Bcl-2 family member Mcl-1 was expected to block the Bim-mediated mitochondrial apoptosis cascade. Therefore, the binding of Mcl-1 and Bim upon treatment with spongistatin 1 was assessed by immunoprecipitation experiments either by precipitating Bim (Figure III.26A) or Mcl-1 (Figure III.26B).

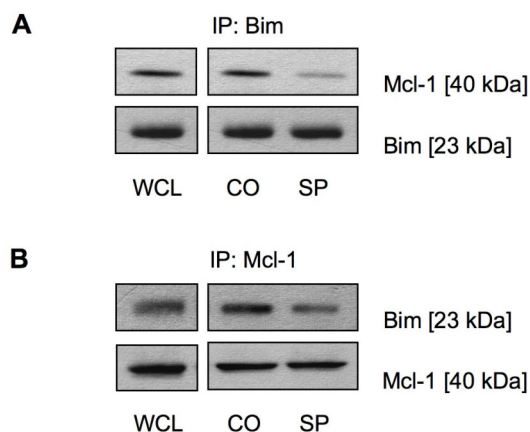


**Figure III.26: Spongistatin 1 disrupts the Mcl-1/Bim complex.**

Cells were left untreated (CO) or stimulated with spongistatin 1 (SP; 500 pM) for 8 h. Bim (**A**) or Mcl-1 (**B**) was precipitated and the interaction with Mcl-1 or Bim was detected by Western Blot analysis, respectively. Equal protein precipitation was controlled by detecting Bim or Mcl-1 with a specific antibody. The whole cell lysate (WCL) was used as control for protein detection. All experiments were carried out three times.

In both settings spongistatin 1 was able to disrupt the Mcl-1/Bim complex, shown by a decrease of the associated proteins, whereas the levels of the precipitated proteins stayed equal. This effect is not due to a degradation of either Mcl-1 or Bim, since it was no change in protein levels of both factors during the whole time of the experiment detectable (Figure III.27).

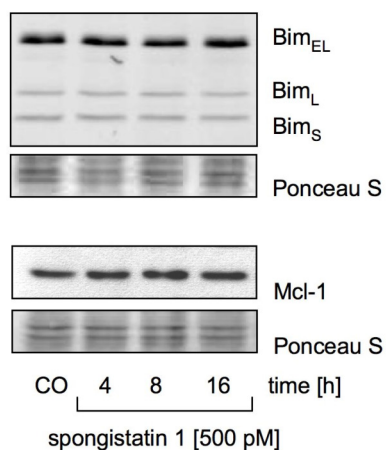


### Figure III.27: Bim and Mcl-1 are not degraded upon spongistatin 1-treatment.

Cells were left untreated (CO) or stimulated with spongistatin 1 (SP; 500 pM) for the indicated times. Bim (*upper panel*) and Mcl-1 (*lower panel*) protein levels were detected by Western Blot analysis, respectively. Equal protein loading was controlled by staining membranes with Ponceau S (a representative section of the stained membrane is shown). One representative blot of three is shown.

### 3.5.3 BIM KNOCKDOWN PREVENTS CELL DEATH BY SPONGISTATIN 1

Elucidating the functional role of Bim in the spongistatin 1-induced cell death, the expression of this protein was downregulated by siRNA. Bim siRNA induced specific gene silencing of Bim over a period of 72 h as determined at protein level. Most importantly, silencing of Bim by siRNA reduced significantly DNA fragmentation upon stimulation with spongistatin 1 (Figure III.28), demonstrating that Bim functions as a major proapoptotic factor in the spongistatin 1-induced cell death.

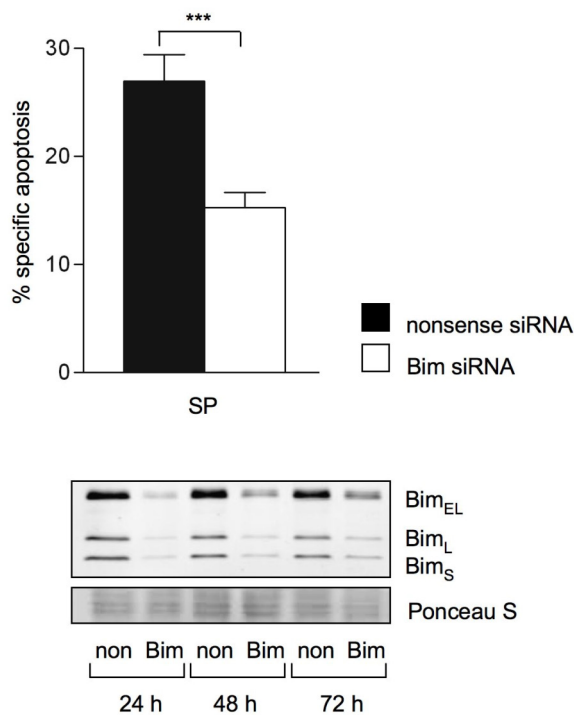


### Figure III.28: Bim siRNA inhibits spongistatin 1-induced cell death.

MCF-7 cells were transfected with oligonucleotides encoding for either Bim siRNA or a nonsense sequence. *Upper panel*, cells were left untreated (CO) or treated with spongistatin 1 (SP; 500 pM) for 48 h. Apoptotic cells were quantified by flow cytometry. Results are represented as the percentage of specific apoptosis. *Bars*, the mean  $\pm$  S.E. of three independent experiments performed in triplicate. \*\*\*,  $p < 0.001$  (ANOVA/Bonferroni). *Lower panel*, downregulation of the Bim protein level was verified by Western Blot using an antibody against the all three splice variants Bim<sub>EL</sub>, Bim<sub>L</sub> and Bim<sub>S</sub>. Equal protein loading was controlled by staining membranes with Ponceau S (a representative section of the stained membrane is shown).

### 3.5.4 BIM FUNCTIONS AS A PROAPOPTOTIC FACTOR UPSTREAM OF MITOCHONDRIA

To verify the notion that Bim acts upstream of mitochondria, Bim was silenced by siRNA and the impact of its downregulation on the release of proapoptotic factors from the mitochondria to the cytosol as well as the translocation to the nucleus was investigated.

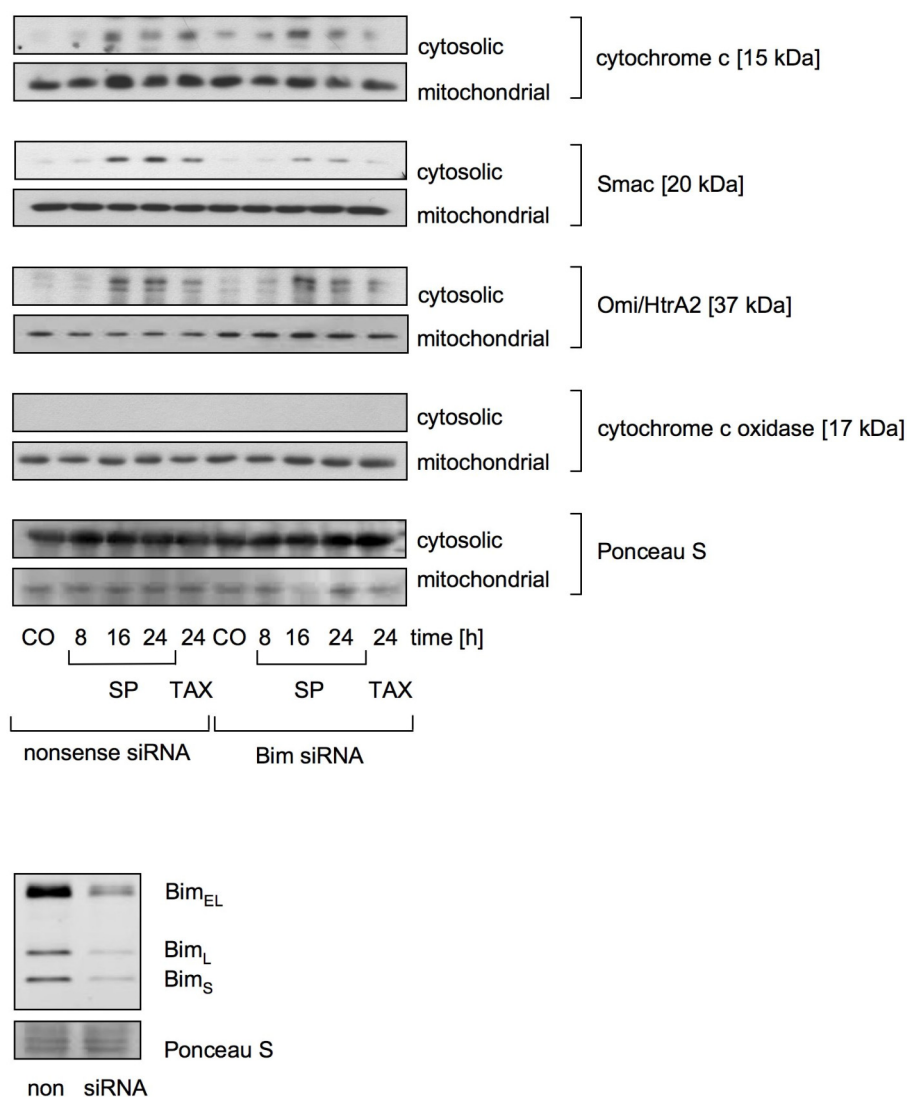


**Figure III.29: Bim functions as a proapoptotic regulator upstream of mitochondria.**

MCF-7 cells were transfected with oligonucleotides encoding for either Bim siRNA or nonsense sequence. *Upper panel*, cells were left untreated (CO) or treated with spongistatin 1 (SP; 500 pM) or as positive control with taxol (TAX; 500 nM) for the indicated times. Cytosol and mitochondrial protein fractions were prepared and cytochrome c, Smac/DIABLO, Omi/HtrA2 were detected by specific antibodies using Western Blot analysis. Cytochrome c oxidase served as control for the quality of the extraction procedure. *Lower panel*, downregulation of the Bim protein level was verified by Western Blot using an antibody against the three splice variants Bim<sub>EL</sub>, Bim<sub>L</sub> and Bim<sub>S</sub>. Equal protein loading was controlled by staining membranes with Ponceau S (a representative section of the stained membrane is shown). All experiments were carried out three times.

Silencing of Bim by siRNA led to a diminished release of Smac from the mitochondria to the cytosol, whereas the release of cytochrome c and Omi/HtrA2 was not affected (Figure III.29). These proteins are thought to be involved in the caspase-mediated apoptotic pathway. As previously shown in Figure III.18, the caspases are not central in the signaling pathway induced by spongistatin 1. Therefore, cytochrome c, Smac and Omi/HtrA2 might also play an inferior role in this signaling cascade.

More importantly, Bim is involved in the caspase-independent apoptotic pathways as it triggered the translocation of mitochondrial AIF and EndoG to the nucleus (Figure III.30). These two factors acting independently of caspases were previously shown to be involved in spongistatin 1-mediated apoptosis (Figure III.21).

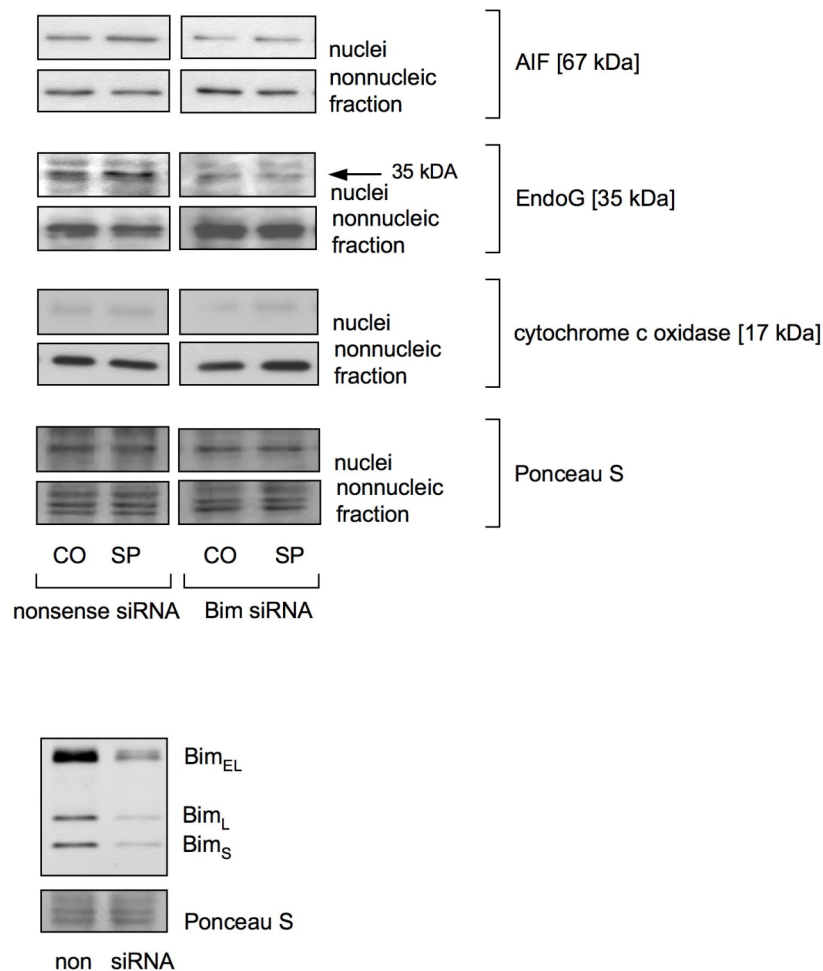


**Figure III.30: Bim is involved in the caspase-independent apoptotic pathway.**

MCF-7 cells were transfected with oligonucleotides encoding for either Bim siRNA or nonsense sequence. *Upper panel*, cells were left untreated (CO) or treated with spongistatin 1 (SP; 500 pM) for 24 hours. Nonnucleic and nuclear protein fractions were prepared and AIF and EndoG were detected by specific antibodies using Western Blot analysis. Cytochrome c oxidase served as a control for the quality of the extraction procedure. *Lower panel*, as a control, the Bim protein levels in cell lysates from nonsense and Bim siRNA transfected cells were analyzed by Western Blot.

In MCF-7 cells transfected with Bim siRNA, no translocation of AIF and EndoG to the nucleus was detectable, whereas in cells transfected with a nonsense sequence AIF and EndoG translocated to the nucleus shown by an increase of these proteins in the nuclear fraction.

Finally, to prove the impact of Bim and caspase-independent players such as EndoG on spongistatin 1-induced apoptosis, cells were cotransfected with Bim and EndoG siRNA. Indeed, a marked reduction in DNA fragmentation equal to the level of the control cells in response to spongistatin 1 exposure could be observed (Figure III.31) indicating that EndoG dominates the cell death pathway triggered by Bim in response to spongistatin 1 treatment. This supports the notion of Bim as a major proapoptotic factor involved in caspase-independent apoptotic signaling pathways.

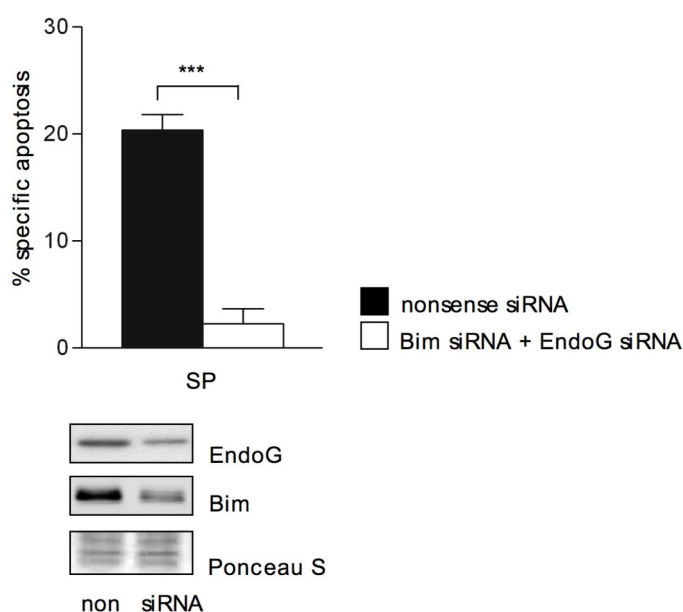


**Figure III.31: Bim and EndoG are the major regulators of spongistatin 1-induced cell death.**

MCF-7 cells were cotransfected with oligonucleotides encoding for either Bim siRNA and EndoG siRNA or nonsense sequence. *Upper panel*, cells were left untreated (CO) or treated with spongistatin 1 (SP; 500 pM) for 48 h. Apoptotic cells were quantified by flow cytometry. Results are represented as the percental specific apoptosis. *Bars*, the mean  $\pm$  S.E. of three independent experiments performed in triplicate. \*\*\*,  $p < 0.001$  (ANOVA/Bonferroni). *Lower panel*, downregulation of Bim and EndoG protein levels were verified by Western Blot. Equal protein loading was controlled by staining membranes with Ponceau S (a representative section of the stained membrane is shown). All experiments were performed three times with consistent results.



## **DISCUSSION**

## IV DISCUSSION

Unfortunately, the anticancer drugs that are nowadays in clinical use have only limited success due to two major problems. First, the high mortality rates associated with cancer are caused by the metastatic spread of tumor cells from the site of their origin. Despite recent advantages in early detection and new therapeutic options for cancer patients, metastatic progression is attributed to 90% of human cancer fatalities and represents the major unsolved problem in cancer therapy. Secondly, a common problem in chemotherapy is the often developed resistance of cancer cells to anticancer agents. Since cytotoxic effects of many anticancer drugs are mediated via the apoptotic pathway, resistance to chemotherapy often reflects an inability of tumor cells to undergo apoptosis [5]. Hence, there is need for the development of novel and pharmacologically effective chemotherapeutic agents as well as characterizing and targeting unusual apoptotic signaling pathways to resensitize cancer cells to chemotherapy. In this respect, the spongistatins are promising substances in the combat against metastatic and chemoresistant cancer cells, particularly because of their exceptional potency on the 60 human cancer cell line panel of the National Cancer Institute (NCI).

### 1 SPONGISTATIN 1, A POTENT ANTICANCER AGENT

The current study presents the marine natural compound spongistatin 1 as a powerful apoptosis inducing agent in various human tumor cell lines. Spongistatin 1 treated cancer cells exhibited characteristic features of apoptotic cell death including cell shrinkage, formation of apoptotic bodies (Figure III.1) and cell cycle arrest at G<sub>2</sub>/M phase (Figure III.4). Of note, spongistatin 1 was able to induce DNA fragmentation, a hallmark of apoptosis, in several cancer cell lines characterized by their insensitivity to many chemotherapeutic drugs or by their increased invasiveness (Figure III.3). The human pancreatic cancer cell line L3.6pl and the human epithelial breast cancer cell line MCF-7 were chosen for further experiments. Both spongistatin 1 as well as the anticancer agent taxol induced DNA fragmentation in MCF-7 cells and L3.6pl cells, however spongistatin 1 was effective at a concentration 1000-fold lower than taxol (Figure III.5). Most importantly, spongistatin 1 showed strong long term effects on the clonogenic survival of both of these cell lines. Spongistatin 1 was able to almost completely suppress the growth of colonies, whereas established anticancer drugs including the tubulin-antagonists taxol and vinblastine in concentrations corresponding to the apoptosis rate of spongistatin 1 reduced the accumulation of colonies to a minor extent (Figure III.5). Thus, the inhibitory effects of spongistatin 1 on clonal tumor cell growth are not only caused by its impact on microtubules, but they seem to be specific for this compound.

Taken together, spongistatin 1 can be regarded as a powerful apoptosis-inducing and growth-inhibiting agent even in metastatic and apoptosis resistant cells. Therefore, it seemed of special interest to clarify the underlying mechanisms of spongistatin 1-induced cytotoxicity, shown in two separate models. First, the effects of spongistatin 1 on critical steps in the metastatic cascade were studied *in vitro* using the highly invasive pancreatic tumor cell line L3.6pl cell. Secondly, apoptotic signaling pathways to circumvent chemoresistance were investigated in the caspase-3 deficient human epithelial breast cancer cell line MCF-7.

## 2 ANTIMETASTATIC EFFECTS OF SPONGISTATIN 1

Pancreatic adenocarcinoma is characterized by aggressive invasion, early metastasis and resistance to chemotherapeutic agents. The 5-year overall survival rate for all patients with pancreatic cancer is only 4%, a statistic which is essentially unchanged from two decades ago despite intensive research [139]. More efficient therapies for pancreatic carcinoma, especially targeting the metastatic process, are thus needed.

The basis of this project represents the strong antimetastatic potential of spongistatin 1 *in vivo*, studied in the orthotopic pancreatic tumor model [112, 136]. Intriguingly, spongistatin 1 was able to decrease the formation of liver metastases by about 78% and lymph node metastases by about 66% (Table III.1). Motivated by these impressive data, the current study focused on the impact of spongistatin 1 on central steps in the metastatic cascade *in vitro*.

### 2.1 SPONGISTATIN 1 INFLUENCES CRITICAL STEPS IN THE METASTATIC PROCESS

The understanding of mediators involved in critical steps in the metastatic process is essential for the development of targeted therapies for pancreatic carcinoma.

Firstly, cell proliferation is one of the key steps in tumorigenesis and metastasis. Metastatic tumor cells are characterized by a strong proliferation in the primary tumor as well as at a secondary site to establish there metastatic foci [140]. Of note, spongistatin 1 strongly inhibited tumor cell proliferation even at remarkably low concentrations in the picomolar range (Figure III.6).

Secondly, an important aspect of the metastatic cascade addresses cell migration and invasion. Tumor cells must invade through the adjacent basement membrane into surrounding tissues and then migrate to and invade the vasculature to disseminate to distant sites. Indeed, *in vitro* experiments, namely the “wound healing” assay and the

modified “Boyden chamber”, revealed antimetastatic properties of spongistatin 1 by inhibiting migration as well as invasion, respectively, even in nontoxic concentrations (Figure III.7, Figure III.8).

These fundamental processes in cancer metastasis involve a dynamic interaction between the tumor cells and the extracellular matrix (ECM) as well as proteolytic remodeling of the ECM [103]. Multiple sets of proteolytic proteins are upregulated and activated during cancer progression. The principle classes of enzymes that degrade the ECM- and cell-associated proteins are the matrix metalloproteinases (MMPs), which are zinc-dependent endopeptidases that cleave and degrade a wide spectrum of ECM components. *In vivo* studies performed by our working group revealed, that MMP-9 was activated in the primary tumor established from L3.6pl cells in the orthotopic pancreatic tumor model. Importantly, spongistatin 1 was able to downregulate MMP-9 at the transcriptional level (data unpublished), thereby probably inhibiting tumor cell invasion.

Thirdly, cell adhesion has an essential role in regulating metastatic processes, particularly at two different steps: On the one hand, tumor cell motility and invasion are dynamic processes involving the formation of adhesions to the ECM at the leading edge of the cell and detachment from the ECM at the trailing edge. Thus, the cell can be put forward by cytoskeletal contraction. On the other hand, metastatic tumor cells in the circulatory system must arrest at a distant site by attachment to the subendothelial ECM [140]. Our data demonstrates an impact of spongistatin 1 on the latter process of tumor cell adhesion, the arrest of detached cells at a secondary site. L3.6pl cells prestimulated with spongistatin 1 for three hours showed a decreased ability to attach on collagen-coated (Figure III.9) surfaces.

In this context, focal adhesion kinase (FAK) is a central player in functional adhesion signaling, cell motility and survival of human solid tumors. These properties may be linked to FAK overexpression or to a constitutive activation of FAK in a subset of metastasizing cancer cells. Increased FAK expression and activity are frequently correlated with malignant or metastatic disease and poor patient prognosis [141]. Several reports have implicated that the activity of FAK correlates with phosphorylation at specific tyrosine residues. Although phosphorylation at Tyr397 might not necessarily reflect FAK kinase activity in different tumor types [107, 142], there is evidence that FAK phosphorylation, especially at the Tyr397 residue, may regulate tumor cell migration. Chatzizacharias et al. [143] demonstrated recently that increased FAK tyrosine phosphorylation and consequently increased FAK signaling seem to drive cells to a more aggressive and even malignant phenotype. Hence, FAK displayed an important aspect in the metastatic process to be addressed in our present study. In fact, the used L3.6pl cells revealed a constitutive activation of FAK by phosphorylation at Tyr397. Treatment with

spongistatin 1 led to a dephosphorylation of FAK at Tyr397 (Figure III.10), which may be linked with an inactivating of this enzyme and a diminished migration and invasion of L3.6pl cells.

## 2.2 APOPTOSIS AND METASTASIS

Matrix-independent passage of cancer cells through blood and/or lymph compartments is an essential component of the metastatic cascade. Therefore, metastatic cancer cells by definition would have to acquire the ability to survive in a detached state. Since detachment of cells from the extracellular matrix induces programmed cell death, metastatic dissemination may depend upon the resistance of metastatic cells to apoptosis. Several previous studies exhibited that most cell lines derived from solid tumors grow in an anchorage-independent manner in suspension culture [144]. Moreover, experimental evidence demonstrated that suppression of anoikis, apoptosis caused by detachment from the ECM, in transformed cells strongly enhances their tumorigenicity *in vivo* [145]. These observations support the hypothesis that induction of apoptosis is one of the key mechanisms for elimination of misplaced cells and may prevent metastatic spread. Indeed, the used metastatic L3.6pl cells were resistant to anoikis and this resistance was abolished by treatment with spongistatin 1. Culturing L3.6pl cells in suspension conditions and not allowing them to adhere did not induce anoikis. Intriguingly, upon treatment with spongistatin 1, these cells overcame anoikis-resistance and showed significant DNA-fragmentation after 24 h (Figure III.11). Thus, spongistatin 1 can be considered as a potential compound in the combat against metastasis, generating a link between apoptosis-induction and metastasis-inhibition.

To investigate the underlying mechanisms of spongistatin 1 on anoikis, we focused on several known factors of the apoptotic machinery that have been shown to be involved in anoikis-resistance and metastasis. There is some experimental evidence indicating that a higher resistance to apoptosis of metastatic cancer cells is associated with the dysfunction of apoptosis regulatory factors. Among them, the Bcl-2 family proteins seem to play a prominent role in both tumorigenesis and metastasis. The antiapoptotic proteins of the Bcl-2 family function in carcinogenesis by preventing apoptosis of tumor cells instead of promoting cell proliferation. Elevated expression of antiapoptotic Bcl-2 was shown to be associated with an increased metastatic phenotype in several human pancreatic cancer cell lines and simultaneously conferred a resistance to apoptotic responsiveness [146]. Furthermore, Fernandez et al. [147] revealed Bcl-x<sub>L</sub> to improve cell survival without cellular adhesion and in the circulation, thereby enhancing anchorage-independent growth, which may cause metastasis. Additionally, Espana et al. [148] demonstrated *in vivo* that an overexpression of Bcl-x<sub>L</sub> in highly metastatic MDA-MB-435 cells enhances

metastatic activity. Although Bcl-2 and Bcl-x<sub>L</sub> are closely related to each other and repress cell death through common mechanisms [149], they are not functionally equivalent. Previous findings indicate that overexpression of Bcl-x<sub>L</sub> correlated better with tumor metastasis than Bcl-2 [147, 148]. Consistent with these findings, we proposed an involvement of both Bcl-2 and Bcl-x<sub>L</sub> in spongistatin 1-mediated cytotoxicity. Western Blot analysis indicated that Bcl-2 was phosphorylated and thereby inactivated upon spongistatin 1 treatment, whereas Bcl-x<sub>L</sub> is both phosphorylated and its protein levels are diminished by spongistatin 1 (Figure III.12). The additional downregulation or degradation of Bcl-x<sub>L</sub> may demonstrate the predominant role of this protein in the metastatic process. Knockdown experiments of Bcl-2 and Bcl-x<sub>L</sub> using siRNA technique confirmed the functional role of these two proteins in anoikis resistance (Figure III.13). We suppose that spongistatin 1 overcomes the resistance to anoikis by inactivating these two proteins. Besides their involvement in resistance to anoikis, Bcl-2 and Bcl-x<sub>L</sub> were previously shown to promote migration and invasion. In a recent study, Du et al. [150] presented Bcl-x<sub>L</sub> as a factor which is able to trigger cell motility and invasion by remodeling the actin cytoskeleton, affecting cell shape and adhesion. Thus, Bcl-x<sub>L</sub> may provide prometastatic properties different from neutralizing proapoptotic Bcl-2 family members. In agreement with these findings, our data support the notion of an involvement of the antiapoptotic proteins Bcl-2 and Bcl-x<sub>L</sub> in cell motility and migration (Figure III.14). Because of their key roles in the regulation of both apoptosis and metastasis, Bcl-2 and Bcl-x<sub>L</sub> display potential targets for chemotherapy.

### 2.3 CONCLUSION AND FURTHER DIRECTIONS

The presented data introduces spongistatin 1 as a potent antimetastatic agent *in vivo* and *in vitro* against the highly invasive and anoikis-resistant pancreatic cancer cells L3.6pl. Spongistatin 1 was shown to affect critical events in the metastatic cascade including proliferation, cell migration, invasion and adhesion. Additionally, our results, namely the inactivation and/or downregulation of the prosurvival proteins Bcl-2 and Bcl-x<sub>L</sub> as well as knockdown experiments of these proteins combined with apoptosis and migration assays, reinforce the hypothesis of a functional link between apoptosis inhibition and metastasis. However, besides this study more functional experiments are necessary to establish the involvement of apoptotic processes in the metastatic cascade. For example, performing metastasis assays with silenced FAK would give some information about the importance of this factor in the distinct metastatic steps. Furthermore, the investigation of downstream targets of FAK would be interesting to get detailed insights into the signaling pathways. Proteins of the Bcl-2 family are both key regulators of the intrinsic apoptotic pathway and important factors in the metastatic process [151]. In this respect, these proteins are currently under investigation by our group. Overexpression as well as silencing of Bcl-2

and Bcl-x<sub>L</sub> in combination with functional metastatic assays, such as the tumor invasion assay, would give important information in the understanding of the functional involvement of antiapoptotic processes in metastasis.

### 3 APOPTOTIC SIGNALING PATHWAYS

In order to elucidate the apoptotic mechanisms of spongistatin 1, we focused on signaling pathways to overcome chemoresistance of the human breast cancer cells MCF-7. As MCF-7 cells are quite insensitive to many chemotherapeutic agents due to a deletion in caspase-3, this cell line represents a good model to study apoptotic mechanisms to combat chemoresistant cells [152]. Breast cancer is the leading cause of cancer death amongst women in developed countries [153]. Despite increased understanding of the molecular aberrations underlying this disease and advances in treatment, therapeutic resistance remains the major obstacle to an effective cure, emphasizing the need for pharmacological therapeutics that trigger unusual signaling pathways to overcome chemoresistance. The principal mediators of apoptosis are caspases, and failure to activate these caspases accounts for cancer cell resistance to apoptosis [154, 155]. Therefore, the triggering of caspase-independent apoptotic pathways is an attractive therapeutic strategy to overcome chemoresistance [156].

#### 3.1 INVOLVEMENT OF THE INTRINSIC APOPTOTIC PATHWAY

Since the intrinsic apoptotic pathway is frequently triggered by chemotherapeutic agents, mitochondrial events upon spongistatin 1 treatment were initially monitored. Critical regulators of this pathway are members of the Bcl-2 protein family. The interplay between opposing members of the Bcl-2 family influences the permeability of the outer mitochondrial membrane. Multidomain proapoptotic proteins, such as Bax, are referred to as essential regulators of apoptosis signaling based on several knock-out studies [157, 158]. In fact, spongistatin 1 was able to trigger the intrinsic mitochondrial pathway by activating Bax (Figure III.15). Moreover, the antiapoptotic proteins Bcl-2 and Bcl-x<sub>L</sub> are phosphorylated in response to spongistatin 1 treatment, causing an inactivation of these proteins. As Bcl-2 phosphorylation is a specific feature of microtubule affecting drugs [82], this phosphorylation may be associated with the tubulin depolymerization and G<sub>2</sub>/M arrest induced by spongistatin 1. The activation of proapoptotic Bax and concomitant inactivation of prosurvival Bcl-2 and Bcl-x<sub>L</sub> by spongistatin 1 unbalances the ratio of pro- and antiapoptotic Bcl-2 proteins, thereby permeabilizing the outer mitochondrial membrane.

The release of mitochondrial intermembrane space proteins to the cytosol is a key event during the intrinsic apoptotic pathway [120, 121]. For instance, cytochrome c is required for the initiation of the apoptosome and activation of caspases, whereas Smac and Omi/HtrA2 are believed to enhance caspase activation through the neutralization of the inhibitors of apoptosis proteins. Although a release of cytochrome c, Smac and Omi/HtrA2 from the intermembrane space of mitochondria to the cytosol could be detected early during spongistatin 1-induced apoptosis, the activation of the caspases occurred late and only slightly (Figure III.17A). In addition, MCF-7 cells reconstituted with caspase-3 did not show a significant increase in DNA-fragmentation upon spongistatin 1 treatment in comparison to MCF-7 cells depleted of caspase-3, whereas the expression of functional caspase-3 greatly enhanced the sensitivity of these cells to staurosporine, a well-known apoptosis-inducing agent able to trigger both the extrinsic and the intrinsic apoptotic pathway [159] (Figure III.17B). Furthermore, the functional role of caspases was assured using the pan-caspase inhibitor Q-VD-OPh. Presence of Q-VD-OPh led to a moderate reduction in DNA fragmentation (Figure III.18). This effect was not limited to MCF-7 cells but also observed in several other tumor cell lines.

These data strongly suggest that caspases, especially caspase-3, are not the key players in the spongistatin 1 induced apoptotic signaling. Tumor cells often develop resistance to apoptosis by deregulation of apoptotic mechanisms, one of them is inactivation and depletion of caspases [5], the core of classical apoptotic pathways. As spongistatin 1 was able to induce apoptosis despite the inferior role of the caspases in spongistatin 1-induced cell death it can be considered as a valuable agent circumventing chemoresistance. Several studies indicate that apoptosis might not even require caspase activation [79, 160], asking for an additional involvement of caspase-independent apoptotic pathways.

### 3.2 CASPASE-INDEPENDENT MECHANISMS

For that reason, our study focused on the involvement of proapoptotic factors working independently of caspases. Mitochondria have been referred to also release factors involved in caspase-independent cell death including Omi/HtrA2, apoptosis-inducing factor (AIF) and endonuclease G (EndoG) [161].

Multiple previous studies demonstrated that the serine protease Omi/HtrA2 promotes apoptosis by mechanisms similar to Smac. Omi/HtrA2 is formed as a precursor and translocates to the mitochondria, where it is processed to its mature form by proteolytic cleavage. Thereby, the IBM motif is exposed allowing Omi/HtrA2 to interact with XIAP and promote caspase-dependent cell death. But unlike Smac, Omi/HtrA2 contributes to caspase-independent apoptosis due to its protease activity in addition to its physical

inhibition of IAPs [162]. Indeed, siRNA-mediated knockdown of Omi/HtrA2 combined with pan-caspase inhibitor zVAD.fmk almost completely protected HeLa cells from undergoing staurosporine-induced cell death, whereas caspase-inhibition alone was significantly less effective [163]. Besides its mitochondrial localization, Omi/HtrA2 was also been detected in the nucleus of resting cells [70]. Thus, Omi/HtrA2 was hypothesized to translocate to the nucleus upon spongistatin 1 treatment and to exert its serine protease activity. However, we could not detect any translocation of Omi/HtrA2 from mitochondria to the nucleus neither by Western Blot analysis nor confocal microscopy (Figure III.20). Additionally, knockdown experiments of Omi/HtrA2 using siRNA techniques confirmed that Omi/HtrA2 did not exhibit a functional role in spongistatin 1-induced cell death (Figure III.21).

The second factor working independent of caspases and elucidated in this study was AIF. AIF is a mitochondrial flavoprotein, its main function during apoptosis is to translocate to the nucleus and initiate large-scale (50kb) DNA fragmentation. *In vitro* studies using recombinant AIF showed [71, 74], that AIF is not able to cleave DNA by itself, but recruits or activates endonucleases to facilitate DNA fragmentation and chromatin condensation [75] building up a so-called “degradeosome” [76]. Third, upon apoptotic stimuli endonuclease G, like AIF, translocates from the mitochondria to the nucleus and contributes extensively to apoptotic nuclear DNA degradation into oligonucleosomal fragments in a caspase-independent way. Of note, upon spongistatin 1 treatment, AIF and EndoG translocated from mitochondria to the nucleus, shown by both Western Blot analysis and confocal microscopy (Figure III.20).

Niikura et al. proposed in a recent study [164] that both AIF and EndoG are essential in the caspase-independent cell death signaling pathway, whereas one of these two factors alone is not able to induce apoptosis. In contrast to these findings, Arnould et al. demonstrated that AIF and EndoG define a caspase-dependent mitochondria-initiated apoptotic DNA degradation pathway [165, 166]. Hence, it remains to be examined whether caspases are required for the release of AIF from mitochondria and for DNA fragmentation, and whether EndoG could be the endonuclease interacting and cooperating with AIF. Our data indicates, that AIF and EndoG collaborate in spongistatin 1-induced cell death. Combined silencing of these genes with siRNA resulted in a marked reduction in DNA fragmentation (75%, Figure III.21) whereas gene silencing of AIF and EndoG individually did not rescue apoptosis in the case of AIF or only by 45% upon EndoG downregulation. Moreover, the functional role of both proteins appeared to be independent of caspase-activation as preincubation with the pan-caspase inhibitor zVAD.fmk did not show a pronounced protection from apoptosis (Figure III.21). These results are in agreement with the findings of Niikura et al. [164]. Our experiments support the notion that AIF alone is not able to induce DNA fragmentation, but enhances the

activity of endonucleases. We hypothesize that EndoG is an endonuclease that interacts and cooperates with AIF in spongistatin 1-induced apoptosis.

### 3.3 INVOLVEMENT OF BIM

The release of mitochondrial proteins, especially AIF and EndoG, is largely regulated by members of the Bcl-2 protein family. Since the BH3-only proteins tBid and Bim execute a highly proapoptotic function by antagonizing all the prosurvival Bcl-2 family proteins [95], they were supposed to be central factors regulating the release of AIF and EndoG from the mitochondria. A functional link between these two proteins and Bim was recently presented by Liou et al. [167], associating Bim<sub>EL</sub> upregulation with the AIF translocation. In two additional studies, BH3-only proteins, especially tBid and Bim, are shown to induce the translocation of EndoG from mitochondria to the nucleus [72, 73].

First, the activation of Bid by cleavage to its truncated form tBid was studied by Western Blot analysis. Upon spongistatin 1 treatment, full-length Bid was not cleaved into its active form tBid (Figure III.22) in contrast to staurosporine, which has been previously described to mediate apoptosis in MCF-7 cells through the contribution of Bid cleavage [168]. However, the necessity of Bid cleavage to its proapoptotic acting relative tBid has been recently challenged by the finding that full-length Bid also mediates apoptosis in epithelial cells without any previous cleavage by caspase-8 or interaction with other Bcl-2 family members [169]. Based on this information, further studies were required to elucidate the involvement of Bid in the spongistatin 1-induced cell death. Initially we pretreated with the small molecular Bid inhibitor BI-6C9, developed in the laboratory of Maurizio Pellecchia (The Burnham Institute, La Jolla, USA), but it did not decrease DNA fragmentation by spongistatin 1 (Figure III.23). As we could not detect any cleavage of Bid to the active form tBid as well no protection by the Bid-inhibitor BI-6C9 upon spongistatin 1 treatment, we concluded that Bid does not participate in the spongistatin 1-mediated apoptotic pathways.

Hence, our study focused on the involvement of Bim in the apoptosis signaling pathway induced by spongistatin 1. Puthalakath et al. demonstrated that under physiological conditions Bim is bound to the dynein light chain (LC8) of microtubules and thereby sequestered from other Bcl-2 family members [123]. Apoptotic stimuli are thought to disrupt this interaction thereby freeing Bim to translocate to the mitochondria and releasing proapoptotic factors from the intermembrane space to the cytosol. In line with the findings of Puthalakath et al. [123], our results confirmed the association of Bim with the microtubular complex in healthy cells. By depolymerizing the tubulin scaffold, spongistatin 1 freed Bim from its sequestration by the microtubules (Figure III.24).

Originally, Bim was described as a Bcl-2 interacting protein capable of initiating the mitochondrial pathway by either directly activating Bax-like proteins or by binding to prosurvival Bcl-2 family members. These interactions disturb the balance between pro- and antiapoptotic Bcl-2 proteins resulting in the release of proapoptotic molecules from the intermembrane space of mitochondria to the cytosol [91]. Recently Weber et al. [170] demonstrated that the Bim<sub>s</sub> apoptosis inducing potential is correlated with mitochondrial localization, but not the ability to bind to Bcl-2. Nevertheless, the essential activity of Bim<sub>s</sub> is assumed to be the activation of Bax. Contrary to this hypothesis, the results of Willis et al. [99] suggest that Bim is able to induce apoptosis without binding Bax. Our immunoprecipitation experiments examining as to whether Bim binds to Bcl-2, Bcl-x<sub>L</sub>, Bax and conformationally changed Bax, respectively, revealed that even in untreated cells Bim is already associated with Bcl-2, Bcl-x<sub>L</sub> and Bax. However, no enhanced translocation of Bim to Bcl-2, Bcl-x<sub>L</sub> and Bax upon induction of apoptosis by spongistatin 1 has been observed (Figure III.25).

Moreover, the activity of Bim has been described to be regulated by the antiapoptotic Bcl-2 family member Mcl-1, possessing a high affinity binding capacity for BH3-only proteins such as Bim and thereby functioning as a reservoir for those proapoptotic proteins [171]. Bim shows a higher affinity for Mcl-1 than Bcl-2 suggesting Bim to counteract Mcl-1 more actively than Bcl-2 [172, 173]. Consistent with this previous observation, our data obtained from immunoprecipitation experiments indicates that spongistatin 1 is able to disrupt the Mcl-1/Bim complex, thereby abolishing the sequestration of the potent proapoptotic protein Bim (Figure III.26). A common view is that antagonizing the prosurvival activity of Mcl-1 requires its elimination from cells via degradation by the proteasome machinery. Indeed, many death stimuli caused a rapid decrease in Mcl-1 levels that correlated with apoptosis [174]. However, a recent study by Lee et al. [175] demonstrated that Bim-induced cell death is not associated with Mcl-1 degradation and functional inactivation of Mcl-1 does not always require its elimination. According to these findings, the disruption of the Mcl-1/Bim complex was not due to the frequently reported degradation [92] neither of Mcl-1 nor Bim, since the protein levels of both factors stayed equal during the entire experiment (Figure III.27).

Bim has been characterized by several previous studies as a critical initiator of apoptosis in various cell lines [91, 176] and animal models [177]. Deletion of the *bim* gene revealed that Bim is essential for hematopoietic homeostasis. For instance, Bouillet et al. [178] showed, that the *bim*<sup>-/-</sup> mice had excess hematopoietic cells and those cells were refractory to certain apoptotic stimuli. Furthermore, a recent study proposed the reexpression of Bim as a strategy to sensitize cells for the treatment with anticancer agents, since enforced expression of Bim in leukemic cells was associated with a time-dependent increase in the percentage of apoptotic cells [179]. Intriguingly, in line with these previous findings,

silencing of Bim by siRNA led to a marked decrease in DNA fragmentation upon stimulation with spongistatin 1, demonstrating that Bim functions as a major proapoptotic factor in the spongistatin 1-induced cell death. Based on the following two facts, we could identify Bim as a central proapoptotic regulator targeted by spongistatin 1 upstream of mitochondria. First, the silencing of Bim by siRNA rescued the cells from apoptosis and led to a diminished release of mitochondrial proteins (Figure III.29). The release of Smac was inhibited significantly, whereas Omi/HtrA2 and cytochrome c were not affected. However, these factors are supposed to play a minor role in the apoptotic pathway by spongistatin 1, because they induced apoptosis mainly by influencing the activity of caspases that are shown to be nonessential in the spongistatin 1-mediated cell death. Secondly and most importantly, the translocation of the caspase-independent acting proteins AIF and EndoG by spongistatin 1 was inhibited in cells silenced with Bim siRNA (Figure III.30). Moreover, cotransfection experiments with Bim siRNA and EndoG siRNA downregulating these proteins indicated that EndoG dominates the potential pathways to cell death triggered by Bim after spongistatin 1 treatment and confirmed a direct functional link between Bim and the caspase-independent factor EndoG (Figure III.31). These findings established the hypothesis of the involvement of Bim in caspase-independent apoptotic pathways.

### 3.4 CONCLUSION

Based on the presented data, we propose the mechanism of spongistatin 1-induced cell death as illustrated in Figure IV.1. The tubulin depolymerizing agent spongistatin 1 releases the BH3-only protein Bim from its sequestration both by the microtubule network and by the antiapoptotic protein Mcl-1. In turn, Bim triggers the translocation of AIF and EndoG from mitochondria to the nucleus leading to caspase-independent apoptosis.

In conclusion, the natural marine compound spongistatin 1 potently induces apoptosis and inhibits long term survival of the human epithelial breast cancer cells MCF-7, which are quite insensitive to many chemotherapeutic drugs due to deletion of caspase-3. The clarified novel mechanism of action makes spongistatin 1 a promising candidate for the sensitization of chemotherapy-resistant tumor cells. Engagement of caspase-independent apoptotic pathways by spongistatin 1 provides a range of valuable targets. Among them, BH3-only proteins like Bim as well as proapoptotic proteins such as AIF and EndoG contribute to cell death in the absence of caspases. Spongistatin 1 proves both to be a valuable tool to discover novel modes of action in apoptotic signaling, especially the involvement of Bim in caspase-independent apoptosis, as well as to be a promising new anticancer agent in the combat against chemoresistance.

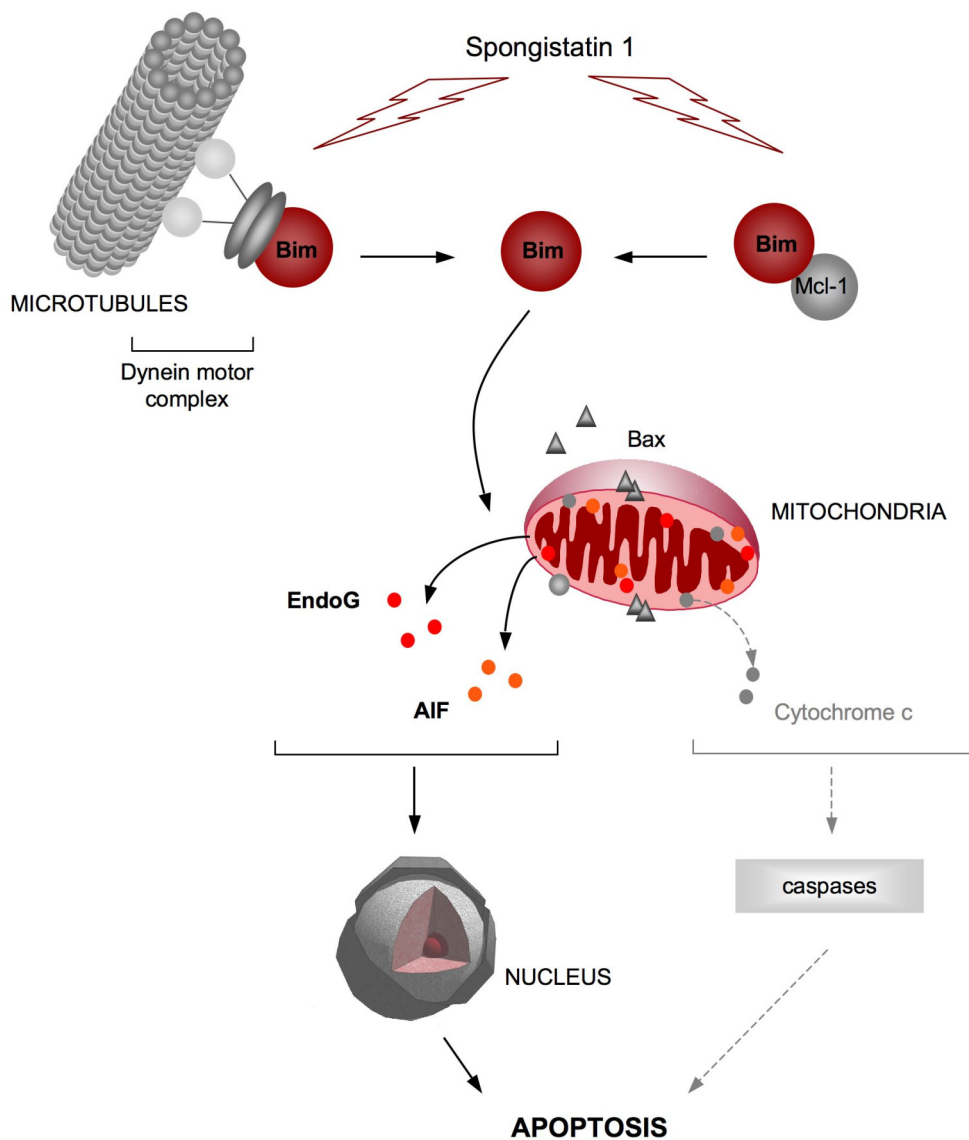


**Figure IV.1: Proposed mechanism of spongistatin 1-induced apoptosis.**

Thick arrows propose the main signaling pathway of spongistatin 1. The tubulin depolymerizing agent spongistatin 1 frees Bim from its sequestration both by the microtubule network and by the antiapoptotic protein Mcl-1. Bim triggers the translocation of AIF and EndoG from mitochondria to the nucleus leading to caspase-independent apoptosis. Thin arrows indicate the inferior role of the caspase-dependent cell death induced by spongistatin 1.



## SUMMARY



## V SUMMARY

Spongistatin 1 is a new experimental chemotherapeutic agent isolated from a marine sponge with **powerful anticancer properties** in a variety of cancer cell lines exerting apoptosis as well as long term effects on the clonogenic survival. The current study presents the impact of spongistatin 1 on the two major problems limiting the success of chemotherapy, namely the metastatic spread of tumor cells to secondary sites and the development of chemoresistance.

Intriguingly, spongistatin 1 revealed **strong antimetastatic effects** in the orthotopic pancreatic tumor model, reducing the formation of liver and lymph node metastases. Based on these impressive *in vivo* data, the antimetastatic potential of spongistatin 1 was monitored *in vitro*. In fact, spongistatin 1 influenced several events in the metastatic process including proliferation, tumor cell migration, invasion and adhesion at a secondary site. Moreover, spongistatin 1 was able to overcome anoikis resistance of metastatic L3.6pl cells, probably through inactivation and/or downregulation of the antiapoptotic proteins **Bcl-2** and **Bcl-x<sub>L</sub>**. Besides their involvement in resistance to anoikis, knockdown studies indicate an essential role of these proteins in cell migration. Spongistatin 1 proves to be a potent antimetastatic agent both by affecting critical steps in the metastatic cascade and by affecting apoptotic pathways thereby circumventing anoikis-resistance.

Investigating the apoptotic mechanisms induced by spongistatin 1 with the focus on signaling pathways to **circumvent chemoresistance**, we were able to identify two facts: First, spongistatin 1 induces the intrinsic pathway of apoptotic cell death, shown by the activation of Bax and the subsequent release of proapoptotic factors from mitochondria to the cytosol. Interestingly, apoptosis occurs mainly **independent of caspases**, involving AIF and EndoG. Upon treatment with spongistatin 1, AIF and EndoG translocate from mitochondria to the nucleus and contribute to spongistatin 1-mediated apoptosis as demonstrated via genetic silencing. Secondly, spongistatin 1 acts as a tubulin depolymerizing agent by freeing the proapoptotic **BH3-only protein Bim** from its sequestration both by the microtubular complex and by the antiapoptotic Bcl-2 family member Mcl-1. Silencing of Bim by siRNA leads to a diminished release of mitochondrial proteins into the cytosol as well as to a decreased translocation of **AIF** and **EndoG** to the nucleus resulting in a protection against DNA fragmentation and apoptosis. We identified Bim as an important factor upstream of the mitochondria executing a central role in the caspase-independent apoptotic signaling pathway induced by spongistatin 1.

Taken together, spongistatin 1 is both an effective tool to characterize **novel modes of action** in the apoptotic pathways as well as a promising new experimental cytotoxic drug. Its strong anticancer potential, especially against metastatic and chemoresistant tumor cells, may render spongistatin 1 a **valuable chemotherapeutic compound** in future.



## REFERENCES

## VI REFERENCES

1. Mann, J., *Natural products in cancer chemotherapy: past, present and future*. Nat Rev Cancer, 2002. **2**(2): p. 143-8.
2. da Rocha, A.B., R.M. Lopes, and G. Schwartzmann, *Natural products in anticancer therapy*. Curr Opin Pharmacol, 2001. **1**(4): p. 364-9.
3. Chin, Y.W., et al., *Drug discovery from natural sources*. Aaps J, 2006. **8**(2): p. E239-53.
4. Rawat, D.S., et al., *Marine peptides and related compounds in clinical trial*. Anticancer Agents Med Chem, 2006. **6**(1): p. 33-40.
5. Igney, F.H. and P.H. Krammer, *Death and anti-death: tumour resistance to apoptosis*. Nat Rev Cancer, 2002. **2**(4): p. 277-88.
6. Fesik, S.W., *Promoting apoptosis as a strategy for cancer drug discovery*. Nat Rev Cancer, 2005. **5**(11): p. 876-85.
7. Amador, M.L., et al., *Progress in the development and acquisition of anticancer agents from marine sources*. Ann Oncol, 2003. **14**(11): p. 1607-15.
8. Sipkema, D., et al., *Marine sponges as pharmacy*. Mar Biotechnol (NY), 2005. **7**(3): p. 142-62.
9. Newman, D.J. and G.M. Cragg, *Marine natural products and related compounds in clinical and advanced preclinical trials*. J Nat Prod, 2004. **67**(8): p. 1216-38.
10. Simmons, T.L., et al., *Marine natural products as anticancer drugs*. Mol Cancer Ther, 2005. **4**(2): p. 333-42.
11. Mollinedo, F. and C. Gajate, *Microtubules, microtubule-interfering agents and apoptosis*. Apoptosis, 2003. **8**(5): p. 413-50.
12. Bhat, K.M. and V. Setaluri, *Microtubule-associated proteins as targets in cancer chemotherapy*. Clin Cancer Res, 2007. **13**(10): p. 2849-54.
13. Jordan, M.A. and L. Wilson, *Microtubules as a target for anticancer drugs*. Nat Rev Cancer, 2004. **4**(4): p. 253-65.
14. Pettit, G.R., *Progress in the Discovery of Biosynthetic Anticancer Drugs*. Journal of Natural Products, 1996. **59**: p. 812-821.
15. Pettit, G.R., *Isolation and Structure of Spongistatin 1*. Journal of Organic Chemistry, 1993. **58**: p. 1302-1304.
16. Pettit, G.R., *Isolation and Structure of the Remarkable Human Cancer Cell Growth Inhibitors Spongistatins 2 and 3 from an Eastern Indian Ocean Spongia sp.* Journal of Chemical Society, Chemical Communications, 1993. **14**: p. 1166-1168.
17. Pettit, G.R., *Isolation and Structure of the powerful human cancer cell growth inhibitors Spongistatins 4 and 5 from an African Spirastrella spinispirulifera (Prolifera)*. Journal of Chemical Society, Chemical Communications, 1993. **24**: p. 1805-1807.
18. Pettit, G.R., *Antineoplastic agents 293. The exceptional Human Cancer Cell Growth Inhibitors Spongistatins 6 and 7*. Natural Product Letters, 1993. **3**(4): p. 239-244.
19. [www.dafni.com](http://www.dafni.com).

20. [www.lalaternadelpopolo.it](http://www.lalaternadelpopolo.it).
21. Pettit, R.K., *A broad-spectrum antifungal from the marine sponge Hyrtios erecta*. International Journal of Antimicrobial Agents, 1998. **9**: p. 147-152.
22. Ovechkina, Y.Y., et al., *Unusual antimicrotubule activity of the antifungal agent spongistatin 1*. Antimicrob Agents Chemother, 1999. **43**(8): p. 1993-9.
23. Paterson, I., et al., *The stereocontrolled total synthesis of altohyrtin A/spongistatin 1: fragment couplings, completion of the synthesis, analogue generation and biological evaluation*. Org Biomol Chem, 2005. **3**(13): p. 2431-40.
24. Bai, R., et al., *Spongistatin 1, a highly cytotoxic, sponge-derived, marine natural product that inhibits mitosis, microtubule assembly, and the binding of vinblastine to tubulin*. Mol Pharmacol, 1993. **44**(4): p. 757-66.
25. Uckun, F.M., *Rationally designed anti-mitotic agents with pro-apoptotic activity*. Curr Pharm Des, 2001. **7**(16): p. 1627-39.
26. Uckun, F.M., et al., *Spongistatins as tubulin targeting agents*. Curr Pharm Des, 2001. **7**(13): p. 1291-6.
27. Catassi, A., et al., *Characterization of apoptosis induced by marine natural products in non small cell lung cancer A549 cells*. Cell Mol Life Sci, 2006. **63**(19-20): p. 2377-86.
28. Schyschka, L., et al., *Spongistatin 1: a new chemosensitizing marine compound that degrades XIAP*. Leukemia, 2008.
29. Fulda, S. and K.M. Debatin, *Extrinsic versus intrinsic apoptosis pathways in anticancer chemotherapy*. Oncogene, 2006. **25**(34): p. 4798-811.
30. Chipuk, J.E. and D.R. Green, *Do inducers of apoptosis trigger caspase-independent cell death?* Nat Rev Mol Cell Biol, 2005. **6**(3): p. 268-75.
31. Assuncao Guimaraes, C. and R. Linden, *Programmed cell deaths. Apoptosis and alternative deathstyles*. Eur J Biochem, 2004. **271**(9): p. 1638-50.
32. Lockshin, R.A. and Z. Zakeri, *Programmed cell death and apoptosis: origins of the theory*. Nat Rev Mol Cell Biol, 2001. **2**(7): p. 545-50.
33. Kerr, J.F., A.H. Wyllie, and A.R. Currie, *Apoptosis: a basic biological phenomenon with wide-ranging implications in tissue kinetics*. Br J Cancer, 1972. **26**(4): p. 239-57.
34. Vaux, D.L., *Apoptosis timeline*. Cell Death Differ, 2002. **9**(4): p. 349-54.
35. Fink, S.L. and B.T. Cookson, *Apoptosis, pyroptosis, and necrosis: mechanistic description of dead and dying eukaryotic cells*. Infect Immun, 2005. **73**(4): p. 1907-16.
36. Leist, M. and M. Jaattela, *Four deaths and a funeral: from caspases to alternative mechanisms*. Nat Rev Mol Cell Biol, 2001. **2**(8): p. 589-98.
37. Jaattela, M., *Multiple cell death pathways as regulators of tumour initiation and progression*. Oncogene, 2004. **23**(16): p. 2746-56.
38. Erwig, L.P. and P.M. Henson, *Clearance of apoptotic cells by phagocytes*. Cell Death Differ, 2008. **15**(2): p. 243-50.
39. Nicotera, P. and G. Melino, *Regulation of the apoptosis-necrosis switch*. Oncogene, 2004. **23**(16): p. 2757-65.

40. Golstein, P. and G. Kroemer, *Cell death by necrosis: towards a molecular definition*. Trends Biochem Sci, 2007. **32**(1): p. 37-43.
41. Broker, L.E., F.A. Kruyt, and G. Giaccone, *Cell death independent of caspases: a review*. Clin Cancer Res, 2005. **11**(9): p. 3155-62.
42. Jaattela, M. and J. Tschopp, *Caspase-independent cell death in T lymphocytes*. Nat Immunol, 2003. **4**(5): p. 416-23.
43. Okada, H. and T.W. Mak, *Pathways of apoptotic and non-apoptotic death in tumour cells*. Nat Rev Cancer, 2004. **4**(8): p. 592-603.
44. Yuan, J., et al., *The C. elegans cell death gene ced-3 encodes a protein similar to mammalian interleukin-1 beta-converting enzyme*. Cell, 1993. **75**(4): p. 641-52.
45. Kumar, S., *Caspase function in programmed cell death*. Cell Death Differ, 2007. **14**(1): p. 32-43.
46. Turk, B. and V. Stoka, *Protease signalling in cell death: caspases versus cysteine cathepsins*. FEBS Lett, 2007. **581**(15): p. 2761-7.
47. Philchenkov, A., *Caspases: potential targets for regulating cell death*. J Cell Mol Med, 2004. **8**(4): p. 432-44.
48. Lavrik, I.N., A. Golks, and P.H. Krammer, *Caspases: pharmacological manipulation of cell death*. J Clin Invest, 2005. **115**(10): p. 2665-72.
49. Lamkanfi, M., et al., *Caspases in cell survival, proliferation and differentiation*. Cell Death Differ, 2007. **14**(1): p. 44-55.
50. Philchenkov, A., et al., *Caspases and cancer: mechanisms of inactivation and new treatment modalities*. Exp Oncol, 2004. **26**(2): p. 82-97.
51. Donepudi, M. and M.G. Grutter, *Structure and zymogen activation of caspases*. Biophys Chem, 2002. **101-102**: p. 145-53.
52. Shi, Y., *Caspase activation, inhibition, and reactivation: a mechanistic view*. Protein Sci, 2004. **13**(8): p. 1979-87.
53. Riedl, S.J. and Y. Shi, *Molecular mechanisms of caspase regulation during apoptosis*. Nat Rev Mol Cell Biol, 2004. **5**(11): p. 897-907.
54. Timmer, J.C. and G.S. Salvesen, *Caspase substrates*. Cell Death Differ, 2007. **14**(1): p. 66-72.
55. Fischer, U., R.U. Janicke, and K. Schulze-Osthoff, *Many cuts to ruin: a comprehensive update of caspase substrates*. Cell Death Differ, 2003. **10**(1): p. 76-100.
56. Eckelman, B.P., G.S. Salvesen, and F.L. Scott, *Human inhibitor of apoptosis proteins: why XIAP is the black sheep of the family*. EMBO Rep, 2006. **7**(10): p. 988-94.
57. Salvesen, G.S. and C.S. Duckett, *IAP proteins: blocking the road to death's door*. Nat Rev Mol Cell Biol, 2002. **3**(6): p. 401-10.
58. Vaux, D.L. and J. Silke, *IAPs, RINGs and ubiquitylation*. Nat Rev Mol Cell Biol, 2005. **6**(4): p. 287-97.
59. Fulda, S., *Inhibitor of apoptosis proteins as targets for anticancer therapy*. Expert Rev Anticancer Ther, 2007. **7**(9): p. 1255-64.

60. Vucic, D. and W.J. Fairbrother, *The inhibitor of apoptosis proteins as therapeutic targets in cancer*. Clin Cancer Res, 2007. **13**(20): p. 5995-6000.
61. Hunter, A.M., E.C. LaCasse, and R.G. Korneluk, *The inhibitors of apoptosis (IAPs) as cancer targets*. Apoptosis, 2007. **12**(9): p. 1543-68.
62. Callus, B.A. and D.L. Vaux, *Caspase inhibitors: viral, cellular and chemical*. Cell Death Differ, 2007. **14**(1): p. 73-8.
63. Jin, Z. and W.S. El-Deiry, *Overview of cell death signaling pathways*. Cancer Biol Ther, 2005. **4**(2): p. 139-63.
64. Kim, R., M. Emi, and K. Tanabe, *Role of mitochondria as the gardens of cell death*. Cancer Chemother Pharmacol, 2006. **57**(5): p. 545-53.
65. Galluzzi, L., et al., *Mitochondria as therapeutic targets for cancer chemotherapy*. Oncogene, 2006. **25**(34): p. 4812-30.
66. Saelens, X., et al., *Toxic proteins released from mitochondria in cell death*. Oncogene, 2004. **23**(16): p. 2861-74.
67. Riedl, S.J. and G.S. Salvesen, *The apoptosome: signalling platform of cell death*. Nat Rev Mol Cell Biol, 2007. **8**(5): p. 405-13.
68. Fadeel, B., A. Ottosson, and S. Pervaiz, *Big wheel keeps on turning: apoptosome regulation and its role in chemoresistance*. Cell Death Differ, 2008. **15**(3): p. 443-52.
69. van Gurp, M., et al., *Mitochondrial intermembrane proteins in cell death*. Biochem Biophys Res Commun, 2003. **304**(3): p. 487-97.
70. Vande Walle, L., M. Lamkanfi, and P. Vandenberghe, *The mitochondrial serine protease HtrA2/Omi: an overview*. Cell Death Differ, 2008. **15**(3): p. 453-60.
71. Susin, S.A., et al., *Molecular characterization of mitochondrial apoptosis-inducing factor*. Nature, 1999. **397**(6718): p. 441-6.
72. Li, L.Y., X. Luo, and X. Wang, *Endonuclease G is an apoptotic DNase when released from mitochondria*. Nature, 2001. **412**(6842): p. 95-9.
73. van Loo, G., et al., *Endonuclease G: a mitochondrial protein released in apoptosis and involved in caspase-independent DNA degradation*. Cell Death Differ, 2001. **8**(12): p. 1136-42.
74. Wang, X., et al., *Mechanisms of AIF-mediated apoptotic DNA degradation in Caenorhabditis elegans*. Science, 2002. **298**(5598): p. 1587-92.
75. Ye, H., et al., *DNA binding is required for the apoptogenic action of apoptosis inducing factor*. Nat Struct Biol, 2002. **9**(9): p. 680-4.
76. Modjtahedi, N., et al., *Apoptosis-inducing factor: vital and lethal*. Trends Cell Biol, 2006. **16**(5): p. 264-72.
77. Cory, S. and J.M. Adams, *The Bcl2 family: regulators of the cellular life-or-death switch*. Nat Rev Cancer, 2002. **2**(9): p. 647-56.
78. Sharpe, J.C., D. Arnoult, and R.J. Youle, *Control of mitochondrial permeability by Bcl-2 family members*. Biochim Biophys Acta, 2004. **1644**(2-3): p. 107-13.

79. Danial, N.N. and S.J. Korsmeyer, *Cell death: critical control points*. Cell, 2004. **116**(2): p. 205-19.
80. Hengartner, M.O., *The biochemistry of apoptosis*. Nature, 2000. **407**(6805): p. 770-6.
81. Armstrong, J.S., *Mitochondria: a target for cancer therapy*. Br J Pharmacol, 2006. **147**(3): p. 239-48.
82. Haldar, S., A. Basu, and C.M. Croce, *Bcl2 is the guardian of microtubule integrity*. Cancer Res, 1997. **57**(2): p. 229-33.
83. Bhalla, K.N., *Microtubule-targeted anticancer agents and apoptosis*. Oncogene, 2003. **22**(56): p. 9075-86.
84. Petros, A.M., E.T. Olejniczak, and S.W. Fesik, *Structural biology of the Bcl-2 family of proteins*. Biochim Biophys Acta, 2004. **1644**(2-3): p. 83-94.
85. Festjens, N., et al., *Bcl-2 family members as sentinels of cellular integrity and role of mitochondrial intermembrane space proteins in apoptotic cell death*. Acta Haematol, 2004. **111**(1-2): p. 7-27.
86. Youle, R.J. and A. Strasser, *The BCL-2 protein family: opposing activities that mediate cell death*. Nat Rev Mol Cell Biol, 2008. **9**(1): p. 47-59.
87. Adams, J.M. and S. Cory, *The Bcl-2 protein family: arbiters of cell survival*. Science, 1998. **281**(5381): p. 1322-6.
88. Burlacu, A., *Regulation of apoptosis by Bcl-2 family proteins*. J Cell Mol Med, 2003. **7**(3): p. 249-57.
89. Hinds, M.G., et al., *Bim, Bad and Bmf: intrinsically unstructured BH3-only proteins that undergo a localized conformational change upon binding to prosurvival Bcl-2 targets*. Cell Death Differ, 2007. **14**(1): p. 128-36.
90. Yin, X.M., *Bid, a BH3-only multi-functional molecule, is at the cross road of life and death*. Gene, 2006. **369**: p. 7-19.
91. O'Connor, L., et al., *Bim: a novel member of the Bcl-2 family that promotes apoptosis*. Embo J, 1998. **17**(2): p. 384-95.
92. Han, J., et al., *Disruption of Mcl-1.Bim complex in granzyme B-mediated mitochondrial apoptosis*. J Biol Chem, 2005. **280**(16): p. 16383-92.
93. Han, J., et al., *Interrelated roles for Mcl-1 and BIM in regulation of TRAIL-mediated mitochondrial apoptosis*. J Biol Chem, 2006. **281**(15): p. 10153-63.
94. Meng, X.W., et al., *Mcl-1 as a buffer for proapoptotic Bcl-2 family members during TRAIL-induced apoptosis: a mechanistic basis for sorafenib (Bay 43-9006)-induced TRAIL sensitization*. J Biol Chem, 2007. **282**(41): p. 29831-46.
95. Willis, S.N. and J.M. Adams, *Life in the balance: how BH3-only proteins induce apoptosis*. Curr Opin Cell Biol, 2005. **17**(6): p. 617-25.
96. Chipuk, J.E., L. Bouchier-Hayes, and D.R. Green, *Mitochondrial outer membrane permeabilization during apoptosis: the innocent bystander scenario*. Cell Death Differ, 2006. **13**(8): p. 1396-402.
97. Adams, J.M. and S. Cory, *The Bcl-2 apoptotic switch in cancer development and therapy*. Oncogene, 2007. **26**(9): p. 1324-37.

98. Letai, A., et al., *Distinct BH3 domains either sensitize or activate mitochondrial apoptosis, serving as prototype cancer therapeutics*. *Cancer Cell*, 2002. **2**(3): p. 183-92.
99. Willis, S.N., et al., *Apoptosis initiated when BH3 ligands engage multiple Bcl-2 homologs, not Bax or Bak*. *Science*, 2007. **315**(5813): p. 856-9.
100. Chen, L., et al., *Differential targeting of prosurvival Bcl-2 proteins by their BH3-only ligands allows complementary apoptotic function*. *Mol Cell*, 2005. **17**(3): p. 393-403.
101. Sahai, E., *Illuminating the metastatic process*. *Nat Rev Cancer*, 2007. **7**(10): p. 737-49.
102. Pantel, K. and R.H. Brakenhoff, *Dissecting the metastatic cascade*. *Nat Rev Cancer*, 2004. **4**(6): p. 448-56.
103. Friedl, P. and K. Wolf, *Tumour-cell invasion and migration: diversity and escape mechanisms*. *Nat Rev Cancer*, 2003. **3**(5): p. 362-74.
104. Gilmore, A.P., *Anoikis*. *Cell Death Differ*, 2005. **12 Suppl 2**: p. 1473-7.
105. Mehlen, P. and A. Puisieux, *Metastasis: a question of life or death*. *Nat Rev Cancer*, 2006. **6**(6): p. 449-58.
106. McLean, G.W., et al., *The role of focal-adhesion kinase in cancer - a new therapeutic opportunity*. *Nat Rev Cancer*, 2005. **5**(7): p. 505-15.
107. Mitra, S.K., D.A. Hanson, and D.D. Schlaepfer, *Focal adhesion kinase: in command and control of cell motility*. *Nat Rev Mol Cell Biol*, 2005. **6**(1): p. 56-68.
108. Pinkas, J., S.S. Martin, and P. Leder, *Bcl-2-mediated cell survival promotes metastasis of EpH4 betaMEKDD mammary epithelial cells*. *Mol Cancer Res*, 2004. **2**(10): p. 551-6.
109. Martin, S.S., et al., *A cytoskeleton-based functional genetic screen identifies Bcl-xL as an enhancer of metastasis, but not primary tumor growth*. *Oncogene*, 2004. **23**(26): p. 4641-5.
110. Bialik, S. and A. Kimchi, *DAP-kinase as a target for drug design in cancer and diseases associated with accelerated cell death*. *Semin Cancer Biol*, 2004. **14**(4): p. 283-94.
111. Engels, I.H., et al., *Caspase-8/FLICE functions as an executioner caspase in anticancer drug-induced apoptosis*. *Oncogene*, 2000. **19**(40): p. 4563-73.
112. Bruns, C.J., et al., *In vivo selection and characterization of metastatic variants from human pancreatic adenocarcinoma by using orthotopic implantation in nude mice*. *Neoplasia*, 1999. **1**(1): p. 50-62.
113. <http://biology.berkeley.edu/crl/cytometry%20compensation.html>.
114. [www.manderson.org/images/1BD\\_LSP\\_Oprical\\_Bench.gif](http://www.manderson.org/images/1BD_LSP_Oprical_Bench.gif).
115. Nicoletti, I., et al., *A rapid and simple method for measuring thymocyte apoptosis by propidium iodide staining and flow cytometry*. *J Immunol Methods*, 1991. **139**(2): p. 271-9.
116. Albini, A., *Tumor and endothelial cell invasion of basement membranes. The matrigel chemoinvasion assay as a tool for dissecting molecular mechanisms*. *Pathol Oncol Res*, 1998. **4**(3): p. 230-41.
117. Albini, A., et al., *The "chemoinvasion assay": a tool to study tumor and endothelial cell invasion of basement membranes*. *Int J Dev Biol*, 2004. **48**(5-6): p. 563-71.

118. Albini, A. and R. Benelli, *The chemoinvasion assay: a method to assess tumor and endothelial cell invasion and its modulation*. Nat Protoc, 2007. **2**(3): p. 504-11.
119. [www.zeiss.de/C1256D18002CC306/0/99C3B5F289AFDB5CC125725F0027D28F/\\$file/45-0066\\_e.pdf](http://www.zeiss.de/C1256D18002CC306/0/99C3B5F289AFDB5CC125725F0027D28F/$file/45-0066_e.pdf).
120. Fulda, S. and K.M. Debatin, *Apoptosis signaling in tumor therapy*. Ann N Y Acad Sci, 2004. **1028**: p. 150-6.
121. Fulda, S. and K.M. Debatin, *Targeting apoptosis pathways in cancer therapy*. Curr Cancer Drug Targets, 2004. **4**(7): p. 569-76.
122. Dirsch, V.M., et al., *Cephalostatin 1 selectively triggers the release of Smac/DIABLO and subsequent apoptosis that is characterized by an increased density of the mitochondrial matrix*. Cancer Res, 2003. **63**(24): p. 8869-76.
123. Puthalakath, H., et al., *The proapoptotic activity of the Bcl-2 family member Bim is regulated by interaction with the dynein motor complex*. Mol Cell, 1999. **3**(3): p. 287-96.
124. Bradford, M.M., *A rapid and sensitive method for the quantitation of microgram quantities of protein utilizing the principle of protein-dye binding*. Anal Biochem, 1976. **72**: p. 248-54.
125. Laemmli, U.K., *Cleavage of structural proteins during the assembly of the head of bacteriophage T4*. Nature, 1970. **227**(5259): p. 680-5.
126. McManus, M.T. and P.A. Sharp, *Gene silencing in mammals by small interfering RNAs*. Nat Rev Genet, 2002. **3**(10): p. 737-47.
127. Sunters, A., et al., *FoxO3a transcriptional regulation of Bim controls apoptosis in paclitaxel-treated breast cancer cell lines*. J Biol Chem, 2003. **278**(50): p. 49795-805.
128. Basnakian, A.G., et al., *Endonuclease G promotes cell death of non-invasive human breast cancer cells*. Exp Cell Res, 2006. **312**(20): p. 4139-49.
129. Park, M.T., et al., *Phytosphingosine in combination with ionizing radiation enhances apoptotic cell death in radiation-resistant cancer cells through ROS-dependent and -independent AIF release*. Blood, 2005. **105**(4): p. 1724-33.
130. Ocker, M., et al., *Variants of bcl-2 specific siRNA for silencing antiapoptotic bcl-2 in pancreatic cancer*. Gut, 2005. **54**(9): p. 1298-308.
131. Zhu, H., et al., *Bcl-XL small interfering RNA suppresses the proliferation of 5-fluorouracil-resistant human colon cancer cells*. Mol Cancer Ther, 2005. **4**(3): p. 451-6.
132. Kurokawa, H., et al., *Alteration of caspase-3 (CPP32/Yama/apopain) in wild-type MCF-7, breast cancer cells*. Oncol Rep, 1999. **6**(1): p. 33-7.
133. Furukawa, Y., et al., *Apaf-1 is a mediator of E2F-1-induced apoptosis*. J Biol Chem, 2002. **277**(42): p. 39760-8.
134. Soengas, M.S., et al., *Inactivation of the apoptosis effector Apaf-1 in malignant melanoma*. Nature, 2001. **409**(6817): p. 207-11.
135. Kortylewski, M., R. Jove, and H. Yu, *Targeting STAT3 affects melanoma on multiple fronts*. Cancer Metastasis Rev, 2005. **24**(2): p. 315-27.

136. Ischenko, I., et al., *Effect of Src kinase inhibition on metastasis and tumor angiogenesis in human pancreatic cancer*. *Angiogenesis*, 2007. **10**(3): p. 167-82.
137. Ward, M.W., et al., *Real time single cell analysis of Bid cleavage and Bid translocation during caspase-dependent and neuronal caspase-independent apoptosis*. *J Biol Chem*, 2006. **281**(9): p. 5837-44.
138. Becattini, B., et al., *Targeting apoptosis via chemical design: inhibition of bid-induced cell death by small organic molecules*. *Chem Biol*, 2004. **11**(8): p. 1107-17.
139. Jemal, A., et al., *Cancer statistics, 2008*. *CA Cancer J Clin*, 2008. **58**(2): p. 71-96.
140. Steeg, P.S., *Tumor metastasis: mechanistic insights and clinical challenges*. *Nat Med*, 2006. **12**(8): p. 895-904.
141. Recher, C., et al., *Expression of focal adhesion kinase in acute myeloid leukemia is associated with enhanced blast migration, increased cellularity, and poor prognosis*. *Cancer Res*, 2004. **64**(9): p. 3191-7.
142. Brunton, V.G., et al., *Identification of Src-specific phosphorylation site on focal adhesion kinase: dissection of the role of Src SH2 and catalytic functions and their consequences for tumor cell behavior*. *Cancer Res*, 2005. **65**(4): p. 1335-42.
143. Chatzizacharias, N.A., G.P. Kouraklis, and S.E. Theocharis, *Disruption of FAK signaling: a side mechanism in cytotoxicity*. *Toxicology*, 2008. **245**(1-2): p. 1-10.
144. Klein, C.A., *The biology and analysis of single disseminated tumour cells*. *Trends Cell Biol*, 2000. **10**(11): p. 489-93.
145. Frankel, A., et al., *Induction of anoikis and suppression of human ovarian tumor growth in vivo by down-regulation of Bcl-X(L)*. *Cancer Res*, 2001. **61**(12): p. 4837-41.
146. Bold, R.J., S. Virudachalam, and D.J. McConkey, *BCL2 expression correlates with metastatic potential in pancreatic cancer cell lines*. *Cancer*, 2001. **92**(5): p. 1122-9.
147. Fernandez, Y., et al., *Bcl-xL promotes metastasis of breast cancer cells by induction of cytokines resistance*. *Cell Death Differ*, 2000. **7**(4): p. 350-9.
148. Espana, L., et al., *Overexpression of Bcl-xL in human breast cancer cells enhances organ-selective lymph node metastasis*. *Breast Cancer Res Treat*, 2004. **87**(1): p. 33-44.
149. Chao, D.T., et al., *Bcl-XL and Bcl-2 repress a common pathway of cell death*. *J Exp Med*, 1995. **182**(3): p. 821-8.
150. Du, Y.C., et al., *Assessing tumor progression factors by somatic gene transfer into a mouse model: Bcl-xL promotes islet tumor cell invasion*. *PLoS Biol*, 2007. **5**(10): p. 2255-69.
151. Zhang, J. and G.T. Bowden, *Targeting Bcl-X(L) for prevention and therapy of skin cancer*. *Mol Carcinog*, 2007. **46**(8): p. 665-70.
152. Simstein, R., et al., *Apoptosis, chemoresistance, and breast cancer: insights from the MCF-7 cell model system*. *Exp Biol Med (Maywood)*, 2003. **228**(9): p. 995-1003.
153. Butt, A.J., et al., *A novel plant toxin, persin, with in vivo activity in the mammary gland, induces Bim-dependent apoptosis in human breast cancer cells*. *Mol Cancer Ther*, 2006. **5**(9): p. 2300-9.

154. Fulda, S. and K.M. Debatin, *Modulation of apoptosis signaling for cancer therapy*. Arch Immunol Ther Exp (Warsz), 2006. **54**(3): p. 173-5.
155. Mashima, T. and T. Tsuruo, *Defects of the apoptotic pathway as therapeutic target against cancer*. Drug Resist Updat, 2005. **8**(6): p. 339-43.
156. Cregan, S.P., V.L. Dawson, and R.S. Slack, *Role of AIF in caspase-dependent and caspase-independent cell death*. Oncogene, 2004. **23**(16): p. 2785-96.
157. Wan, K.F., et al., *Chelerythrine induces apoptosis through a Bax/Bak-independent mitochondrial mechanism*. J Biol Chem, 2008. **283**(13): p. 8423-33.
158. Gavalda, N., et al., *Bax deficiency promotes an up-regulation of Bim(EL) and Bak during striatal and cortical postnatal development, and after excitotoxic injury*. Mol Cell Neurosci, 2008. **37**(4): p. 663-72.
159. Zhang, X.D., S.K. Gillespie, and P. Hersey, *Staurosporine induces apoptosis of melanoma by both caspase-dependent and -independent apoptotic pathways*. Mol Cancer Ther, 2004. **3**(2): p. 187-97.
160. Kroemer, G. and S.J. Martin, *Caspase-independent cell death*. Nat Med, 2005. **11**(7): p. 725-30.
161. Lorenzo, H.K. and S.A. Susin, *Mitochondrial effectors in caspase-independent cell death*. FEBS Lett, 2004. **557**(1-3): p. 14-20.
162. Liu, H.R., et al., *Role of Omi/HtrA2 in apoptotic cell death after myocardial ischemia and reperfusion*. Circulation, 2005. **111**(1): p. 90-6.
163. Kuninaka, S., et al., *The tumor suppressor WARTS activates the Omi / HtrA2-dependent pathway of cell death*. Oncogene, 2005. **24**(34): p. 5287-98.
164. Niikura, Y., et al., *BUB1 mediation of caspase-independent mitotic death determines cell fate*. J Cell Biol, 2007.
165. Arnoult, D., et al., *Mitochondrial release of AIF and EndoG requires caspase activation downstream of Bax/Bak-mediated permeabilization*. Embo J, 2003. **22**(17): p. 4385-99.
166. Arnoult, D., et al., *Mitochondrial release of apoptosis-inducing factor occurs downstream of cytochrome c release in response to several proapoptotic stimuli*. J Cell Biol, 2002. **159**(6): p. 923-9.
167. Liou, A.K., et al., *BimEL up-regulation potentiates AIF translocation and cell death in response to MPTP*. Faseb J, 2005. **19**(10): p. 1350-2.
168. Tang, D., J.M. Lahti, and V.J. Kidd, *Caspase-8 activation and bid cleavage contribute to MCF7 cellular execution in a caspase-3-dependent manner during staurosporine-mediated apoptosis*. J Biol Chem, 2000. **275**(13): p. 9303-7.
169. Valentijn, A.J. and A.P. Gilmore, *Translocation of full-length Bid to mitochondria during anoikis*. J Biol Chem, 2004. **279**(31): p. 32848-57.
170. Weber, A., et al., *BimS-induced apoptosis requires mitochondrial localization but not interaction with anti-apoptotic Bcl-2 proteins*. J Cell Biol, 2007. **177**(4): p. 625-36.
171. Kim, S.H., M.S. Ricci, and W.S. El-Deiry, *Mcl-1: a gateway to TRAIL sensitization*. Cancer Res, 2008. **68**(7): p. 2062-4.

172. Wuilleme-Toumi, S., et al., *Reciprocal protection of Mcl-1 and Bim from ubiquitin-proteasome degradation*. *Biochem Biophys Res Commun*, 2007. **361**(4): p. 865-9.
173. Gomez-Bougie, P., R. Bataille, and M. Amiot, *Endogenous association of Bim BH3-only protein with Mcl-1, Bcl-xL and Bcl-2 on mitochondria in human B cells*. *Eur J Immunol*, 2005. **35**(3): p. 971-6.
174. Brunelle, J.K., et al., *Loss of Mcl-1 protein and inhibition of electron transport chain together induce anoxic cell death*. *Mol Cell Biol*, 2007. **27**(4): p. 1222-35.
175. Lee, E.F., et al., *A novel BH3 ligand that selectively targets Mcl-1 reveals that apoptosis can proceed without Mcl-1 degradation*. *J Cell Biol*, 2008. **180**(2): p. 341-55.
176. O'Reilly, L.A., et al., *The proapoptotic BH3-only protein bim is expressed in hematopoietic, epithelial, neuronal, and germ cells*. *Am J Pathol*, 2000. **157**(2): p. 449-61.
177. Bouillet, P., et al., *Degenerative disorders caused by Bcl-2 deficiency prevented by loss of its BH3-only antagonist Bim*. *Dev Cell*, 2001. **1**(5): p. 645-53.
178. Bouillet, P., et al., *Proapoptotic Bcl-2 relative Bim required for certain apoptotic responses, leukocyte homeostasis, and to preclude autoimmunity*. *Science*, 1999. **286**(5445): p. 1735-8.
179. Aichberger, K.J., et al., *Low-level expression of proapoptotic Bcl-2-interacting mediator in leukemic cells in patients with chronic myeloid leukemia: role of BCR/ABL, characterization of underlying signaling pathways, and reexpression by novel pharmacologic compounds*. *Cancer Res*, 2005. **65**(20): p. 9436-44.

TITEL <http://ghr.nlm.nih.gov/handbook/illustrations/apoptosismacrophage>



## APPENDIX

## VII APPENDIX

### 1 ABBREVIATIONS

AIF	Apoptosis inducing factor
ANOVA	Analysis of variance between groups
ANT	Adenine nucleotide translocator
Apaf-1	Apoptotic-protease-activating factor-1
APS	Ammonium persulfate
ATCC	American Type Culture Collection
ATP / dATP	Adenosine-5'-triphosphate / 2'-desoxyadenosine-5'-triphosphate
BAD	Bcl-2 antagonist of cell death
Bak	Bcl-2 antagonist killer 1
Bax	Bcl-2-associated X protein
Bcl	B-cell lymphoma
BH	Bcl-2 homology
Bid	Bcl-2 interacting domain death agonist
Bik	Bcl-2 interacting killer
Bim	Bcl-2 interacting mediator of cell death
BIR	Baculoviral IAP repeat
Bmf	Bcl-2 modifying factor
bp	Base pair
BSA	Bovine serum albumin
CAD	Caspase-activated DNase
CARD	Caspase recruitment domain
Cdc42	Cell division cycle 42
CDK	Cyclin-dependent kinase
CED	Cell-death abnormality
c-FLIP	Cellular FLICE-inhibitory protein
c-IAP 1 / c-IAP 2	Cellular inhibitor of apoptosis 1/2
CrmA	Cytokine response modifier A
DAPK	Death-associated protein kinase
DD	Death domain
DED	Death effector domain
DEPC	Diethylcarbonate
DIABLO	Direct IAP binding protein with low pI
DISC	Death-inducing signaling complex
DLC	Dynein light chain
DMSO	Dimethylsulfoxide

---

DNA	Desoxyribonucleic acid
DR4 / DR5	Death receptor 4/5
ds	Double strand
DTT	Dithiothreitol
ECL	Enhanced chemiluminescence
ECM	Extracellular matrix
EDTA	Ethylenediaminetetraacetic acid
EGTA	Ethylene glycol-bis(2-aminoethylether) tetraacetic acid
ELISA	Enzyme-linked immunosorbent assay
EndoG	Endonuclease G
ERK	Extracellular signal-regulated kinase
FACS	Fluorescence-activated cell sorter
FADD	Fas-associated death domain
FAK	Focal adhesion kinase
FasL	Fas ligand
FAT	Focal-adhesion targeting
FCS	Foetal calf serum
FERM	Protein4.1, ezrin, radixin and moesin homology
FL	Fluorescence
FSC	Forward scatter
GFP	Green fluorescent protein
HEPES	N-(2-Hydroxyethyl)piperazine-N'-(2-ethanesulfonic acid)
HFS	Hypotonic fluorochrome solution
Hrk	Harakiri
HRP	Horseradish peroxidase
HSP	Heat-shock protein
HtrA2	High-temperature-requirement protein A2
IAP	Inhibitor of apoptosis
ICAD	Inhibitor of caspase-activated DNase
ICE	Interleukin-1 $\beta$ converting enzyme
JNK	c-Jun N-terminal kinase
kDa	Kilo Dalton
MAPK	Mitogen activated protein kinase
Mcl-1	Myeloid cell leukemia-1
MMP	Matrix metalloproteinase
MMP	Mitochondrial membrane permeabilization
mRNA	Messenger ribonucleic acid

---

MTT	3-(4,5-Dimethylthiazol-2-yl)-2,5-diphenyl tetrazolium bromide
NADH	Nicotinamide adenine dinucleotide
NAIP	Neutral apoptosis inhibitory protein
NCI	National Cancer Institute
NF-kB	Nuclear factor kappa B
nt	Nucleotide
OMM	Outer mitochondrial membrane
p-	Phospho-
p38 MAPK	p38 mitogen-activated protein kinase
PAA	Polyacrylamide
PARP	Poly(ADP-ribose) polymerase
PBS	Phosphate buffered saline
PCD	Programmed cell death
PI	Propidium iodide
PIDD	p53-induced protein with a DD
PI3k	Phosphoinositide-3-OH kinase
PKA	Protein kinase A
PKB	Protein kinase B
PKC	Protein kinase C
PMSF	Phenylmethylsulfonylfluoride
Poly-HEMA	Polyhydroxyethylmethacrylate
PRR	Proline-rich region
PS	Phosphatidylserine
PSR	Phosphatidylserine receptor
PTPC	Permeability transition pore complex
Puma	p53-upregulated modulator of apoptosis
Q-VD-OPh	N-(2-Quinolyl)valyl-aspartyl-(2,6-difluorophenoxy)methylketone
RAIDD	RIP associatd ICH-1/CED-3-homologous protein with DD
RING	Really interesting new gene
RISC	RNA interference silencing complex
RNAi	RNA interference
SDS	Sodium dodecyl sulfate
SDS-PAGE	Sodium dodecyl sulfate polyacrylamide gel electrophoresis
SEM	Standard error of the mean
shRNA	Short hairpin RNA

---

siRNA	Short interfering RNA
Smac	Second mitochondria-derived activator of caspases
SSC	Side scatter
TBS-T	Tris-buffered saline with tween
T/E	Trypsin/EDTA
TEMED	N, N, N', N' tetramethylenediamine
TNF	Tumor necrosis factor
TNF-R1	Tumor necrosis factor receptor 1
TRAIL	TNF-related apoptosis-inducing ligand
TRAIL-R1/TRAIL-R2	TNF-receptor associated apoptosis-inducing ligand receptor 1/2
TRAF2	TNF-receptor associated factor 2
UV	Ultraviolet
VDAC	Voltage-dependent anion channel
WB	Western Blot
XIAP	X-chromosome-linked inhibitor of apoptosis
zVAD.fmk	N-benzyloxycarbonyl-Val-Ala-Asp(OMe)-fluoromethylketone

## 2 ALPHABETICAL LIST OF COMPANIES

Active Motif	Rixensart, Belgium
Alexis	Grünberg, Germany
AGFA	Cologne, Germany
Amaxa	Cologne, Germany
Ambion	Hamburg, Germany
Amersham Biosciences	Freiburg, Germany
Applichem	Darmstadt, Germany
Applied Biosystems	Foster City, CA, USA
BD Biosciences	Heidelberg, Germany
BD PharMingen	Heidelberg, Germany
Beckman Coulter	Krefeld, Germany
Becton Dickinson	Heidelberg, Germany
Biochrome	Berlin, Germany
Biomers.net	Ulm, Germany
Biometra	Göttingen, Germany
Biomol	Hamburg, Germany
Bio-Rad	Munich, Germany
Biotrend Chemikalien GmbH	Cologne, Germany
Biozol	Eching, Germany
Calbiochem	Schwalbach, Germany
Canon	Krefeld, Germany
Cell Signaling	Frankfurt, Germany
Cytoskeleton	Offenbach, Germany
Dharmacon	Lafayette, CO, USA
Dianova	Hamburg, Germany
EliLilly	Bad Homburg, Germany
Fermentas	St. Leon-Rot, Germany
Fuji	Düsseldorf, Germany
Gibco/Invitrogen	Karlsruhe, Germany
Immunotech	Marseille, France
Invitrogen	Karlsruhe, Germany
Kodak	Rochester, USA
Li-Cor Biosciences	Lincoln, NE
Merck Biosciences	Darmstadt, Germany
Millipore	Schwalbach, Germany
Minerva Biolabs	Berlin, Germany
Molecular Probes/Invitrogen	Karlsruhe, Germany
NatuTac	Frankfurt, Germany

---

Olympus Optical	Hamburg, Germany
PAA Laboratories	Cölbe, Germany
PAN Biotech	Aidenbach, Germany
PeptoTech	Rocky Hill, NY, USA
Peqlab Biotechnologie GmbH	Erlangen, Germany
Perkin Elmer	Überlingen, Germany
Peske	Aindling-Arnhofen, Germany
Prosci incorporated	Poway, USA
Promega	Heidelberg, Germany
Promocell	Heidelberg, Germany
R&D Systems	Minneapolis, USA
Roche	Mannheim, Germany
Roth GmbH	Karlsruhe, Germany
Santa Cruz	Heidelberg, Germany
S.CO LifeScience	Garching, Germany
SERVA Electrophoresis GmbH	Heidelberg, Germany
Sigma-Aldrich	Taufkirchen, Germany
SLT Labinstruments	Crailsheim, Germany
Stratagene	La Jolla, USA
Tecan	Crailsheim, Germany
TILL Photonics	Gräfelfing, Germany
TPP	Trasadingen, Switzerland
Upstate	Lake Placid, NY, USA
USB	Cleveland, USA
Zeiss	Oberkochen, Germany



### 3 PUBLICATIONS

#### 3.1 POSTER PRESENTATIONS

U. M. Schneiders, L. Schyschka, N. Barth, A. M. Vollmar

Characterisation of apoptosis signal transduction induced by spongistatin 1 in MCF-7 cells.

48<sup>th</sup> Spring Meeting of the Deutsche Gesellschaft für experimentelle und klinische Pharmakologie und Toxikologie, March 13-15, 2006, Mainz, Germany.

Naunyn-Schmiedeberg's Archive of Pharmacology, Vol. 375

U. M. Schneiders, A.M. Vollmar

Spongistatin 1 induces apoptosis involving the BH3-only protein Bim and the endonuclease G.

15<sup>th</sup> Euroconference on Apoptosis, October 26-31, 2007, Portoroz, Slovenia

Poster No. P-207

#### 3.2 ORIGINAL PUBLICATIONS

U. M. Schneiders, L. Schyschka, A. Rudy, A. M. Vollmar

Spongistatin 1, a marine compound, induces apoptosis involving the BH3-only protein Bim and endonuclease G.

*submitted*

A. Rothmeier\*, U. M. Schneiders\*, I. Ischenko, C. Bruns, S. Zahler, A. M. Vollmar

Inhibition of MMP-9 and Bcl-x<sub>L</sub> by spongistatin 1 reduces pancreatic tumor progression and metastasis *in vitro* and *in vivo*.

\* These authors contributed equally to this work.

*in preparation*

#### 3.3 BOOK CONTRIBUTIONS

Co-authorship:

Ammon, Hermann P.T. (Hrsg.), Mutschler, Ernst (Hrsg.), Scholz, Hasso (Hrsg.)  
Arzneimittelinformation und -beratung in der Apotheke.

Monographs of analgetic drugs.

Deutscher Apotheker Verlag Stuttgart

*in press*

## 4 CURRICULUM VITAE

### Personal data

Name	Uta Monika Schneiders
Date of birth	1979-07-27
Place of birth	Saarbrücken, Germany
Nationality	german
Marital status	unmarried

### Science

Since 08/2005	Ph.D. thesis Institut of Pharmaceutical Biology, Prof. Dr. A. M. Vollmar Department of Pharmacy - Center of Drug Research, Ludwig-Maximilians-University, Munich, Germany
Since 12/2005	Advanced training as Specialist in Pharmaceutical Analysis Institut of Pharmaceutical Chemistry, Prof. Dr. F. Bracher Department of Pharmacy - Center of Drug Research, Ludwig-Maximilians-University, Munich, Germany
Since 02/2006	Pharmacist Riesefeld Apotheke, Munich, Germany
06/2005	3rd State Examination, Licensure as Pharmacist
11/2004 - 04/2005	“First year resident“ as Pharmacist, Department of Cardiovascular, Dr. Hanna Tinnel Bayer Health Care AG, Research Center Wuppertal, Germany
05-10/2004	“First year resident“ as Pharmacist, Apotheke am Engelbecken, Berlin, Germany
04/2004	2nd State Examination
06-09/2002	Internship as trainee in Pharmacology, Department of Pharmacology, Prof. Dr. Lucia Sivilotti School of Pharmacy, University of London, United Kingdom
09/2001	1st State Examination
10/1999 - 04/2004	Studies of Pharmacy, Ruprecht-Karls-University, Heidelberg, Germany

### Education

1990 - 1999	Grammar School: Johannes-Kepler-Gymnasium, Lebach, Germany
1986 - 1990	Primary School: St. Michael-Grundschule, Lebach, Germany

## 5 ACKNOWLEDGEMENTS

First of all, I would like to thank Prof. Dr. Angelika M. Vollmar for giving me the opportunity to perform this work in her laboratories. Her encouragement and her constant scientific guidance were exceeding helpful and motivating to me.

Furthermore, I want to thank my thesis committee, especially Prof. Dr. Christian Wahl-Schott for acting as second examiner.

Special thanks go to Dr. Paul Groot-Kormelink for sparking my interest in scientific work. During my time in the lab of Prof. Lucia Sivilotti, University of London, he taught me in a variety of molecular biological techniques, never forgetting how to have fun at work.

Many thanks go to the “chemists” from building C, especially Dr. Florian Plößl, Dr. Martin Giera, Marco Keller and Melanie Hass for their warm reception in the supervision of the first semester and for endless fun both during the time in the practical course and after work. I would also express my gratitude to Dr. Hanns-Jürgen Krauss for giving me the opportunity to take part in the “Weiterbildung zum Fachapotheker für pharmazeutische Analytik” and for his permanent support doing this.

Special thanks go to all former and present members of the working group for such a motivating, pleasant and relaxing working atmosphere. I would also express my gratitude to the technical staff for their cooperativeness. Many thanks go to PD. Dr. Stefan Zahler for his expert guidance and patience foremost in the use of the confocal microscope. I am very grateful to Dr. Anita Rudy for her permanent support in an excellent manner, for the introduction in different research techniques and always being around for practical advice in the lab and inspiring discussions. Furthermore, I want to thank her for the great time during the 15<sup>th</sup> Euroconference on Apoptosis in Portoroz. Many thanks go to Christine Weber for reading the manuscript. My dearest thanks go to Martin Bubik, Nina Berberich and also Christoph Mayer and Sandra Hemmers for their friendship, for the numerous amusing coffee breaks and for the wonderful time I could spend with them in- and outside the lab. Without you, I would never had such great hiking tours in the mountains and barbecue sessions on the balcony.

A very special and heartfelt thankyou to Manuel Ruf for his unlimited comprehension, his enduring patience with me and for just being there whenever I needed him.

Last but not least I have to express my deepest gratitude to my family and all my friends. Without their encouragement and support, this work would not exist. Thank you so much!

